Metatranscriptomic Insights into the Microbiomes of Canine and Feline Struvite Uroliths and Investigation of the Oral–Urolith Axis

By

ASHLEIGH MARIE FLORES

DISSERTATION

Submitted in partial satisfaction of the requirements for the degree of

DOCTOR OF PHILOSOPHY

in

Integrative Pathobiology

in the

OFFICE OF GRADUATE STUDIES

of the

UNIVERSITY OF CALIFORNIA

DAVIS

Approved:

Bart C Weimer, Chair

Jodi L Westropp

Maria M Soltero-Rivera

Committee in Charge

2025

DEDICATION

For Binero, Boots, Charlotte, Rosey and Mikey

ACKNOWLEDGEMENTS

I would like to sincerely thank my dissertation committee for their invaluable insights and mentorship; I appreciate your guidance and encouragement with this endeavor. Thank you to my lab mates for your help and support throughout my PhD journey.

A heartfelt thank you to Dr. Sara Thomasy, your belief in my potential and your unwavering support have been instrumental in my success, I would not be where I am without you today. Thank you to Dr. Brian Leonard for their support during commencement. I would like to thank everyone involved with the Veterinary Scientist Training Program (VSTP) at UC Davis. Participating in this program has been an invaluable opportunity that shaped my career path and enabled me to achieve far more than I imagined.

To my partner in life, Dr. Luke Domulevicz, thank you for your constant love, support, and unwavering patience as I've worked towards earning my PhD and DVM. I know this is a long road but I could not do this without you! To our handicapable tribe of fur children — Mikey, Little Nubby, Mama Nubby, Peabs, Molly, Gir, Meow Meow, and Little Wing — thank you for the unconditional love and joy you bring every day.

Thank you to my mom, grandma, and the rest of my family for always loving and supporting me, for always encouraging me when times are tough, and for your patience as I continue my education…two more years to go!

TABLE OF CONTENTS

ABSTRACT

Struvite urolithiasis remains a significant clinical concern in companion animals, with recurrent cases frequently observed in both dogs and cats. While struvite stones from dogs have long been associated with bacterial urinary tract infections (UTIs), the microbial contribution to struvite formation remains largely uncharacterized. To address this gap, we hypothesized that struvite stones harbor a microbiome that actively contributes to ammonia production via urease activity. To test this, we applied shotgun metatranscriptomics to characterize the transcriptionally active microbial communities within struvite stones from dogs and cats.

Stones from dogs harbored a robustly active and complex microbial community with predominantly active taxa being *Staphylococcus*, *Enterococcus, Porphyromonas,* and *Bacillus*. Functional analyses revealed active expression of key pathways involved in ammonia production, derived from microbial metabolism via urease, the arginine deiminase (ADI) pathway, and deamination of nitrogenous substrates. Notably, *Staphylococcus* actively expressed urease, which accounted for 28.3% of its total ammonia-related gene expression with other metabolic routes being 17.5% (Arginine Deaminase Pathway) and 54.3% (deamination routes). Among the ammonia-producing pathways, deamination emerged as the dominant mechanism across all predominant taxa. Other constituents that enable struvite formation including phosphate mobilization and biofilm formation were actively expressed by multiple taxa. Unexpectedly, *Porphyromonas* was active in stones in dogs, which prompted the investigation of the oral/stone axis. This analysis found that many organisms were shared between the two sites, suggesting a plausible relationship between the oral cavity and the urinary stone

microbiome that warrants further investigation. Together, these findings highlight the functional complexity of the dog stone microbiome and suggest that polymicrobial metabolic activity plays a central role in shaping the biochemical conditions that drive struvite stone formation that in part was derived from organisms commonly associated with the oral cavity.

Struvite uroliths from cats have historically been considered sterile due to their propensity to yield negative results on standard aerobic urine cultures. To evaluate this long-standing assumption, we applied metatranscriptomics to examine the activity of the microbiome from these stones. We extended our analysis to compare the stone microbiome with those of both healthy and FCGS-affected oral cavities. Despite negative culture results in some cases, all feline stone samples exhibited robust microbial activity. We found that a complex and active microbiome existed within cat struvite stones that contained a diverse microbial membership. *Staphylococcus* and *Enterococcus* dominated the active members of the microbiome; however, a broad range of taxa were observed in the stone microbiome. Importantly, extensive microbial overlap was observed between the stone and oral microbiomes, with the stone community showing greater compositional similarity to that of FCGS-affected individuals than to the microbiome of the healthy cohort. Functional analyses demonstrated active expression of ammonia-generating, phosphate-liberating, and biofilm-formation pathways. Microbial expression of genes associated urease, the ADI pathway, and deamination of nitrogenous substrates, were observed in multiple genera. Urease gene expression occurred exclusively in *Staphylococcus* and comprised 34.1% of all ammonia-producing pathways expressed by this genus. Again, oral organisms were

found in the stone microbiome, including *Pasteurella multocida*, an organism associated with the oral cavity, was found in the struvite stones. Cat stones were not sterile and contained a very robust and active microbiome that produced ammonia from multiple biochemical routes. As with dogs, the oral/stone axis was observed with healthy and FCGS cats.

Collectively, this study found that struvite stones from two different animal species contained a robust microbiome that was active and produces transcripts the transduce ammonia production via multiple routes. These observations challenge the paradigm that struvite uroliths—especially in cats—are sterile and provide evidence that the microbial community is cooperating to produce multiple constituents in struvite formation. Both dog and cat stones harbored polymicrobial communities whose combined metabolic activity was responsive to the local biochemical environment to produce ammonia via multiple routes along with expression of genes needed for phosphate liberation and biofilm formation that collectively provided the substrates and pH needed for struvite formation. Additionally, these results strongly support the existence of an oral–stone microbial axis in both animal species. However, different oral bacteria are important in stones between dogs and cats. This work extends our understanding of microbial contributions to struvite stone formation, underscores the limitations of culture-based diagnostics in detecting relevant organisms, and expands the biochemical routes that can lead to struvite formation beyond urease alone.

Chapter 1:

Introduction

INTRODUCTION

In 1931, Blout noted that “from the very inception of veterinary science the importance of recognizing signs associated with the presence of urinary calculi has been regarded as paramount,” reflecting on the fact that similar conditions in humans have been addressed since antiquity (1). Urolithiasis, the formation of mineral concretions within the urinary tract, has been identified in over 925 animal species across terrestrial and aquatic environments (2,3). Near the turn of the 20th century, veterinarians described urolithiasis as a widespread disease for which a cure "was out of the question" (4). Today, urolithiasis remains a common and recurrent cause of morbidity, and occasionally mortality, in dogs and cats worldwide, with struvite ($NH_4MgPO_4 \cdot 6H_2O$) being one of the most common stone types (5,6). In both dogs and cats, struvite accounts for around half of all urolith submissions globally (7). Clinically, these stones can result in discomfort, inflammation, and in severe cases, life-threatening complications such as urethral obstruction, uremia, or renal failure (8,9).

For decades, standard aerobic urine culture (AUC) has been the clinical gold standard for detecting urinary pathogens in urine and stone specimens (10). Yet, discord between stone and urine AUC occurs commonly in both species (11,12). AUC utility is limited by its inability to detect slow-growing, fastidious, or anaerobic microbes, many of which may still contribute to stone pathogenesis (10,13). In dogs and humans, struvite stones have historically been associated with urinary tract infections (UTIs), particularly those involving urease-producing microorganisms (14). Common pathogens isolated from urine and stones in affected dogs include *Staphylococcus* spp., *Proteus* spp., *Klebsiella* spp., and *Enterococcus* spp. (11,14). In contrast, uroliths in cats have

long been considered sterile, as they rarely yield culturable organisms via AUCs (15,16). Bacterial growth is detected in approximately 10% of urine cultures associated with struvite cases in cats, compared to about 40% in dogs (5,6). More recent studies have reported culture-positive rates as high as 62% in cat struvite stones, further challenging the assumption of sterility for this animal (16), yet no study has definitively proven the role of microorganisms in this animal.

Struvite stones can recur postoperatively despite owner adherence to current recommended management practices (17). An estimated 21-35% of dogs with the disease will experience recurrence within the first 12 months following stone removal (14,17,18). While the recurrence rate of struvite urolithiasis in cats is not as well established, it has been reported to occur in 2.7–19.1% of cases, with an average time to recurrence of 20–29 months (19,20). This propensity for recurrence, coupled with the chronic pain and inflammation often associated with the condition, can significantly impact patient quality of life (21).

Medical dissolution remains the preferred first-line treatment for struvite urolithiasis in dogs and cats (15,22). In dogs, dissolution diets combined with antibiotics are commonly prescribed, though there are no definitive guidelines on the timing or duration of antimicrobial therapy (22). Despite these interventions, struvite urolithiasis remains a persistent concern in dogs, and its incidence has increased in cats over recent decades, suggesting that current prevention strategies may be insufficient for long-term prevention (5,6).

Investigation into the pathogenesis of struvite stones can be distilled into three key questions, as framed by Das and colleagues (23): 1) What types of stones form in

the presence of bacteria? 2) What types of bacteria promote stone formation? and 3) What are the biochemical mechanisms underlying infectious stone formation? Although it has recently been proposed that struvite stones may result from multiple microbially encoded metabolic pathways (24), investigation beyond urease production remains underexplored but may hold significant untapped potential for advancing our understanding of stone pathogenesis and subsequent treatment options.

While urease activity is widely recognized as an important source of ammonia in struvite stone formation, even weakly ureolytic or non-ureolytic organisms have been shown to induce struvite precipitation in sterile urine, supporting the role of urease-limited and urease-independent mechanisms in disease pathogenesis (25). Among these, amino acid deamination, was proposed nearly a century ago as a contributor to urinary ammonia in cats (1), but has received comparatively little attention in the context of struvite stone pathogenesis. Additional microbial pathways, including the arginine deiminase (ADI) pathway and dissimilatory nitrate reduction to ammonia (DNRA), are also well-characterized routes of ammonia production (26–28). Despite their widely known existence in bacteria these biochemical pathways remain unexplored in the context of struvite urolithiasis. A deeper understanding of these mechanisms is essential for understanding microbial contribution to struvite formation.

The limitations of culture-based diagnostics remain a major barrier to progress in this area. Although AUC is the most common diagnostic tool used for identifying pathogens in urine and uroliths, it likely underrepresents the microbial diversity present in these samples (10,22). Across multiple studies, 15–70% of struvite uroliths in humans yielded culturable organisms (29). This wide range is likely due, in part, to the fact that

AUC protocols are optimized for detecting known urinary tract infection (UTI) pathogens and do not provide the environment for many other organisms that contribute to struvite stone formation to grow in a clinical laboratory (10). A culture-independent approach can provide an alternative method to characterize the microbial communities within struvite uroliths.

Relative to human medicine, minimal work has been directed at urolithiasis in dogs and cats. Use of culture-dependent methods is largely focused on 16s rRNA gene sequencing that provides general information (30–32). Unfortunately, this amplicon-based method does not provide consistent taxonomic resolution or biochemical pathway information, leaving a large gap in knowledge and understanding of the contribution of the microbiome to struvite formation (33–35). Advances in shotgun RNA-sequencing (metatranscriptomics) allows simultaneous identification of microbial taxa and their biochemical functions from the same sample with high accuracy (35). This technique produces a consistent level of taxonomic and metabolic information, allowing for reliable bacterial detection, identification, and relative activity across the entire microbiome. Using ultra-deep metatranscriptomic sequencing in struvite stones can provide bacterial strain identification for comparison between body sites, but also bacterial functional regulation for pathway determination of ammonia production (36,37). This improvement in resolution and accuracy over amplicon approaches will allow for more accurate identification of microbes, specifically those that are actively participating in struvite formation.

Furthermore, the functional profiles of microbes associated with struvite uroliths have not been investigated, particularly in dogs and cats, for their role in struvite growth

in vivo, which limits treatment options. The clinical significance of struvite urolithiasis, combined with advances in analytical tools, warrants deeper investigation into alternative microbial pathways that generate precursors required for struvite precipitation. Better understanding the role of the microbiome in struvite urolith formation can help inform future treatment options by applying what we know about microbial mechanisms to possible clinical interventions.

Beyond the urinary tract, the oral cavity has emerged as a potential reservoir for microbes implicated in diseases at distant organ sites including atherosclerosis, Alzheimer's disease, pancreatic cancer, colon cancer and chronic kidney disease (38,39) Periodontal disease is common in both humans and companion animals, with prevalence rates exceeding 60–80% in dogs and cats (40) . Previous studies have shown that animals with periodontitis exhibit increased bacterial translocation, which is associated with a higher risk of urinary stone formation (41,42). Oral bacteria can translocate to distant organ sites when epithelial barriers are disrupted, a process linked to both local pathology and systemic physiological changes (41,43,44). Pregnancy is known to increase oral inflammation and impair endothelial function in both dogs and humans, conditions that could promote the movement of oral microbes into the bloodstream (45–47). To explore potential links between oral and urinary microbiomes, struvite stones were compared with oral samples from healthy, pregnant dams. While pregnancy was not a focus of subsequent analysis, it provided a physiologically relevant context in which microbial translocation from the oral cavity may be more pronounced, supporting their use as a comparison group.

In cats, feline chronic gingivostomatitis (FCGS) is a severe oral inflammatory condition that disrupts mucosal integrity and alters local immune responses, making microbial translocation more likely (36,37,48). It is thought that oral organisms can enter the bloodstream by making products that degrade endothelial tight junction proteins, increasing vascular permeability (49). Histopathologic evidence from FCGS-affected cats indicates disruption of epithelial integrity and local immune dysregulation, which may facilitate microbial dissemination out of the oral cavity and into circulation (42,48). Cats with FCGS exhibit altered oral microbiomes with elevated levels of Gram-negative and anaerobic bacteria, some of which are capable of ammonia production that is fundamental to struvite formation (36,41,48,50,51). This aspect of oral bacteria translocation is virtually unexplored in stone formation leaving a gap in understanding if oral health impacts risk of stone formation. By comparing the oral microbiomes of healthy and FCGS-affected cats may help determine whether oral disease increases specific microorganisms between the oral cavity and the urinary tract that may contribute to struvite formation.

This dissertation investigates microbial contributions to struvite urolithiasis in companion animals through a combination of literature review and metatranscriptomic studies. To address existing gaps in our understanding of the microbial role in struvite stone pathogenesis, shotgun metatranscriptomics was applied to comprehensively characterize the transcriptionally active microbial communities within struvite stones removed from dogs and cats. Focus was given to functional pathways involved in ammonia production, phosphate mobilization, and biofilm formation. By comparing microbial profiles in stones to those in the oral cavity, this work also explored the

potential for an oral–urinary microbial axis that may contribute to stone formation and recurrence. Chapter 1 provides a comprehensive overview of struvite urolithiasis in dogs and cats beginning with a historical context and draws parallels to human struvite urolithiasis to highlight key aspects of microbial involvement, urinary pathophysiology, diagnostic limitations, and treatment strategies. Chapter 2 examines struvite stones in dogs using metatranscriptomics to characterize the transcriptionally active microbiota within struvite stones and investigate functional pathways relevant to stone pathogenesis. Taxonomic comparisons were made to the oral microbiome of clinically healthy dogs. Chapter 3 extends this approach and study methods to cats for evaluation microbial taxa and activity within feline struvite stones, with taxonomic comparisons to both healthy and FCGS-affected oral microbiomes. Particular attention was given to the relationship between oral disease and stone composition.

Together, these studies offer novel insights into the microbial ecology of struvite stones and reveal previously underappreciated functional pathways that may contribute to stone formation and recurrence and defines the relative proportion of biochemical routes that produce ammonia from multiple taxa. This work advances our understanding of microbial pathogenesis in struvite urolithiasis and contributes new knowledge to support the development of future diagnostic and therapeutic strategies in veterinary medicine.

References

1. Blout WP. Urinary Calculi. The Veterinary Journal. 1931 Dec;87(12):561–76.

2. Robinson MR, Norris RD, Sur RL, Preminger GM. Urolithiasis: Not Just a 2-Legged Animal Disease. Vol. 179, Journal of Urology. 2008. p. 46–52.

3. Osborne CA, Albasan H, Lulich JP, Nwaokorie E, Koehler LA, Ulrich LK. Quantitative Analysis of 4468 Uroliths Retrieved from Farm Animals, Exotic Species, and Wildlife Submitted to the Minnesota Urolith Center: 1981 to 2007. Vol. 39, Veterinary Clinics of North America - Small Animal Practice. 2009. p. 65–78.

4. Perry JF. Diseases of The Urinary Organs. In: Dogs Their Management and Treatment in Disease: A Study of the Theory and Practice of Canine Medicine. 2nd ed. J. Loring Thayer; 1891. p. 89–104.

5. Kopecny L, Palm CA, Segev G, Westropp JL. Urolithiasis in dogs: Evaluation of trends in urolith composition and risk factors (2006-2018). Journal of Veterinary Internal Medicine. 2021 May;35(3):1406–15.

6. Kopecny L, Palm CA, Segev G, Larsen JA, Westropp JL. Urolithiasis in cats: Evaluation of trends in urolith composition and risk factors (2005-2018). Journal of Veterinary Internal Medicine. 2021 May;35(3):1397.

7. Center MU. 2023 Minnesota Urolith Center Global Data [Internet]. University of Minnesota; 2024 Feb. Available from: z.umn.edu/2023GlobalUrolith

8. Eyral V, Pichard D, Mariaud V, Manassero M, Maurey C. Struvite ureterolithiasis associated with ureolytic bacterial pyelonephritis in a cat. Journal of Feline Medicine and Surgery Open Reports. 2025 Jan;11(1).

9. Defarges A, Evason M, Dunn M, Berent A. Urolithiasis in Small Animals. In: Clinical Small Animal Internal Medicine. Wiley; 2020. p. 1123–56.

10. Perry LA, Kass PH, Johnson DL, Ruby AL, Shiraki R, Westropp JL. Evaluation of culture techniques and bacterial cultures from uroliths. Journal of Veterinary Diagnostic Investigation. 2013 Mar;25(2):199–202.

11. Legaria MC, Barberis C, Famiglietti A, Gregorio SD, Stecher D, Rodriguez CH, et al. Urinary tract infection caused by anaerobic bacteria. Utility of anaerobic urine culture. Vol. 78, Anaerobe. Academic Press; 2022.

12. Detkalaya O, Kornkasem S, Vichukit K, Suksamranthaweerat M, Aponrat P. Association between uropathogens and the occurrence of magnesium ammonium phosphate and calcium oxalate in cats with urolithiasis: a retrospective study (2016-2021). Journal of feline medicine and surgery. 2025 Apr;27(4).

13. Osborne CA, Lulich JP, Polzin DJ, Allen TA, Kruger JM, Bartges JW, et al. Medical Dissolution and Prevention of Canine Struvite Urolithiasis- Twenty Years of Experience. Vet Clin North Am Small Anim Pract. 1999 Jan;29(1):73–111.

14. Ling GV. Urinary Stone Disease. In: Lower Urinary Tract Diseases of Dogs and Cats: Diagnosis, Medical Management, Prevention [Internet]. Mosby-Year Book, Inc.; 1995. p. 144–77. Available from: https://uc-nrlf.caiasoft.com/reports/caiasoftBRW.php

15. Osborne CA, Klausner JS, Polzin DJ, Griffith DP. Etiopathogenesis of canine struvite urolithiasis. Am J Vet Res. 1986 Jan;16(1):67–86.

16. Westropp JL. Feline Lower Urinary Tract Disorders: A Comprehensive, Tailored Management Approach. In VMX Small Animal Proceedings, Nephrology & Urology; 2020. p. 483–8. Available from: https://cabidigitallibrary.org

17. Brown NO, Parks JL, Greene RW. Recurrence of Canine Uroliths 1974. Journal of the American Veterinary Medical Association. 1977 Feb;170(4):419–22.

18. Jummai T, Boonyayatra S, Tangjitjaroen W, Akatvipat A. View of Factors affecting the recurrence of canine urolithiasis in the lower urinary tract after surgical removal. Veterinary Integrative Sciences. 2018;3(17):197–210.

19. Albasan H, Osborne CA, Lulich JP, Lekcharoensuk C, Koehler LA, Ulrich LK, et al. Rate and frequency of recurrence of uroliths after an initial ammonium urate, calcium oxalate, or struvite urolith in cats. Scientific Reports JAVMA. 2009 Dec;235(12).

20. Bohonowych RO, Parks JL, Greene RW. Cystic Calculi in Cats in a Hospital Population. Journal of the American Veterinary Medical Association. 1978;73(3):301–3.

21. Cooper E, Scansen BA. Obstructive Uropathy. In: Clinical Small Animal Internal Medicine [Internet]. Wiley; 2020. p. 1109–22. Available from: https://onlinelibrary.wiley.com/doi/10.1002/9781119501237.ch122

22. Westropp JL, Sykes JE. Infections of the Genitourinary Tract. In: Sykes JE, editor. Greene's Infectious Diseases of the Dog and Cat. 5th ed. Elsevier; 2023. p. 1669–87.

23. Das P, Gupta G, Velu V, Awasthi R, Dua K, Malipeddi H. Formation of struvite urinary stones and approaches towards the inhibition—A review. Vol. 96, Biomedicine and Pharmacotherapy. Elsevier Masson SAS; 2017. p. 361–70.

24. Wallace B, Chmiel JA, Al KF, Bjazevic J, Burton JP, Goldberg HA, et al. The Role of Urinary Modulators in the Development of Infectious Kidney Stones. Journal of Endourology. 2023 Mar;37(3):358–66.

25. Rivadeneyra MA, Gutierrez-Calderó A, Rivadeneyra AM, Ramos-Cormenzana A. A Study of Struvite Precipitation and Urease Activity in Bacteria Isolated from Patients with Urinary Infections and Their Possible Involvement in the Formation of Renal Calculi. Urol Int. 1999 Sep;63:188–92.

26. Abdelal AT. Arginine Catabolism by Microorganisms. Annual Review of Microbiology. 1979 Oct;33:139–68.

27. Zuniga M, Perez G, Gonzalez-Candelas F. Evolution of arginine deiminase (ADI) pathway genes. Molecular Phylogenetics and Evolution. 2002 May;25:429–44.

28. Wiebe MA, Brannon JR, Steiner BD, Bamidele A, Schrimpe-Rutledge AC, Codreanu SG, et al. Serine Deamination Is a New Acid Tolerance Mechanism Observed in Uropathogenic Escherichia coli. mBio. 2022 Dec;13(6).

29. Schwaderer AL, Wolfe AJ. The association between bacteria and urinary stones. Annals of Translational Medicine [Internet]. 2017 Jan;5(2). Available from: /pmc/articles/PMC5300853/ /pmc/articles/PMC5300853/?report=abstract https://www.ncbi.nlm.nih.gov/pmc/articles/PMC5300853/

30. Melgarejo T, Oakley BB, Krumbeck JA, Tang S, Krantz A, Linde A. Assessment of bacterial and fungal populations in urine from clinically healthy dogs using next-generation sequencing. Journal of Veterinary Internal Medicine. 2021 May;35(3):1416–26.

31. Burton EN, Cohn LA, Reinero CN, Rindt H, Moore SG, Ericsson AC. Characterization of the urinary microbiome in healthy dogs. PLoS ONE. 2017 May;12(5).

32. Alasmar M, El-Khodery S, Youssef M, El-Ashker M. A narrative review of current perspectives on urinary tract infections in dogs and cats. Vol. 2023, CAB Reviews: Perspectives in Agriculture, Veterinary Science, Nutrition and Natural Resources. CABI International; 2023.

33. Matchado MS, Rühlemann M, Reitmeier S, Kacprowski T, Frost F, Haller D, et al. On the limits of 16S rRNA gene-based metagenome prediction and functional profiling. Microbial Genomics. 2024 Feb;10(2).

34. O'Callaghan JL, Willner D, Buttini M, Huygens F, Pelzer ES. Limitations of 16S rRNA Gene Sequencing to Characterize Lactobacillus Species in the Upper Genital Tract. Frontiers in Cell and Developmental Biology. 2021 Jul;9.

35. Aguiar-Pulido V, Huang W, Suarez-Ulloa V, Cickovski T, Mathee K, Narasimhan G. Metagenomics, metatranscriptomics, and metabolomics approaches for microbiome analysis. Vol. 12, Evolutionary Bioinformatics. Libertas Academica Ltd.; 2016. p. 5–16.

36. Shaw CA, Soltero-Rivera M, Profeta R, Weimer BC. Case Report: Inflammation-Driven Species-Level Shifts in the Oral Microbiome of Refractory Feline Chronic Gingivostomatitis. Bacteria. 2025 Mar;4(1):1–0.

37. Shaw CA, Soltero-Rivera M, Profeta R, Weimer BC. Case Report: Shift from Aggressive Periodontitis to Feline Chronic Gingivostomatitis Is Linked to Increased Microbial Diversity. Pathogens. 2025 Mar;14(3).

38. Lim MY, Kim JH, Nam YD. Oral microbiome correlates with selected clinical biomarkers in individuals with no significant systemic disease. Frontiers in Cellular and Infection Microbiology. 2023;13.

39. Fu D, Shu X, Zhou G, Ji M, Liao G, Zou L. Connection between oral health and chronic diseases. MedComm. 2025 Jan;6(1):e70052.

40. Logan EI. Dietary Influences on Periodontal Health in Dogs and Cats. Vol. 36, Veterinary Clinics of North America - Small Animal Practice. 2006. p. 1385–401.

41. Lee DB, Verstraete FJM, Arzi B. An Update on Feline Chronic Gingivostomatitis. Veterinary Clinics of North America - Small Animal Practice. 2020 Sep;50(5):973–82.

42. Vapniarsky N, Simpson DL, Arzi B, Taechangam N, Walker NJ, Garrity C, et al. Histological, Immunological, and Genetic Analysis of Feline Chronic Gingivostomatitis. Frontiers in Veterinary Science. 2020 Jun;7.

43. Sudhakara P, Gupta A, Bhardwaj A, Wilson A. Oral dysbiotic communities and their implications in systemic diseases. Dentistry Journal. 2018 Jun;6(2).

44. Chopra A, Franco-Duarte R, Rajagopal A, Choowong P, Soares P, Rito T, et al. Exploring the presence of oral bacteria in non-oral sites of patients with cardiovascular diseases using whole metagenomic data. Scientific Reports. 2024 Dec;14(1).

45. Jennifer R, Williana B, Chad L, Richard W, Ben P. Evaluation of Gingivitis in Pregnant Beagle Dogs. Journal of Veterinary Dentistry. 2019 Sep;36(3):179–85.

46. Kornacki J, Gutaj P, Kalantarova A, Sibiak R, Jankowski M, Wender-Ozegowska E. Endothelial dysfunction in pregnancy complications. Biomedicines. 2021 Dec;9(12).

47. Marcickiewicz J, Jamka M, Walkowiak J. A Potential Link Between Oral Microbiota and Female Reproductive Health. Vol. 13, Microorganisms. Multidisciplinary Digital Publishing Institute (MDPI); 2025.

48. Soltero-Rivera M, Shaw C, Arzi B, Lommer M, Weimer BC. Feline Chronic Gingivostomatitis Diagnosis and Treatment through Transcriptomic Insights. Pathogens. 2024 Mar;13(3).

49. Li Q, Ouyang X, Lin J. The impact of periodontitis on vascular endothelial dysfunction. Vol. 12, Frontiers in Cellular and Infection Microbiology. Frontiers Media S.A.; 2022.

50. Dolieslager SMJ, Riggio MP, Lennon A, Lappin DF, Johnston N, Taylor D, et al. Identification of bacteria associated with feline chronic gingivostomatitis using culture-dependent and culture-independent methods. Veterinary Microbiology. 2011 Feb;148(1):93–8.

51. Rodrigues MX, Bicalho RC, Fiani N, Lima SF, Peralta S. The subgingival microbial community of feline periodontitis and gingivostomatitis: characterization and comparison between diseased and healthy cats. Scientific Reports. 2019 Dec;9(1).

Chapter 2:

Literature Review: Microbial Contributions to Struvite Urolithiasis

The Urinary Microbiome and its Role in Struvite Urolithiasis: A Disease that Spans Human and Veterinary Medicine

Ashleigh M. Flores[1], Jodi L. Westropp[2*] Bart C. Weimer[1*]

[1]University of California, Davis, School of Veterinary Medicine, Dept. of Population Health and Reproduction, 100K Pathogen Genome Project, Davis, CA, USA

[2]University of California, School of Veterinary Medicine, Dept. of Medicine and Epidemiology, Davis, CA, USA

***Correspondence:**

bcweimer@ucdavis.edu

jlwestropp@ucdavis.edu

Keywords: urolith, urinary stone, bladder stone, calculi

Abstract

Struvite urolithiasis is a common and clinically important disease in both humans and companion animals, particularly dogs and cats. Unlike cats, in dogs, urease-producing bacteria, primary Staphylococcus spp. are the primary cause for struvite formation, while struvite in cats is thought be due to a number of non-infectious etiologies such as a diet and genetics. Emerging research suggests that additional microbial processes and community interactions might also contribute to struvite development. This review explores the evolving understanding of the urinary microbiome's role in struvite stone formation, including alternative pathways of ammonia production, phosphate release, and the influence of bacterial biofilms. It also discusses limitations of standard diagnostic methods and highlights how advanced sequencing technologies are reshaping our knowledge of microbial involvement in urinary tract health. The promise of next-generation sequencing and metatranscriptomics to better characterize the urinary microbiome offers a new avenue to expand upon current knowledge in the field. A deeper understanding of microbial metabolism and community interactions might inform novel strategies for prevention, diagnosis, and treatment of struvite urolithiasis in both human and veterinary medicine

Introduction

Pathophysiology and epidemiology of struvite formation

Urolithiasis has remained a persistent health concern in humans and animals for centuries (1,2). More than 925 mammalian and non-mammalian species from terrestrial and aquatic habitats develop struvite urolithiasis (2,3). Struvite comprises 10–15% of human stones in the U.S. and is associated with substantial clinical and economic challenges (4,5). Struvite urolithiasis is reported in dogs and cats and is one of the most common types of uroliths submitted to urinary stone analysis laboratories from these species (6,7). In humans recurrence a 10% recurrence rate is reported, however, this rate increases to 85% if residual stone fragments remain following stone removal, presumably because these fragments act as a nidus for infection (4,5). Struvite uroliths recur in an estimated 21–35% of dogs within a year of removal (8–10). In cats, reported recurrence rates range from 2.7–19.1%, with an average interval of 20–29 months (8,9). In cats, reported recurrence rates range from 2.7–19.1%, with an average interval of 20–29 months (11,12). Collectively, struvite stones present a significant risk to the health and well-being of humans, dogs and cats.

While most struvite uroliths in dogs and cats form in the bladder, nephroliths (so called ‘staghorn’ calculi) and ureteroliths are more common in humans (13) but have also been reported in dogs (14). Struvite ureterolithiasis is not reported in the cat. Reported risk factors include being a small or toy breed dog and female sex (15). In cats, Persian and Himalayan breeds are over-represented, and either sex can be affected. In dogs, no clear breed associations have been identified, though some studies report overrepresentation of small breeds such as mixed breeds, Shih Tzus, and

Bichon Frisés (15,16). Dogs and cats with cystolithiasis usually display lower urinary signs such as stranguria, pollakiuria, hematuria, and potentially urethral obstruction (17–19). Typically dogs and cats with lower urinary tract urolithiasis lack systemic signs, but those with kidney or ureteral uroliths might present with signs associated with acute kidney injury, especially if the urolith is causing partial or complete ureteral obstruction (17,19–21). Signs such as abdominal pain, lethargy, anorexia or an elevated body temperature could be present when the dog has concurrent pyelonephritis (17). In cats and dogs, complete ureteral or urethral obstruction can cause serious illness in as little as 1-2 days with mortality in just 3-5 days (17). Even when obstruction has not occurred, stone removal is important as retention can predispose dogs (and possibly cats) to recurrent bacteriuria and further struvite stone formation (17). Despite the differences in anatomic location, the underlying pathophysiology of struvite urolithiasis is similar in dogs and humans and possibly cats (2).

Urease-producing bacteria are commonly associated with struvite crystallization and subsequent stone formation in both *in vitro* and *in vivo* settings (22–27) in dogs. Some researchers have even proposed that bacterial urease production might be the sole mechanism by which bacteria contribute to the formation of struvite stones (28–32) in dogs and humans. Urease catalyzes the hydrolysis of urea, a process that generates high concentrations of ammonia and subsequent alkalinization of the urine, oftentimes pH>8, creating favorable conditions for the precipitation of struvite ($NH_4MgPO_4 \cdot 6H_2O$) (33). However, the most common urease-producing bacteria such as *Staphylococcus* spp. in dogs and *Proteus* spp. in humans (8), are not always identified in urine or urolith cultures from affected individuals (34). Moreover, in humans with urinary tract infections

(UTI) with a urease-producing bacteria, fewer than 20% develop struvite stones, suggesting that urease alone is not sufficient for stone formation and that additional biochemical pathways might also contribute to elevated urinary ammonia levels and subsequent struvite crystallization (35,36).

In contrast to dogs and humans, bacteria are rarely cultured from cats with struvite urolithiasis, leaving the mechanisms underlying struvite formation in this species poorly understood (37,38). Struvite urolithiasis in this species is likely multifactorial, involving genetic, environmental, and dietary factors (7,39,40). However, the proportion of struvite-containing uroliths in cats has increased significantly in recent decades (7). While bacteria are less commonly cultured from struvite stones in cats (10.9%) compared to dogs (41.8%) (6,7),and urease-producing organisms are also less frequent, other microbial pathways that generate ammonia might contribute to struvite lithogenicity. However, these mechanisms have not been well investigated (41). Enhancing our understanding of these pathways could lead to improved clinical diagnostics and more effective treatment strategies for both cats and dogs. The strong emphasis that has been placed on bacterial urease production in relation to struvite stone formation has contributed to a narrow perspective on the disease's etiology within the field, despite the occurrence of the disease across species. It is becoming increasingly apparent that the traditional urease-producing bacteria are not the only contributors to the disease process and the formation of stones (41,42). Other well-established bacterial metabolic pathways that produce ammonia, such as protein/amino-acid deamination and dissimilatory nitrate reduction to ammonia (DNRA)

have not been investigated for their role in struvite formation in humans and animals and should be considered with regard to this disease (43–45).

Standard Diagnostic Approach for Struvite Urolithiasis in dogs, cats and humans

Urinalysis is a valuable resource that can offer clinicians substantial insights into a patient's urinary and systemic health (46,47). In cases of suspected struvite urolithiasis in dogs and cats, urine specimens, including urinalysis, sediment examination, and aerobic bacterial urine culture are recommended as first-line diagnostics to assist with identifying the mineral content present in the stone prior to removal (48–50). Cystocentesis for urine collection is considered the gold standard in veterinary medicine (51–53). Aerobic bacterial urine cultures with susceptibility testing are needed to identify the presence or absence of common uropathogens as well as to guide treatment (54). This information, combined with imaging studies, usually digital radiography, and occasionally ultrasonography, are needed to diagnose and treat dogs and cats with struvite urolithiasis (19). Twenty-four-hour urine collections are evaluated in some humans to assess potential risk factors for struvite urolithiasis, but this diagnostic is not performed in client owned dogs and cats (55).

After a stone is removed, polarized light microscopy and infrared spectroscopy are the recommended diagnostic tests to provide a layer-by-layer mineral analysis of the urolith (6). Aerobic bacterial cultures from stone specimens removed from humans and dogs are not usually indicated, especially if a urine culture yielded bacterial growth and clinical signs resolved after stone dissolution/removal (56–58). However, these data might help determine other associated pathogens and therefore expand our knowledge

about the pathophysiology of struvite formation, particularly when urine cultures are negative (42).

While the diagnostic approach for dogs and cats with suspected struvite urolithiasis has not changed over the years, recurrence rates remain static (6). Though we recognize these traditional culture-based methods have been valuable in the past, they center around the idea of single organism causality based upon taxonomic identification of organisms. The selective nature of this method likely underestimates the number of organisms in the uroliths, providing an incomplete and potentially misleading picture of the true composition and diversity of the microbes present (56,59,60).

To help further address limitations of aerobic UC, techniques like Enhanced Quantitative Urine Culture (EQUC) were created. First described in 2014, this method employs a broad range of growth media, culture conditions, and incubation times (54). It allows for detection of slow-growing, fastidious, anaerobic, or those bacteria not commonly associated with UTIs (61). Aerobic UC failed to detect 67% of uropathogens relative to EQUCs and a 90% false-negative rate for all bacterial (54,62). This raises the question of whether other organisms that do not grow well using aerobic UCs conditions could be causal (56,59,61,63). Despite its advantages, EQUC is time and resource intensive and is not offered in most clinical settings outside of large, research hospitals (63).

The Chemistry of Struvite Formation and The Role of Urea

Struvite is comprised of Mg^{2+}, NH_3, and PO_4^{3-} in an equimolar (1:1:1) ratio with a chemical formula of: $Mg^{2+} + NH_3 + PO_4^{3-} + 6H_2O \rightleftharpoons Mg\,NH_4PO_4 \cdot 6\,H_2O$ (64), all of which

are normal constituents of urine (32). However, when the concentration of the ions increases and the urine becomes supersaturated, precipitation of struvite can occur with a change in the pH≥7.2 (65). While supersaturation of mineral precursors is important, supersaturated urine is also observed in non-stone forming dogs and cats, suggesting that additional factors are needed for struvite crystal formation (65).

Urine alkalinity (pH≥7.2) is one of the principle chemical forces that promotes struvite formation (5). Dissolution can occur in stable urine conditions with an approximate urine pH ≤6.3 (66). Urease-producing bacteria aid in increasing urine alkalinity that potentiates the precipitation of magnesium, ammonium, and phosphate (67). In humans, normal urinary pH tends to be slightly acidic, pH=5.5-7.5, similar to the normal urinary pH in the dog and cat, 7.0-7.5, and 6.3-7.0, respectively (68–70). Along with urinary pH, other environmental factors such as urine osmolality, oxygen levels, and nutrient availability significantly influence microbial colonization (71). However, how such factors influence struvite formation in vivo is not well studied or understood.

Although the in vivo effects of these environmental factors on struvite formation remain unclear, they might contribute to the structured growth of the stone. As a struvite stone grows, concentric laminations develop, radiating from a central core (72). The crystals within the laminations of a struvite stone act as a scaffolding, held together by a biofilm of exopolysaccharide produced by the microbiome and where microbial inhabitants reside in a complex community (22–24,27,73). In the late 1980s and early 1990s, Nickel, McLean, and colleagues conducted revolutionary research that depicted bacterial microcolonies within struvite stones using scanning electron microscopy (SEM) and transmission electron microscopy (TEM) (22–24,27). In 2021, Saw et. al (74)

employed multiple microscopy technique, including brightfield, polarization, confocal, super-resolution autofluorescence, and Raman microscopy, to demonstrate the presence of microbes embedded within various urinary stone types, including struvite, as components of the biofilm matrix integral to the stone structure. The relationship between bacteria and the stones is irrefutable based on these microscopy techniques, though the exact biochemical mechanisms by which they contribute to biofilm and stone formation remains unclear.

The Role of Bacterial Biofilms in Struvite Stone Formation

Biofilm formation is a complex and multifaceted process that plays a crucial role in the development of struvite stones (Fig. 1) (23,24). This “glue-like” substance forms when bacterial cells produce exopolysaccharide material and attach irreversibly to a surface, such as the uroepithelium, or to each other, and encase themselves in the polysaccharide matrix (75,76). Compared to planktonic bacteria, those within the biofilm exhibit phenotypic differences in gene expression, growth rate, and nutrient sharing (75,76). Additionally, organisms like *Staphylococcus* spp., *Proteus* spp., and *Klebsiella* spp. can produce exopolysaccharides as part of metabolic changes and virulence shifts that facilitate bacterial adherence to the uroepithelium and promote biofilm formation (77–81). *Klebsiella* spp. are known to form robust biofilms, in part due to their ability to produce large quantities of extracellular polysaccharides, which are upregulated during biofilm development (78,79).

The biofilm's complex matrix helps with bacterial adherence, communication, and coordination of metabolic activities, all contributing to biofilm formation and persistence

in a structure that changes metabolism, nutrient sharing (e.g. cross-feeding), virulence, and antibiotic resistance (75,82). Bacteria benefit from the biofilm they produce as it provides enhanced protection against the host immune response and antimicrobials, which can lead to persistent infections that are non-responsive to treatment (75,82). Struvite crystals can further stabilize and protect the biofilm, increasing bacterial resistance (83). This defense mechanism is so effective that organisms within the stone can remain viable for years (8).

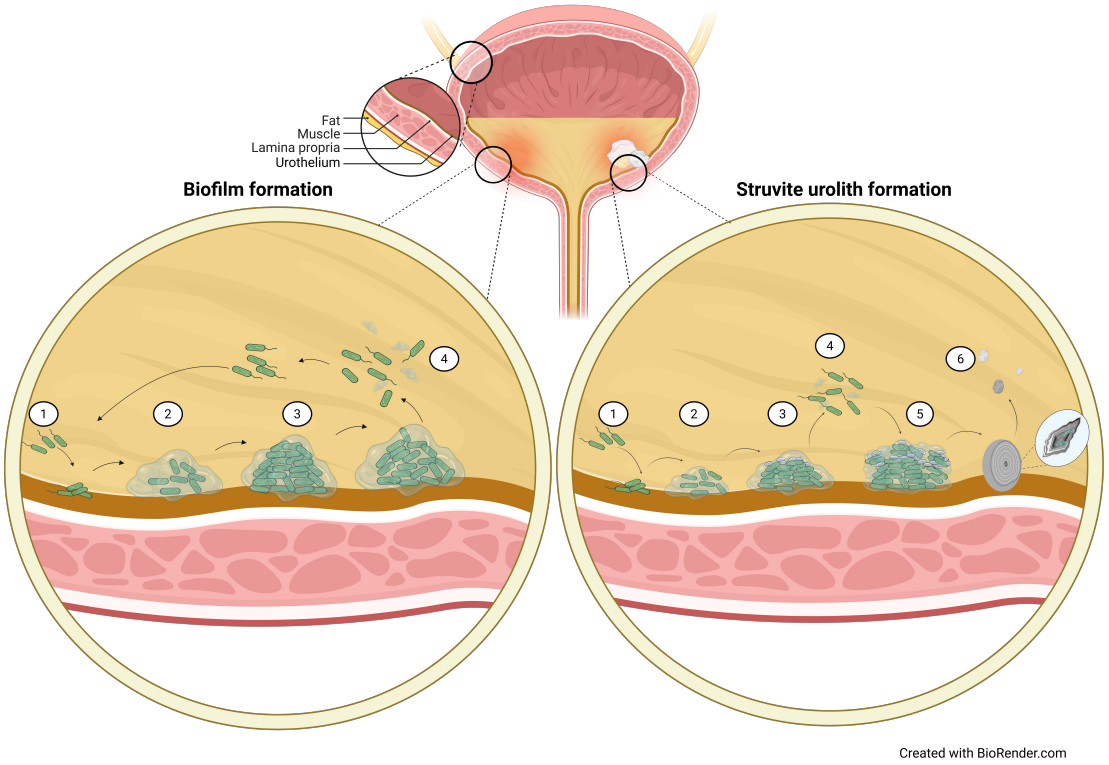

Figure 1. The process of biofilm formation and the process of biofilm formation in the context of struvite urolith formation. 1) Bacteria attachment: Biofilm formation involves bacterial adhesion and increasing urinary pH 2) Microcolony formation: The formation of microcolonies and the excretion of extracellular polysaccharides (EPS) that protect the bacteria from the host immune response and antimicrobials, 3) Maturation & crystal formation: Bacteria and crystals become encase as excretion of EPS continues with microcolony growth and crystal formation occurs within the EPS and in the surrounding urine 4) Dispersal of planktonic bacteria: Through methods not completely

understood, some of the bacteria detach from the microcolonies and become planktonic to form additional microcolonies. 5) Planktonic bacteria attach to crystals: With stone formation, planktonic bacteria attach to the surface of pre-existing crystals and form more microcolonies formation which potentiate EPS production and crystal formation. 6) Urolith formation: The cycle repeats to form a struvite stone that grows with each cycle. The process is repeated until a mature biofilm forms with the bacteria encased in biofilm within the stone, on stone surfaces, the urothelium, and the urinary tract. Pieces of biofilm can also act as a nidus for additional stones to form.

Microbial Metabolism and Biofilm Formation in Struvite Stone Pathogenesis

In addition to forming biofilms, uropathogenic bacteria express a range of virulence factors that contribute to struvite stone formation. These include enzymes such as phosphatases, proteases, nucleases, and lipases that degrade host tissues and organic substrates, releasing ions that can promote struvite crystallization (80,84,85). Adhesins and fimbriae further facilitate bacterial attachment to the uroepithelium, and many of these surface structures are upregulated during biofilm formation (75). For example, *Proteus mirabilis* expresses multiple biofilm-associated factors, including fimbriae, capsular polysaccharide, and a unique swarming motility that enhances its ability to colonize the urinary tract (75,80,86). Swarming enables bacterial migration across surfaces, while fimbriae and the capsule promote adhesion and biofilm development. Similarly, a recent study of *Staphylococcus aureus* isolates from struvite stones identified widespread presence of the pore-forming toxin hla (93.3%, 28/30 isolates) and the fibronectin-binding adhesin fnbA (73.3%, 22/30 isolates), both of which are associated with epithelial adherence and biofilm formation (87). These virulence mechanisms, often induced under biofilm conditions, work synergistically with stress response pathways to support bacterial persistence at the epithelial surface.

Urease Negative Bacteria in Struvite

A retrospective, multi-institutional study confirmed that while *Proteus* remained a common bacterial urinary isolate in humans with struvite stones, *E. coli* and *Enterococcus* were also frequently cultured (88), suggesting struvite stones might be also associated with other uropathogens (88). An additional study also found *P. mirabilis* to be the most isolated urease producer identified in the struvite stones removed from humans (42). However, nearly half of all of these struvite stone samples (47.1%, 8/17) contained urease-negative organisms. Furthermore, *E. coli* was found in 29.4% (5/17) of all of these specimens even though it was estimated that 99% of all *E. coli* strains are urease negative (42,67). The authors also found that 45.2% of struvite stones in humans yielded no bacterial growth from the stone, highlighting the need for culture-independent diagnostics. This study suggests the diverse urinary microbiome includes previously overlooked organisms that might contribute to struvite stone formation, including those that do not produce urease (42).

Urinary microbiome: Ammonia Production Beyond Urease?

While urease has long been recognized as a potent microbial virulence factor in urolithiasis, producing two moles of ammonia and one mole of CO_2 per mole of urea hydrolyzed, other microbial pathways can also contribute substantially to the ammonia pool (33,41) Microbes have urease-independent ammonia-generating pathways including amino acid deamination, dissimilatory nitrate reduction to ammonia (DNRA), and the arginine deiminase (ADI) pathway (44,89–91). Given that many uropathogens

exist in biofilms and that struvite formation is strongly influenced by urine alkalinization, it is essential to consider that these alternative microbial metabolic routes, beyond urease, might also contribute to struvite formation within the urinary tract.

The DNRA and the ADI pathway each produce one mole of ammonia per mole of substrate (nitrate or arginine, respectively) (90,92). DNRA is an anaerobic process in which microbes reduce nitrate and nitrite to ammonia (90). It is facilitated by paired reductases: Nap/NrfA or Nar/Nir, depending on environmental oxygen levels. The Nap system operates under low-oxygen conditions, while Nar is active in anaerobic conditions (93). The final step of nitrite reduction to ammonia occurs via the cytochrome c nitrite reductase NrfA which is considered a marker of DNRA (93–95). The *nrfA* gene is broadly distributed across microbial taxa including Bacteroidetes, Firmicutes, and Proteobacteria (96). Many microbes are capable of DNRA including, but not limited to, pathogens associated with struvite urolithiasis including *Staphylococcus* spp., *Proteus* spp., and *Klebsiella* spp. (97). However, DNRA may not be restricted to only bacteria that express *nrfA*. Interestingly, *nirD* was upregulated nearly five-fold in mice with UPEC-associated UTIs compared to UPEC grown in the laboratory, suggesting that this route to produce ammonia may participate in stone formation (98).

Ammonia generation can also result from protein deamination. Multiple pathways for arginine degradation have been described in microorganisms, and some may coexist within a single organism (99–101). Generally, absent in higher order eukaryotes, the ADI pathway is used by many bacteria, degrading arginine to ultimately produce citrulline and ammonia are produced to generate energy for the organism (102) This pathway is well characterized in the gastrointestinal tract and has been described

in organisms relevant to the urinary tract including several species of Mycoplasma: *Mycoplasma salivarium*, *Mycoplasma hominis*, and *Mycoplasma fermentans* (44,102). Epidemiologic studies have linked *Ureaplasma urealyticum* to chronic urinary symptoms (103). Baka et al. reported that *U. urealyticum* was detected in just over half of 153 women with chronic urinary symptoms, while *Mycoplasma hominis* was detected in approximately 3% of patients—always in co-occurrence with *U. urealyticum*—suggesting potential metabolic interactions between these uropathogens that may synergistically supply nitrogen substrates to other members of the urinary microbiota (104). Though most often studied in non-urinary environments (44), these urease-independent processes are increasingly relevant to the urinary tract, particularly in the context of biofilm-based communities where substrate availability and oxygen availability likely vary at different stages in stone growth.

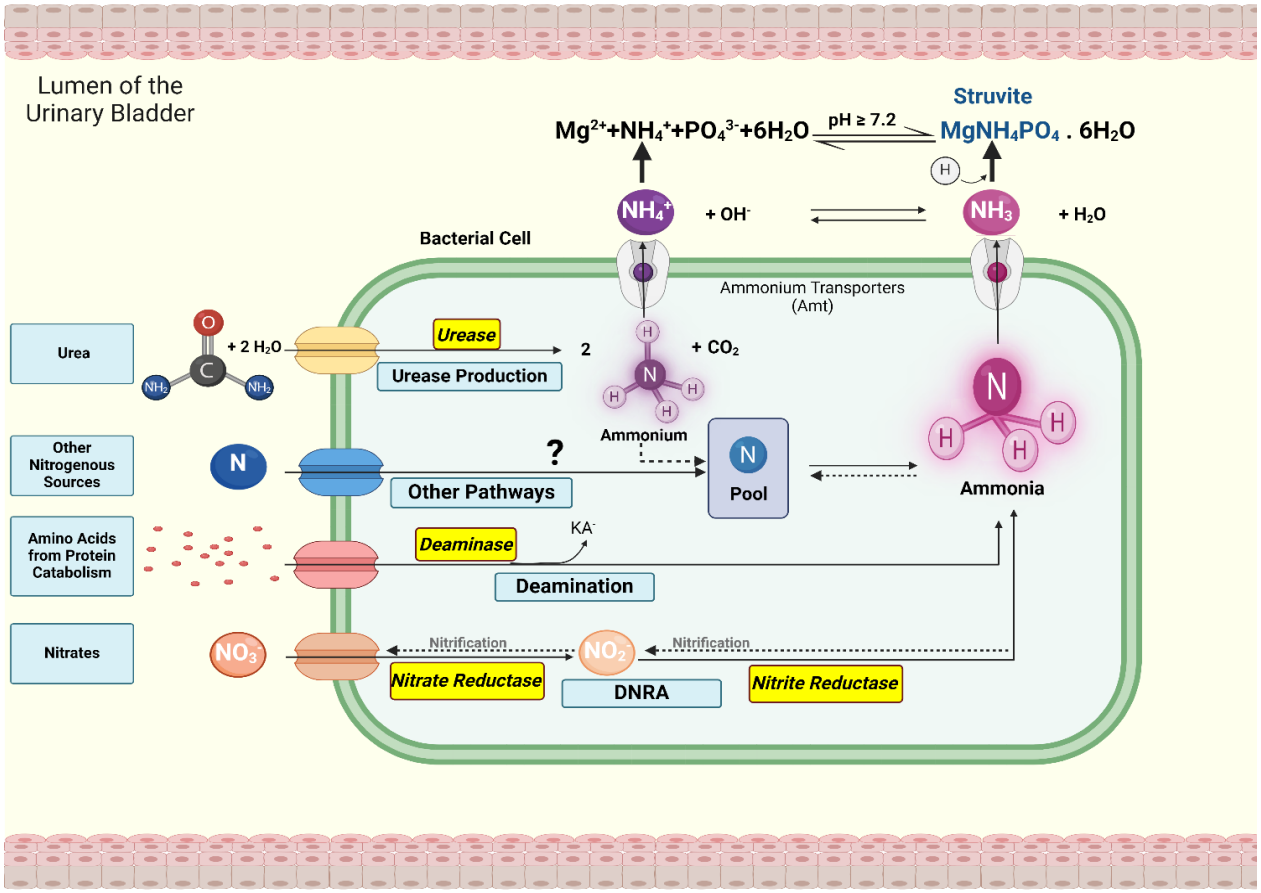

Figure 2 Established and potential microbial biochemical pathways that increase ammonia in host urine, thereby contributing to struvite stone formation. This schematic summarizes potential microbial metabolic routes contributing to ammonia generation within the urinary bladder. Urea, amino acids, and nitrate serve as nitrogenous substrates for bacteria. The urease pathway, classically associated with struvite urolithiasis, hydrolyzes urea into ammonium (NH_4^+) and CO_2, with ammonium exported via transporters or converted to ammonia (NH_3), raising pH and facilitating struvite ($MgNH_4PO_4 \cdot 6H_2O$) precipitation (8). Urease-independent pathways also contribute to the ammonia pool. These include amino acid deamination via deaminase enzymes, and dissimilatory nitrate reduction to ammonia (DNRA), which reduces nitrate (NO_3^-) and nitrite (NO_2^-) to ammonium through nitrate and nitrite reductases. Together, these pathways demonstrate how both urease-positive and urease-negative organisms might contribute to urinary alkalinization and struvite stone formation. Created using Biorender.com.

Is urine sterile?

The controversy surrounding the sterility of the urinary tract has been ongoing for centuries. The “sterile urine paradigm”, the concept that healthy urine does not contain microbes, has roots dating back to the mid-1800s, a time when germ theory was being discovered and popularized (105). Louis Pasteur attempted to disprove spontaneous generation of microbial life by exposing a sample of boiled urine to air, resulting in increased turbidity relative to urine that remained in a sealed vessel (62). Two decades later, William Robert performed a similar experiment and observed increased turbidity in urine specimens that were exposed to air or tap water compared to unexposed specimens (62,105). Therefore, these early researchers incorrectly concluded that fresh urine from otherwise healthy individuals should be free of bacteria (105). The creation of the modern aerobic bacterial UC and the Kass criterion in the 1950s, both of which are still used in clinical microbiology today, garnered wide-spread support of the “sterile urine paradigm” (105).

In the 1970s, Rosalind Maskell, a medical microbiologist published the first report challenging the long-held “sterile urine paradigm” (106,107). Maskell observed that some patients (humans?) experienced symptoms consistent with urinary tract infection (UTI) despite negative urine cultures (106–108). She recognized that many organisms present in urine, particularly anaerobes and other fastidious bacteria, were not recoverable using standard culture methods (108). Thus, she concluded that conventional UC techniques were insufficient for diagnosing all UTI (108). Despite the significance of these insights, Maskell’s work was largely overlooked for decades. It wasn’t until 2012 that Wolf et al., in consultation with Maskell, used 16S rRNA gene

sequencing (16S) to confirm the presence of a urinary microbiome, validating her earlier observations (109).

By the end of the 1970s, asymptomatic bacteriuria was acknowledged to exist, suggesting that many organisms can colonize the urinary tract with no appreciable symptoms or signs in the human, dog or cat (46). Asymptomatic bacteriuria, termed subclinical bacteriuria in veterinary medicine, has since been documented in up to 5% of healthy women and at even higher rates in postmenopausal women (58,110,111). It is also present in approximately 2–9% of dogs (112,113), and in 6% of middle-aged cats and up to 13% of geriatric cats (114–116). These findings suggest that the mere presence of bacteria in urine does not necessarily indicate disease. Indeed, treatment of subclinical bacteriuria is generally discouraged, as antimicrobial therapy might cause more harm than benefit and perpetuate antimicrobial resistance. Some colonizing strains might actually be protective for urinary tract health, rather than acting as pathogens (117).

The composition of the urinary microbiome is now recognized as a key determinant of urinary health, where shifts in taxonomic and functional profiles might contribute to the onset and progression of various urological diseases, including struvite? urolithiasis (71,110,118–122). The perspective that the urinary tract harbors a dynamic and interactive microbiome, rather than being a sterile environment, fundamentally challenges the collective previous presumptions and necessitated the adoption of more advanced metagenomic approaches to further our understanding of it (109). The diversity and activity of microbes in urine, including the expression of virulence genes, combined with potential weaknesses in host immune defenses, might

be important factors that result in the presence or absence of clinical signs and subsequent development of struvite urolithiasis in dogs and even cats (82,123).

Urinary Microbiome Research in Healthy Humans, Dogs, and Cats

The presence of a urinary microbiome in clinically healthy dogs was first reported by Burton and colleagues in 2017 (124). Four dominant bacterial taxa in male (n=10; 1 intact) and female dogs (n=10; spayed) were identified: P*seudomonas* spp.*, Acinetobacter* spp.*, Sphingobium* spp. and *Bradyrhizobiaceae* (124). *Streptococcus* and *Staphylococcus* have also been identified as predominant organisms in free catch (ie, urogenital microbiome analysis) urine specimens from dogs (125). Melgarejo et al. used 16S and found diverse microbial communities within urine specimens obtained from dogs via cystocentesis, despite the animals having negative UC results (126). The sequencing data, however, revealed that all specimens contained microbes including 231 bacterial genera, of which 20 were known pathogens (126). The authors concluded that the urinary microbiome of healthy dogs has diverse bacterial species, confirming the work conducted by Maskell decades prior (126).

Struvite crystals were also associated with bacterial richness and community structure, while not statistically significant (P= 0.07), this finding is clinically relevant. One dog had the greatest urinary microbial diversity (87 genera) and the highest degree of struvite crystalluria (4+) despite the absence of clinical signs associated with the bacteriuria. Five of 10 of the most abundant organisms in the dog's urine (*Sporosarcina pasteurii*, *Viribacter* spp., *Mycobacterium* spp., *Rhodobiaceae* spp., and *Sporosarcina contaminans*) were urease-producing bacteria that had not been cultured previously

from urine specimens from dogs. They concluded that the urinary microbiome from healthy dogs has a diverse microbial composition, further highlighting the limitations aerobic UC. Although beyond the scope of their study, the authors remarked that these findings pose interesting questions regarding microbial virulence factors and the role of the host immune system, presenting interesting questions that should be investigated in future work (126).

While data are more limited in cats, 16S has also been used to determine the composition of the urinary microbiome in 17 cats with chronic kidney disease (CKD) and 14 clinically healthy control cats (127). *Pseudomonas* was found in 50% of the urine specimens from healthy cats and *E. coli* appeared more common in the urine from cats with CKD (127).

Next-Generation Sequencing and the Urinary Microbiome

Modern, next-generation sequencing (NGS) has provided insight into the role of the microbiota in health and disease that were unattainable using previous culture-based methods. Several recent review articles on NGS technologies for readers unfamiliar with the background and use of these methods are cited here (128–130). NGS methods within the field of metagenomics have revolutionized our understanding of the urinary microbiome. These powerful diagnostics have revealed that the urinary tract harbors a diverse array of microorganisms, even in the absence of clinical signs (124,127,131,132). Advances in modern molecular sequencing methods have challenged outdated concepts like the “sterile urine paradigm”, revealing a complex and diverse array of microbes in the urinary tract, even in healthy individuals (109,132–134).

The depth of sequence is an important consideration when using any NGS method to study the microbiome, sequencing at a higher depth leads to greater data accumulation compared to more shallow sequencing, resulting in a more accurate and complete view of microbial community members (135,136).

The role of 16S vs. shotgun metagenomic sequencing

In addition to 16S ribosomal RNA gene sequencing (rRNA) and enhanced quantitative urine cultures (EQUC) (124,126,127,137–139), shotgun metagenomic sequencing has many advantages. Despite 16s being less expensive and labor intensive than metagenomic sequencing, it is inferior for investigating diseases such as struvite urolithiasis can be misleading because the shallow depth (~10,000–200,000 reads per sample) and taxonomic resolution of 16s can be inconsistent, making analysis difficult (42,128). Shotgun metagenomic sequencing allows for a higher level of taxonomic resolution (~5 million–200+ million reads per sample), and identification of bacteria beyond the species level (128). Furthermore, 16S implements an amplicon-based approach, using a single marker gene to evaluate species diversity and therefore, the entire metagenome is not being sequenced (42,128).16s provides limited resolution between closely related species and differences associated with variable region diversity (42). However, a limitation of both 16s and shotgun metagenomic sequencing methods is their inability to differentiate live or metabolically active cells from dead or inactive cells (128). EQUC can be used in conjunction with these diagnostics to attempt to surpass this shortcoming; however, the use of more robust

metagenomic methods like transcriptomics has the ability to determine the functional profile and gain much more accurate, higher resolution taxonomic information.

Studies utilizing metagenomics to analyze the urinary microbiome are limited (138,140,141). Kachroo and colleagues published the first study that implemented metagenomics to classify the urinary microbiome of human patients with CaOx stones (138). *Lactobacillus crispatus* was enriched in the urine from the control group compared to those with CaOx urolithiasis, whereas those with CaOx stones had *Pseudomonas aeruginosa* and *Burkholderia* spp. most commonly identified (138). The authors also attempted to do pathway enrichment analysis to try to identify metabolic pathways that were over expressed or under expressed in either group. However, other studies have demonstrated that while shotgun metagenomics is useful to identify a microbiome's taxonomic composition and the taxa relative abundance, it does not provide quality information about differential gene content (142,143). The functional profile of a microbial community is best inferred using shotgun metatranscriptomic sequencing. When choosing a NGS method, the advantages and disadvantages of each should be considered (Fig. 3) (144).To date, no studies using shotgun metagenomics or NGS have been published in humans, cats or dogs with struvite urolithiasis.

Metatranscriptomic Sequencing

Metatranscriptomic sequencing is an approach that involves sequencing the entire transcriptome (RNA) of a microbial community (128). This approach is a more robust method for capturing bacterial metabolism in real time because of the nature of

transcription in which DNA is actively being converted to RNA (145). In bacteria, the function of a gene is often directly tied to the rate of its transcription due to a process called coupled transcription-translation that does not occur in eukaryotes (145). This is particularly useful with prokaryotic DNA in which no post-translational modification is needed, as in eukaryotes (128,142,143). Not only can transcriptomic approaches like RNAseq provide a superior view into the taxonomic profile of the urinary microbiome, but it can also elucidate the functional profile of the microbial community, which could provide insights into the pathophysiology of urological diseases such as UTIs and struvite urolithiasis (138,143).

Accurately identifying the taxonomic composition of the urinary microbiome is an important first step, as it allows us to focus on the key microbial players and their relative abundance within the urinary tract (128). However, understanding the functional profile of the urinary microbiome and the community's collective metabolic capabilities is even more important to improve our approach to managing urological diseases in human and veterinary patients. Linking microbial community membership with biochemical function creates translational opportunities and supports more targeted diagnostics and therapeutics. Just as crucial is an understanding of microbial interactions, such as co-occurrence patterns and biofilm formation, which can reveal synergistic or competitive relationships that drive pathogenicity or persistence. These insights offer potential mechanisms for alternative, non-antibiotic therapies, such as disrupting biofilms or introducing beneficial competitors, ultimately strengthening antimicrobial stewardship by reducing unnecessary or ineffective antibiotic use. There is

a need to link community membership with the biochemical capabilities that can be used for translational opportunities

Techniques for Uropathogen Identification

	SUC	EQUC	MALDI-TOF	Multiplex PCR	Shotgun Metagenomics	Total RNAseq
	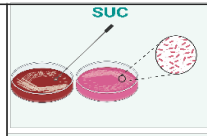	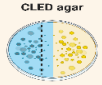		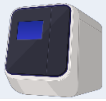	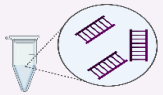	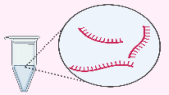
Use	Bacterial ID, Susceptibility Testing	Expanded Organism ID, Susceptibility Testing	Organism ID, Susceptibility Testing	Organism ID, Susceptibility Testing	Organism ID, AMR, Host-Microbe Interactions	Organism ID, Gene Expression, AMR, Host-Microbe Interactions
Target	Common veterinary isolates: *S. pseudintermedius* *K. pneumoniae* *E. faecalis* *P. mirabilis* UPEC	Organisms not detected on SUC Slow growing Fastidious organisms Anaerobes	Cultured Organisms or Organisms in Whole Sample	Organisms in Whole Sample	Organisms in Whole Sample, Entire Microbial Community	Organisms in Whole Sample, Entire Microbial Community
Pros	No specialized equipment Widely Available ↓ Relative Cost	↓ False (-) compared to SUC ↓ Relative Cost	Can be Culture-Independent ↑ Sensitivity compared to culture Time to Report ≤ 24 hrs (varies)	Can be Culture-Independent ↑ Sensitivity compared to culture Time to Report ≤ 24 hrs (varies)	Culture-Independent Community-wide ID: Taxonomy ↑ Accurcy of Community Composition ID DNA stability	Culture-Independent Community-wide ID: Taxonomy Function ↑ Accurcy of Community Composition ID Detects active cells
Cons	↑ False (-) Highly Selective Susceptible to contamination Time to Report ~24-48 hrs	Resource Intensive Somewhat Selective At large institutions Time to Report ~48-72 hrs	Culture -dependent Specialized equipment Sample Destroyed ↑ Cost than culture methods Poor discrimination between similar/ related organisms At large institutions Time to Report ≤ 24 hrs (varies)	Primer Dependent Specialized equipment ↑ Cost than culture methods At large institutions Time to Report ≤ 24 hrs (varies)	Seq. Depth Matters Detects inactive cells ↑ Relative Cost Specialized Intensive Analysis Not Used Clinically Time to Report ≤ 24 hrs (varies)	Seq. Depth Matters RNA<DNA stability ↑ Relative Cost Specialized Training and Equipment Intensive Analysis Not Used Clinically Time to Report ≤ 24 hrs (varies)

Figure 3 A comparison of traditional and newer methods for microbial identification and microbiome analysis. Created using Biorender.com.

Conclusions

Current culture methods approach diagnosis from a perspective of single organism causality, without considering the possibility of microbial community cooperation within the urinary microbiome in struvite urolithiasis. While urease-producing organism have long been implicated in struvite stone formation in dogs and humans, the concept of intra-microbiome community cooperation contributing to this disease process has not been previously considered. While most urine and urolith cultures from cats with struvite urolithiasis are negative for growth, advanced RNAseq testing might elucidate new information for this species.

By looking beyond these specific organisms and their production of urease, a more comprehensive understanding of the microbial community's collective contribution to the pathophysiology of struvite stone formation can be gained. As veterinary medicine continues to evolve, the incorporation of metagenomic technologies to comprehensively characterize the urinary microbiome can help us further our knowledge regarding struvite urolithiasis formation. This could lead to advancements in clinical diagnostics or treatments that target the metabolic activity occurring as part of community cooperation, rather than just focusing treatment on a predominant organism(s) detected using traditional methods. Diagnostic approaches could shift toward molecular-based methods that detect microbial gene expression or community metabolic potential, rather than relying solely on organism isolation. Such tools might improve the identification of fastidious, anaerobic, or low-abundance bacteria contributing to struvite formation and enable earlier, more precise intervention. Underlying mechanisms of microbial activity might present a widespread target for future treatments to limit stone formation, going

beyond the current practice of prescribing antimicrobials based solely on aerobic UC results and antimicrobial sensitivity testing. This enhanced understanding of the urinary microbiome might also pave the way for the development of novel, microbiome-based therapies (Fig. 4).

As our understanding grows of the relationship between the urinary microbiome and the host, whether human, dog, or cat, the necessity to transcend simplistic culture-based approaches and embrace a more comprehensive and holistic assessment of the urinary microbiome becomes increasingly evident. This is essential to better elucidate the intricate interplay between the urinary microbiome urinary tract health and disease like struvite urolithiasis.

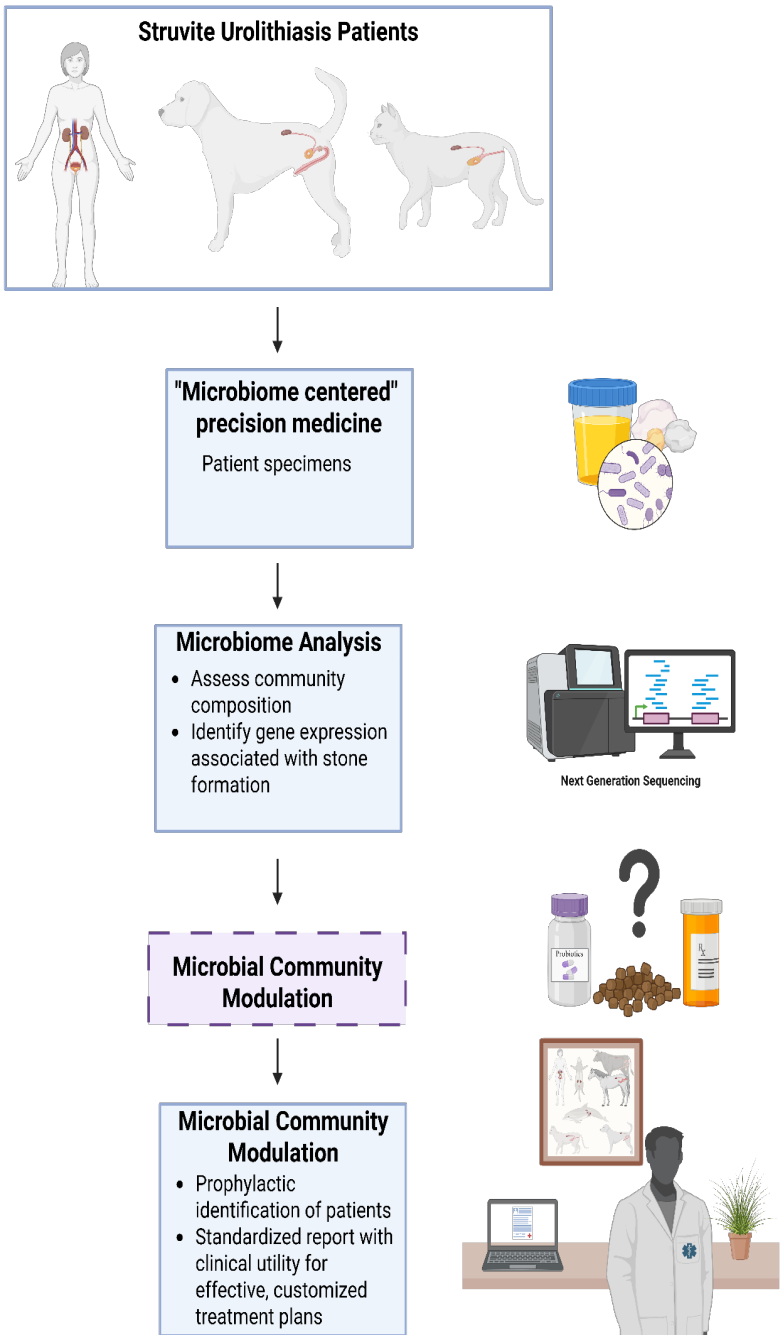

Figure 4 Possible future clinical applications of microbiome analysis via shotgun metagenomics and metatranscriptomics to improve disease outcomes and patient care in both human and veterinary patients.

Funding

Financial support for AMF was supported by the MSTP T32 (NIH Grant T32GM136559), NIH TL1 Training Grant (5TL1DK139565-02) through the LAUNCH Program, UCSF. The funding sources were not involved in writing the report or in the decision to submit this article for publication.

Conflicts of Interest: The authors declare no conflicts of interest.

References

1. Perry JF. Diseases of The Urinary Organs. In: Dogs Their Management and Treatment in Disease: A Study of the Theory and Practice of Canine Medicine. 2nd ed. J. Loring Thayer; 1891. p. 89–104.

2. Robinson MR, Norris RD, Sur RL, Preminger GM. Urolithiasis: Not Just a 2-Legged Animal Disease. Vol. 179, Journal of Urology. 2008. p. 46–52.

3. Osborne CA, Albasan H, Lulich JP, Nwaokorie E, Koehler LA, Ulrich LK. Quantitative Analysis of 4468 Uroliths Retrieved from Farm Animals, Exotic Species, and Wildlife Submitted to the Minnesota Urolith Center: 1981 to 2007. Vol. 39, Veterinary Clinics of North America - Small Animal Practice. 2009. p. 65–78.

4. Reis S, Danilovic A, Vicentini FC, Torricelli FCM, Srougi M, Mazzucchi E. The challenge of cystine and struvite stone formers: Clinical, metabolic and surgical assessment. Int Braz J Urol. 2016;42(5):977–85.

5. Flannigan R, Choy WH, Chew B, Lange D. Renal struvite stones - Pathogenesis, microbiology, and management strategies. Nat Rev Urol. 2014;11(6):333–41.

6. Kopecny L, Palm CA, Segev G, Westropp JL. Urolithiasis in dogs: Evaluation of trends in urolith composition and risk factors (2006-2018). J Vet Intern Med. 2021 May;35(3):1406–15.

7. Kopecny L, Palm CA, Segev G, Larsen JA, Westropp JL. Urolithiasis in cats: Evaluation of trends in urolith composition and risk factors (2005-2018). J Vet Intern Med. 2021 May;35(3):1397.

8. Osborne CA, Klausner JS, Polzin DJ, Griffith DP. Etiopathogenesis of canine struvite urolithiasis. Am J Vet Res. 1986 Jan;16(1):67–86.

9. Brown NO, Parks JL, Greene RW. Recurrence of Canine Uroliths 1974. J Am Vet Med Assoc. 1977 Feb;170(4):419–22.

10. Jummai T, Boonyayatra S, Tangjitjaroen W, Akatvipat A. View of Factors affecting the recurrence of canine urolithiasis in the lower urinary tract after surgical removal. Vet Integr Sci. 2018;3(17):197–210.

11. Albasan H, Osborne CA, Lulich JP, Lekcharoensuk C, Koehler LA, Ulrich LK, et al. Rate and frequency of recurrence of uroliths after an initial ammonium urate, calcium oxalate, or struvite urolith in cats. Sci Rep JAVMA. 2009 Dec;235(12).

12. Bohonowych RO, Parks JL, Greene RW. Cystic Calculi in Cats in a Hospital Population. J Am Vet Med Assoc. 1978;73(3):301–3.

13. Chamberlin JD, Clayman RV. Medical Treatment of a Staghorn Calculus: The Ultimate Noninvasive Therapy. J Endourol Case Rep. 2015 Dec;1(1):21–3.

14. Pereira J, Pereira JDA, Bonci MM, Makita MT, Botteon RDCCM, Souza MMS de, et al. Urinary infection by Citrobacter koseri (C. diversus) in a dog affected by nephrolithiasis. Pubvet. 2021 Jan;15(02):1–6.

15. Ling GV, Ruby AL, Johnson DL, Thurmond M, Franti CE. Renal calculi in dogs and cats: prevalence, mineral type, breed, age, and gender interrelationships (1981-1993). J Vet Intern Med Am Coll Vet Intern Med. 1998;12(1):11–21.

16. Houston DM, Moore AEP, Favrin MG, Hoff B. Canine urolithiasis: A look at over 16 000 urolith submissions to the Canadian Veterinary Urolith Centre from February 1998 to April 2003. Can Vet J. 2004;45:225–30.

17. Cooper E, Scansen BA. Obstructive Uropathy. In: Clinical Small Animal Internal Medicine [Internet]. Wiley; 2020. p. 1109–22. Available from: https://onlinelibrary.wiley.com/doi/10.1002/9781119501237.ch122

18. Defarges A, Evason M, Dunn M, Berent A. Urolithiasis in Small Animals. In: Clinical Small Animal Internal Medicine. Wiley; 2020. p. 1123–56.

19. Lulich JP, Berent AC, Adams LG, Westropp JL, Bartges JW, Osborne CA. ACVIM Small Animal Consensus Recommendations on the Treatment and Prevention of Uroliths in Dogs and Cats. J Vet Intern Med. 2016 Sept;30(5):1564–74.

20. Taylor S, Boysen S, Buffington T, Chalhoub S, Defauw P, Delgado MM, et al. 2025 iCatCare consensus guidelines on the diagnosis and management of lower urinary tract diseases in cats. J Feline Med Surg. 2025 Feb;27(2):1098612X241309176.

21. Manoharan SA, Berent AC, Weisse CW, Purdon K, Bagley D. Medical dissolution of presumptive upper urinary tract struvite uroliths in 6 dogs (2012-2018). J Vet Intern Med. 2024 Nov;

22. Nickel JC, Olson M, McLean RJC, Grant SK, Costerton JW. An Ecological Study of Infected Urinary Stone Genesis in an Animal Model. Br J Urol. 1987;59(1):21–30.

23. McLean RJ, Nickel JC, Noakes VC, Costerton JW. An In Vitro Ultrastructural Study of Infectious Kidney Stone Genesis. Am Soc Microbiol. 1985;49(3):805–11.

24. Nickel JC, Emtage J, Costerton JW. Ultrastructural Microbial Ecology of Infection Induced Urinary Stones. J Urol. 1985;133(4):622–7.

25. Olson ME, Nickel JC, Costerton JW. Animal Model of Human Disease Infection-Induced Struvite Urolithiasis in Rats. Vol. 135, Americanj ournal ofPathology. 1989.

26. Mclean RJC, Downey J, Clapham L, Nickel JC. A simple technique for studying struvite crystal growth in vitro. Vol. 18, Urol Res. 1990 p. 39–43.

27. Nickel JC, Costerton JW, Mclean' RJC, Olson M. Bacterial biofilms: influence on the pathogenesis, diagnosis and treatment of urinary tract infections [Internet]. Vol. 33,

Journal of Antimicrobial Chemotherapy. 1994 p. 31–41. Available from: https://academic.oup.com/jac/article/33/suppl_A/31/723390

28. Griffith DP, Musher DM, Itin C. Urease the Primary Cause of Infection-Induced Urinary Stones. Invest Urol. 1976;13(5):346–50.

29. Yadav SN, Ahmed N, Nath AJ, Mahanta D, Kalita MK. Urinalysis in dog and cat: A review. Vet World. 2020 Oct;13(10):2133–41.

30. Das P, Gupta G, Velu V, Awasthi R, Dua K, Malipeddi H. Formation of struvite urinary stones and approaches towards the inhibition—A review. Vol. 96, Biomedicine and Pharmacotherapy. Elsevier Masson SAS; 2017. p. 361–70.

31. Prien EL. Studies in urolithiasis. III. Physicochemical principles in stone formation and prevention. J Urol. 1955 Apr;73(4):627–52.

32. Wang LP, Wong Y, Griffith DP. Treatment Options in Struvite Stones. Urol Clin North Am. 1997 Feb;24(1):149–62.

33. Estiu G, Merz KM. The hydrolysis of urea and the proficiency of urease. J Am Chem Soc. 2004 June;126(22):6932–44.

34. Halinski A, Bhatti KH, Boeri L, Cloutier J, Davidoff K, Elqady A, et al. Spectrum of Bacterial Pathogens from Urinary Infections Associated with Struvite and Metabolic Stones. Diagnostics. 2023 Jan;13(1).

35. Margel D, Ehrlich Y, Brown N, Lask D, Livne PM, Lifshitz DA. Clinical implication of routine stone culture in percutaneous nephrolithotomy - A prospective study. Urology. 2006 Jan;67(1):26–9.

36. Alford A, Furrow E, Borofsky M, Lulich J. Animal models of naturally occurring stone disease. Vol. 17, Nature Reviews Urology. Nature Research; 2020. p. 691–705.

37. Palma D, Langston C, Gisselman K, McCue J. Feline Struvite Urolithiasis. Compendium: Continuing Education for Veterinarians®. Vetlearn.com; 2009. p. E1–8.

38. Gomes VR, Ariza PC, Silva MAM, Schulz FJ, Oliveira HF, Queiroz LL, et al. Mineral composition and clinical aspects of urolithiasis in cats in Brazil. Arq Bras Med Vet E Zootec. 2022;74(4):649–61.

39. Grauer GF. Feline Struvite & Calcium Oxalate Urolithiasis. Today's Veterinary Practice. 2015. p. 14–20.

40. Houston DM, Vanstone NP, Moore AEP, Weese HE, Weese JS. Evaluation of 21426 feline bladder urolith submissions to the Canadian Veterinary Urolith Centre (1998–2014). Can Vet J. 2016 Feb;57(2):196–201.

41. Wallace B, Chmiel JA, Al KF, Bjazevic J, Burton JP, Goldberg HA, et al. The Role of Urinary Modulators in the Development of Infectious Kidney Stones. J Endourol. 2023 Mar;37(3):358–66.

42. Machado J da C, Renteria JM, Nascimento MM do, Cunha ACA, Vieira GM, Manso JEF. Association between urinary lithiasis, other than struvite by crystallography and non-ureolytic bacteria. Urolithiasis. 2024 Dec;52(1).

43. Wiebe MA, Brannon JR, Steiner BD, Bamidele A, Schrimpe-Rutledge AC, Codreanu SG, et al. Serine Deamination Is a New Acid Tolerance Mechanism Observed in Uropathogenic Escherichia coli. mBio. 2022 Dec;13(6).

44. Bergen WG, Wu G. Intestinal nitrogen recycling and utilization in health and disease. Vol. 139, Journal of Nutrition. 2009. p. 821–5.

45. Martín-Rodríguez AJ, Rhen M, Melican K, Richter-Dahlfors A. Nitrate Metabolism Modulates Biosynthesis of Biofilm Components in Uropathogenic Escherichia coli and Acts as a Fitness Factor During Experimental Urinary Tract Infection. Front Microbiol. 2020 Jan;11.

46. Roberts KB. The diagnosis of UTI: Liquid gold and the problem of gold standards. Vol. 135, Pediatrics. American Academy of Pediatrics; 2015. p. 1126–7.

47. Satyal U, Srivastava A, Abbosh PH. Urine Biopsy—Liquid Gold for Molecular Detection and Surveillance of Bladder Cancer. Vol. 9, Frontiers in Oncology. Frontiers Media S.A.; 2019.

48. Reine NJ, Langston CE. Urinalysis interpretation: How to squeeze out the maximum information from a small sample. Clin Tech Small Anim Pract. 2005;20(1 SPEC.ISS.):2–10.

49. Piech TL, Wycislo KL. Importance of Urinalysis. Vol. 49, Veterinary Clinics of North America - Small Animal Practice. W.B. Saunders; 2019. p. 233–45.

50. Callens AJ, Bartges JW. Urinalysis. Vol. 45, Veterinary Clinics of North America - Small Animal Practice. W.B. Saunders; 2015. p. 621–37.

51. Pryles CV, Atkin MD, Morse TS, Welch KJ. Comparative Bacteriologic Study of Urine Obtained from Children by Percutaneous Suprapubic Aspiration of the Bladder and by Catheter. Pediatrics. 1959 Dec;24(6):983–91.

52. Coffey EL, Gomez AM, Ericsson AC, Burton EN, Granick JL, Lulich JP, et al. The impact of urine collection method on canine urinary microbiota detection: a cross-sectional study. BMC Microbiol. 2023 Dec;23(1).

53. Pohl HG, Groah SL, Pérez-Losada M, Ljungberg I, Sprague BM, Chandal N, et al. The urine microbiome of healthy men and women differs by urine collection method. Int Neurourol J. 2020;24(1):41–51.

54. Price TK, Dune T, Hilt EE, Thomas-White KJ, Kliethermes S, Brincat C, et al. The clinical urine culture: Enhanced techniques improve detection of clinically relevant microorganisms. J Clin Microbiol. 2016 May;54(5):1216–22.

55. Boyd C, Wood K, Whitaker D, Ashorobi O, Harvey L, Oster R, et al. Accuracy in 24-hour Urine Collection at a Tertiary Center. Rev Urol. 2018;20(3):119–24.

56. Perry LA, Kass PH, Johnson DL, Ruby AL, Shiraki R, Westropp JL. Evaluation of culture techniques and bacterial cultures from uroliths. J Vet Diagn Invest. 2013 Mar;25(2):199–202.

57. Flokas ME, Andreatos N, Alevizakos M, Kalbasi A, Onur P, Mylonakis E. Inappropriate Management of Asymptomatic Patients with Positive Urine Cultures: A Systematic Review and Meta-analysis. Vol. 4, Open Forum Infectious Diseases. Oxford University Press; 2017.

58. Nicolle LE, Gupta K, Bradley SF, Colgan R, DeMuri GP, Drekonja D, et al. Clinical practice guideline for the management of asymptomatic bacteriuria: 2019 update by the Infectious Diseases Society of America. Vol. 68, Clinical Infectious Diseases. Oxford University Press; 2019. p. E83–E75.

59. Legaria MC, Barberis C, Famiglietti A, Gregorio SD, Stecher D, Rodriguez CH, et al. Urinary tract infection caused by anaerobic bacteria. Utility of anaerobic urine culture. Vol. 78, Anaerobe. Academic Press; 2022.

60. Westropp JL, Sykes JE. Infections of the Genitourinary Tract. In: Sykes JE, editor. Greene's Infectious Diseases of the Dog and Cat. 5th ed. Elsevier; 2023. p. 1669–87.

61. Xu R, Deebel N, Casals R, Dutta R, Mirzazadeh M. A new gold rush: A review of current and developing diagnostic tools for urinary tract infections. Vol. 11, Diagnostics. Multidisciplinary Digital Publishing Institute (MDPI); 2021.

62. Brubaker L, Chai TC, Horsley H, Khasriya R, Moreland RB, Wolfe AJ. Tarnished gold—the "standard" urine culture: reassessing the characteristics of a criterion standard for detecting urinary microbes. Vol. 3, Frontiers in Urology. Frontiers Media SA; 2023.

63. Festa RA, Luke N, Mathur M, Parnell L, Wang D, Zhao X, et al. A test combining multiplex-PCR with pooled antibiotic susceptibility testing has high correlation with expanded urine culture for detection of live bacteria in urine samples of suspected UTI patients. Diagn Microbiol Infect Dis. 2023 Oct;107(2).

64. Polat S, Eral HB. Effect of hyaluronic acid on the struvite crystallization: A structural, morphological, and thermal analysis study. J Cryst Growth. 2022 Aug;592.

65. Espinosa-Ortiz EJ, Gerlach R. Struvite Stone Formation by Ureolytic Biofilms. In: The Role of Bacteria in Urology. Springer International Publishing; 2019. p. 61–70.

66. Thomas B, Tolley D. Concurrent urinary tract infection and stone disease: Pathogenesis, diagnosis and management. Vol. 5, Nature Clinical Practice Urology. 2008. p. 668–75.

67. Konieczna I, Arnowiec P, Kwinkowski M, Kolesiska B, Frczyk J, Kamiski Z, et al. Bacterial Urease and its Role in Long-Lasting Human Diseases [Internet]. 2012. Available from: http://mgv2.cmbi.ru.nl

68. Bono AJM, Leslie SW, Affiliations WCR, Beaumont OUW. Uncomplicated Urinary Tract Infections. In: StatPearls (Internet) [Internet]. StatPearls Publishing LLC; 2023. Available from: https://www.ncbi.nlm.nih.gov/books/NBK470195/

69. Rose C, Parker A, Jefferson B, Cartmell E. The characterization of feces and urine: A review of the literature to inform advanced treatment technology. Crit Rev Environ Sci Technol. 2015 Sept;45(17):1827–79.

70. Putchakayala R, Haritha GS. Urinary system diseases of dogs and cats. In: Introduction to Diseases, Diagnosis, and Management of Dogs and Cats. Elsevier; 2023. p. 147–61.

71. Neugent ML, Hulyalkar NV, Nguyen VH, Zimmern PE, Nisco NJD. Advances in understanding the human urinary microbiome and its potential role in urinary tract infection. mBio. 2020 Mar;11(2).

72. Boyce WH. Organic Matrix of Human Urinary Concretions. Am J Med. 1968 Nov;45(5):673–83.

73. Aggarwal N, Kitano S, Puah GRY, Kittelmann S, Hwang IY, Chang MW. Microbiome and Human Health: Current Understanding, Engineering, and Enabling Technologies. Vol. 123, Chemical Reviews. American Chemical Society; 2023. p. 31–72.

74. Saw JJ, Sivaguru M, Wilson EM, Dong Y, Sanford RA, Fields CJ, et al. In Vivo Entombment of Bacteria and Fungi during Calcium Oxalate, Brushite, and Struvite Urolithiasis. Kidney360. 2021 Feb;2(2):298–311.

75. Zhao A, Sun J, Liu Y. Understanding bacterial biofilms: From definition to treatment strategies. Vol. 13, Frontiers in Cellular and Infection Microbiology. Frontiers Media S.A.; 2023.

76. Wickramasinghe NN, Hlaing MM, Ravensdale JT, Coorey R, Chandry PS, Dykes GA. Characterization of the biofilm matrix composition of psychrotrophic, meat spoilage pseudomonads. Sci Rep. 2020 Dec;10(1).

77. Hanke ML, Kielian T. Deciphering mechanisms of Staphylococcal biofilm evasion of host immunity. Vol. 2, Frontiers in cellular and infection microbiology. 2012. p. 62.

78. Bandeira M, Borges V, Gomes JP, Duarte A, Jordao L. Insights on klebsiella pneumoniae biofilms assembled on different surfaces using phenotypic and genotypic approaches. Microorganisms. 2017 June;5(2).

79. Beckman RL, Cella E, Azarian T, Rendueles O, Fleeman RM. Diverse polysaccharide production and biofilm formation abilities of clinical Klebsiella pneumoniae. Npj Biofilms Microbiomes. 2024 Dec 19;10(1):151.

80. Wasfi R, Hamed SM, Amer MA, Fahmy LI. Proteus mirabilis Biofilm: Development and Therapeutic Strategies. Vol. 10, Frontiers in Cellular and Infection Microbiology. Frontiers Media S.A.; 2020.

81. Aniba R, Dihmane A, Raqraq H, Ressmi A, Nayme K, Timinouni M, et al. Exploring staphylococcus in urinary tract infections: A systematic review and meta-analysis on the epidemiology, antibiotic resistance and biofilm formation. Vol. 110, Diagnostic Microbiology and Infectious Disease. Elsevier Inc.; 2024.

82. Cangui-Panchi SP, Ñacato-Toapanta AL, Enríquez-Martínez LJ, Salinas-Delgado GA, Reyes J, Garzon-Chavez D, et al. Battle royale: Immune response on biofilms – host-pathogen interactions. Vol. 4, Current Research in Immunology. Elsevier B.V.; 2023.

83. Kim A, Ahn J, Choi WS, Park HK, Kim S, Paick SH, et al. What is the cause of recurrent urinary tract infection? Contemporary microscopic concepts of pathophysiology. Int Neurourol J. 2021 Sept;25(3):192–201.

84. Govindarajan DK, Kandaswamy K. Virulence factors of uropathogens and their role in host pathogen interactions. Cell Surf. 2022 Dec;8.

85. Bünsow D, Tantawy E, Ostermeier T, Bähre H, Garbe A, Larsen J, et al. Methicillin-resistant Staphylococcus pseudintermedius synthesizes deoxyadenosine to cause persistent infection. Virulence. 2021;12(1):989–1002.

86. Rocha SPD, Pelayo JS, Elias WP. Fimbriae of uropathogenic Proteus mirabilis. Vol. 51, FEMS Immunology and Medical Microbiology. 2007. p. 1–7.

87. Ahmed AE, Abol-Enein H, Awadalla A, Degla HE, El-Shehaby OA. Investigation of Virulence Genes of the Predominant Bacteria Associated with Renal Stones and their Correlation with Postoperative Septic Complications. Infect Drug Resist. 2022;15:3643–55.

88. Flannigan RK, Battison A, De S, Humphreys MR, Bader M, Lellig E, et al. Evaluating factors that dictate struvite stone composition: A multi institutional clinical experience from the EDGE Research Consortium. Can Urol Assoc J. 2018 Apr;12(4):131–6.

89. Aliko A, Kamińska M, Bergum B, Gawron K, Benedyk M, Lamont RJ, et al. Impact of Porphyromonas gingivalis Peptidylarginine Deiminase on Bacterial Biofilm

Formation, Epithelial Cell Invasion, and Epithelial Cell Transcriptional Landscape. Sci Rep. 2018 Dec;8(1).

90. Zhao Y, Li Q, Cui Q, Ni SQ. Nitrogen recovery through fermentative dissimilatory nitrate reduction to ammonium (DNRA): Carbon source comparison and metabolic pathway. Chem Eng J. 2022 Aug;441.

91. Elhawy MI, Huc-Brandt S, Pätzold L, Gannoun-Zaki L, Abdrabou AMM, Bischoff M, et al. The phosphoarginine phosphatase ptpb from staphylococcus aureus is involved in bacterial stress adaptation during infection. Cells. 2021 Mar;10(3):1–17.

92. Zuniga M, Perez G, Gonzalez-Candelas F. Evolution of arginine deiminase (ADI) pathway genes. Mol Phylogenet Evol. 2002 May;25:429–44.

93. Wang C, He T, Zhang M, Zheng C, Yang L, Yang L. Review of the mechanisms involved in dissimilatory nitrate reduction to ammonium and the efficacies of these mechanisms in the environment. Vol. 345, Environmental Pollution. Elsevier Ltd; 2024.

94. Yang T, Xin Y, Zhang L, Gu Z, Li Y, Ding Z, et al. Characterization on the aerobic denitrification process of Bacillus strains. Biomass Bioenergy. 2020 Sept;140.

95. Yang J, Feng L, Pi S, Cui D, Ma F, Zhao H ping, et al. A critical review of aerobic denitrification: Insights into the intracellular electron transfer. Sci Total Environ. 2020 Aug;731.

96. Mohan SB, Schmid M, Jetten M, Cole J. Detection and widespread distribution of the nrfA gene encoding nitrite reduction to ammonia, a short circuit in the biological nitrogen cycle that competes with denitrification. FEMS Microbiol Ecol. 2004 Sept;49(3):433–43.

97. Papava V, Didbaridze T, Zaalishvili Z, Gogokhia N, Maziashvili G. The Role of Urinary Nitrite in Predicting Bacterial Resistance in Urine Culture Analysis Among Patients With Uncomplicated Urinary Tract Infection. Cureus. 2022 June;

98. Snyder JA, Haugen BJ, Buckles EL, Lockatell CV, Johnson DE, Donnenberg MS, et al. Transcriptome of uropathogenic Escherichia coli during urinary tract infection. Infect Immun. 2004 Nov;72(11):6373–81.

99. Abdelal AT. Arginine Catabolism by Microorganisms. Annu Rev Microbiol. 1979 Oct;33:139–68.

100. Cunin R, Glansdorff N, Pierard A, Stalon V. Biosynthesis and Metabolism of Arginine in Bacteria. Mlicrobiological Rev. 1986 Sept;50(3):314–52.

101. Safrhansova L, Hlozkova K, Starkova J. Targeting amino acid metabolism in cancer. In: Buqué A, Lorenzo G, editors. International Review of Cell and Molecular Biology. Academic; 2022. p. 37–79.

102. Yiwen C, Yueyue W, Lianmei Q, Cuiming Z, Xiaoxing Y. Infection strategies of mycoplasmas: Unraveling the panoply of virulence factors. Virulence. 2021;12(1):788–817.

103. Reyes L, Reinhard M, Brown MB. Different inflammatory responses are associated with Ureaplasma parvum-induced UTI and urolith formation. BMC Infect Dis. 2009 Jan;9.

104. Baka S, Kouskouni E, Antonopoulou S, Sioutis D, Papakonstantinou M, Hassiakos D, et al. Prevalence of Ureaplasma urealyticum and Mycoplasma hominis in Women With Chronic Urinary Symptoms. Urology. 2009 July;74(1):62–6.

105. Thomas-White K, Brady M, Wolfe AJ, Mueller ER. The Bladder Is Not Sterile: History and Current Discoveries on the Urinary Microbiome. Vol. 11, Current Bladder Dysfunction Reports. Current Medicine Group LLC 1; 2016. p. 18–24.

106. Maskell R, Allen J, Pead L. The Puzzle of “Urethral Syndrome”: A Possible Answer? The Lancet. 1979 May;313(8125):1058–9.

107. Maskell RM. The natural history of urinary tract infection in women. Med Hypotheses. 2010 May;74(5):802–6.

108. Maskell R, Pead L, Sanderson RA. Fastidious Bacteria and the Urethral Syndrome: A 2-Year Clinical and Bacteriological Study of 51 Women. The Lancet. 1983 Dec;322(8362):1277–80.

109. Wolfe AJ, Toh E, Shibata N, Rong R, Kenton K, FitzGerald MP, et al. Evidence of uncultivated bacteria in the adult female bladder. J Clin Microbiol. 2012 Apr;50(4):1376–83.

110. Lizbeth P, Naranjo Z, María E, Gutiérrez R, Andrea M, Onofre Z, et al. Urolithiasis and its Interplay with the Urinary Microbiome: A Comprehensive Exploration. Int J Med Sci Clin Res Stud. 2023 Nov;03(11):2627–30.

111. Raz R. Urinary Tract Infection in Postmenopausal Women. Korean J Urol. 2011;52(12):801.

112. Mcghie J, Stayt J, Hosgood G. Prevalence of bacteriuria in dogs without clinical signs of urinary tract infection presenting for elective surgical procedures. Aust Vet J. 2014;92(1–2):33–7.

113. Wan SY, Hartmann FA, Jooss MK, Viviano KR. Prevalence and clinical outcome of subclinical bacteriuria in female dogs. J Am Vet Med Assoc. 2014 July;245(1):106–12.

114. Moberg FS, Langhorn R, Bertelsen PV, Pilegaard LM, Sørensen TM, Bjørnvad CR, et al. Subclinical bacteriuria in a mixed population of 179 middle-aged and elderly cats: a prospective cross-sectional study. J Feline Med Surg. 2020 Aug;22(8):678–84.

115. Puchot ML, Cook AK, Pohlit C. Subclinical bacteriuria in cats: prevalence, findings on contemporaneous urinalyses and clinical risk factors. J Feline Med Surg. 2017 Dec;19(12):1238–44.

116. White JD, Cave NJ, Grinberg A, Thomas DG, Heuer C. Subclinical Bacteriuria in Older Cats and its Association with Survival. J Vet Intern Med. 2016 Nov;30(6):1824–9.

117. Segev G, Chen H, Dear JD, Martínez López B, Pires J, Klumpp DJ, et al. Evaluation of the efficacy of a live *Escherichia coli* biotherapeutic product (ASYMPTOMATIC BACTERIURIA *E. coli* 212). J Vet Intern Med. 2024 Sept;38(5):2548–55.

118. Lemberger U, Pjevac P, Hausmann B, Berry D, Moser D, Jahrreis V, et al. The microbiome of kidney stones and urine of patients with nephrolithiasis. Urolithiasis. 2023 Dec;51(1).

119. Chorbińska J, Krajewski W, Nowak Ł, Małkiewicz B, Giudice FD, Szydełko T. Urinary Microbiome in Bladder Diseases—Review. Vol. 11, Biomedicines. Multidisciplinary Digital Publishing Institute (MDPI); 2023.

120. Hiergeist A, Gessner A. Clinical implications of the microbiome in urinary tract diseases. Vol. 27, Current Opinion in Urology. Lippincott Williams and Wilkins; 2017. p. 93–8.

121. Schneeweiss J, Koch M, Umek W. The human urinary microbiome and how it relates to urogynecology. Int Urogynecology J. 2016 Sept;27(9):1307–12.

122. Kustrimovic N, Bilato G, Mortara L, Baci D. The Urinary Microbiome in Health and Disease: Relevance for Bladder Cancer. Vol. 25, International Journal of Molecular Sciences. Multidisciplinary Digital Publishing Institute (MDPI); 2024.

123. Mariano LL, Ingersoll MA. The immune response to infection in the bladder. Vol. 17, Nature Reviews Urology. Nature Research; 2020. p. 439–58.

124. Burton EN, Cohn LA, Reinero CN, Rindt H, Moore SG, Ericsson AC. Characterization of the urinary microbiome in healthy dogs. PLoS ONE. 2017 May;12(5).

125. Mrofchak R, Madden C, Evans MV, Kisseberth WC, Dhawan D, Knapp DW, et al. Urine and fecal microbiota in a canine model of bladder cancer and comparison of canine and human urine microbiota. Life. 2022;15(1):1245–63.

126. Melgarejo T, Oakley BB, Krumbeck JA, Tang S, Krantz A, Linde A. Assessment of bacterial and fungal populations in urine from clinically healthy dogs using next-generation sequencing. J Vet Intern Med. 2021 May;35(3):1416–26.

127. Kim Y, Carrai M, Leung MHY, Chin J, Li J, Lee PKH, et al. Dysbiosis of the Urinary Bladder Microbiome in Cats with Chronic Kidney Disease. 2021; Available from: https://doi.org/10.1128/mSystems

128. Aguiar-Pulido V, Huang W, Suarez-Ulloa V, Cickovski T, Mathee K, Narasimhan G. Metagenomics, metatranscriptomics, and metabolomics approaches for microbiome analysis. Vol. 12, Evolutionary Bioinformatics. Libertas Academica Ltd.; 2016. p. 5–16.

129. Matchado MS, Rühlemann M, Reitmeier S, Kacprowski T, Frost F, Haller D, et al. On the limits of 16S rRNA gene-based metagenome prediction and functional profiling. Microb Genomics. 2024 Feb;10(2).

130. Han H, Lee JY. Microbiome Analysis Using Next-Generation Sequencing in Urinary Tract Infections. Urogenit Tract Infect. 2022;17(1):1–7.

131. Fouts DE, Pieper R, Szpakowski S, Pohl H, Knoblach S, Suh MJ, et al. Integrated next-generation sequencing of 16S rDNA and metaproteomics differentiate the healthy urine microbiome from asymptomatic bacteriuria in neuropathic bladder associated with spinal cord injury. J Transl Med. 2012 Aug;10(1).

132. Lewis DA, Brown R, Williams J, White P, Jacobson SK, Marchesi JR, et al. The human urinary microbiome; bacterial DNA in voided urine of asymptomatic adults. Front Cell Infect Microbiol. 2013;4(AUG).

133. Hilt EE, McKinley K, Pearce MM, Rosenfeld AB, Zilliox MJ, Mueller ER, et al. Urine is not sterile: Use of enhanced urine culture techniques to detect resident bacterial flora in the adult female bladder. J Clin Microbiol. 2014;52(3):871–6.

134. Siddiqui H, Nederbragt AJ, Lagesen K, Jeansson SL, Jakobsen KS. Assessing diversity of the female urine microbiota by high throughput sequencing of 16S rDNA amplicons. BMC Microbiol. 2011 Dec;11(1).

135. Liu J, Wang X, Xie H, Zhong Q, Xia Y. Analysis and evaluation of different sequencing depths from 5 to 20 million reads in shotgun metagenomic sequencing, with optimal minimum depth being recommended. Genome. 2022 Sept;65(9):491–504.

136. Sims D, Sudbery I, Ilott NE, Heger A, Ponting CP. Sequencing depth and coverage: Key considerations in genomic analyses. Vol. 15, Nature Reviews Genetics. 2014. p. 121–32.

137. Kachroo N, Lange D, Penniston KL, Stern J, Tasian G, Bajic P, et al. Standardization of microbiome studies for urolithiasis: an international consensus agreement. Vol. 18, Nature Reviews Urology. Nature Research; 2021. p. 303–11.

138. Kachroo N, Monga M, Miller AW. Comparative functional analysis of the urinary tract microbiome for individuals with or without calcium oxalate calculi. Urolithiasis. 2022 June;50(3):303–17.

139. Wolfe AJ, Brubaker L. Urobiome updates: advances in urinary microbiome research. Vol. 16, Nature Reviews Urology. Nature Publishing Group; 2019. p. 73–4.

140. Garretto A, Thomas-White K, Wolfe AJ, Putonti C. Detecting viral genomes in the female urinary microbiome. J Gen Virol. 2018 Aug;99(8):1141–6.

141. Rani A, Ranjan R, McGee HS, Andropolis KE, Panchal DV, Hajjiri Z, et al. Urinary microbiome of kidney transplant patients reveals dysbiosis with potential for antibiotic resistance. Transl Res. 2017 Mar;181:59–70.

142. Jovel J, Nimaga A, Jordan T, O'Keefe S, Patterson J, Thiesen A, et al. Metagenomics Versus Metatranscriptomics of the Murine Gut Microbiome for Assessing Microbial Metabolism During Inflammation. Front Microbiol. 2022 Feb;13.

143. Spatz S, Afonso CL. Non-Targeted RNA Sequencing: Towards the Development of Universal Clinical Diagnosis Methods for Human and Veterinary Infectious Diseases. Vol. 11, Veterinary Sciences. Multidisciplinary Digital Publishing Institute (MDPI); 2024.

144. Hempel CA, Wright N, Harvie J, Hleap JS, Adamowicz SJ, Steinke D. Metagenomics versus total RNA sequencing: most accurate data-processing tools, microbial identification accuracy and perspectives for ecological assessments. Nucleic Acids Res. 2022 Sept;50(16):9279–93.

145. Irastortza-Olaziregi M, Amster-Choder O. Coupled Transcription-Translation in Prokaryotes: An Old Couple With New Surprises. Vol. 11, Frontiers in Microbiology. Frontiers Media S.A.; 2021.

Chapter 3:

Oral & Stone Microbiomes of the Dog

Elucidating the Microbiome of the Struvite Urolith from Dogs and its Relationship to the Oral Cavity

Ashleigh M Flores[1#], Rodrigo Profeta[1#], Jodi L Westropp[2*], Maria Soltero-Rivera[3*], Bart C Weimer[1*]
[1]Department of Population Health and Reproduction, 100K Pathogen Genome Project, School of Veterinary Medicine, University of California, Davis, Davis, CA, USA
[2] Department of Veterinary Medicine and Epidemiology, School of Veterinary Medicine, University of California, Davis, Davis, CA, USA
[3] Department of Surgical and Radiological Sciences, School of Veterinary Medicine, University of California, Davis, Davis, CA, USA

[#]authors contributed equally to this work

***Correspondence:**
bcweimer@ucdavis.edu
jlwestropp@ucdavis.edu
msoltero@ucdavis.edu

Keywords: urolith, urinary stone, calculi, dentistry, lithiasis, MAP, metatranscriptomics, canine, oral microbiome

Contributions:
AMF: project design, data analysis, visualization, data interpretation, writing and editing; RP: sequence analysis, bioinformatics, data analysis, visualization, editing; JLW: funding, project design, data interpretation, writing and editing, MSR: funding, project design, data interpretation, writing and editing; BCW: funding, project design, data interpretation, writing and editing

ABSTRACT

Urolithiasis is a prevalent condition reported in over 925 mammalian and non-mammalian species worldwide. Struvite uroliths comprise roughly half of all uroliths submitted to stone laboratories from dogs, and submissions remain steady over time. Over 15 different bacterial genera have been associated with struvite stones in dogs with the most commonly isolated being *Staphylococcus spp.*, and less frequently *Proteus*, *Klebsiella*. Over 15 different bacterial genera have been associated with struvite stones in dogs with *Staphylococcus spp.* being the most commonly isolated, and less frequently *Proteus*, *Klebsiella*. Ammonia production largely from urease activity coupled with subsequent urine alkalinization are widely considered central to struvite stone formation. However, investigation into alternative microbial routes for ammonia production in the context of this disease is lacking and questions remain regarding the extent of bacterial association with stone formation. Using shotgun metatranscriptomics, we found a complex microbiome with 481 genera with the most transcriptionally active being *Staphylococcus*, *Enterococcus*, and *Porphyromonas*. Multiple ammonia-producing pathways were actively expressed by multiple members of the stone microbiome. Genes for phosphate liberation and biofilm formation were also expressed in these organisms. *Enterococcus* and *Porphyromonas* also contributed to ammonia production by expression of multiple routes while *Staphylococcus* expressed only urease. Deamination accounted for the most ammonia-producing activity, with additional contributions from urease and the arginine deiminase (ADI) pathway in *Enterococcus*. All organisms expressed genes needed for phosphate and biofilm formation. The unexpected observation and transcriptional high activity of

Porphyromonas prompted a comparative analysis with the oral microbiome, revealing extensive overlap in microbial membership, suggesting that the oral cavity may serve as a reservoir for stone-associated bacteria. Together, these results uncovered a likely link between the oral and stone microbiomes in the dog, suggesting the existence of an oral-stone microbial axis that may contribute to struvite urolith formation.

INTRODUCTION

Struvite urolithiasis has been recognized in humans and dogs for over a century (1,2). It remains a prevalent and recurrent disease associated with significant morbidity—and, in some cases, mortality—in dogs worldwide (3–8). Over 50% of uroliths removed from dogs and submitted to stone laboratories are composed of struvite (3,9) with an estimated 21-35% recurrence within the first year following stone removal (10–12). Struvite urolithiasis most often occurs in the bladder of dogs however nephrolithiasis and ureterolithiasis can lead to pyelonephritis, ureteral obstruction, and signs of acute kidney injury (13).

Struvite stones form when crystals of magnesium, ammonium, and phosphate precipitate within a microbial biofilm that often adhere to the bladder mucosa to coalesce into a nidus (14,15). The most common organism associated with struvite urolithiasis in dogs is *Staphylococcus*, and less often *Proteus*, and *Klebsiella*, and rarely *Enterococcus* (3,16,17). While the first three are known urease-producing bacteria, the latter is not. Furthermore, more than 18 different genera have been identified in struvite stones removed from humans and dogs (3,10,11,16–38).

Ammonia contributes both to the composition of struvite ($MgNH_4PO_4 \cdot 6H_2O$) and to elevated urinary pH, which promotes the precipitation of ammonium and phosphate and drives struvite stone formation (39). The formation of ammonia required for struvite stone development has traditionally been explained by a urease-centric model with phosphate sourced from dietary intake and renal excretion (40), however, microbial activity within biofilms may contribute additional phosphate to the local environment. Several uropathogens, including *Staphylococcus* and *Proteus* are capable of expressing these enzymes (41,42) but to what extent they influence stone formation in vivo remains an open question.

Bacteria produce an extracellular matrix (ECM) essential for the initiation and growth of struvite crystals, with the bacterially derived glycocalyx facilitating adhesion, offering protection, and binding mineral components (43,44). Formation of struvite stones often contain numerous bacteria that proliferate within the protective biofilm, shielding them from host defenses and environmental influences, including antibiotics, making the disease difficult to treat (14,17). Various biofilm types serve as the scaffolding that facilitates struvite crystal aggregation and stone formation (14,15,45). In addition to bacteria and their products, host-derived substances such as urinary mucoproteins and glycosaminoglycans (GAGs) may become incorporated into the biofilm matrix (45,46). These host components can enhance the stabilization and aggregation of struvite crystals, further promoting stone development (46). As microcolonies mature within the stone, continued bacterial proliferation and the accumulation of exopolysaccharides (EPS) mucoproteins, and GAGs support ongoing struvite deposition, driven by elevated pH (14,43,45). Mineral precipitation is thought to

occur rapidly at the biofilm–urine interface, where the external flow of urine efficiently transports ions to the porous biofilm (47). In vitro studies have shown that urea and ammonia concentrations are highest at this interface (48). This same region marks the initial zone of struvite crystal deposition, consistent with the layered laminations that radiate from a central nidus in struvite stones (39). As the biofilm thickens and becomes more dense, zones of high saturation with struvite precursors form, further increasing the likelihood of mineral precipitation in and around the biofilm (47,48). However, urea becomes depleted at greater depths (48,49), suggesting that urease-driven hydrolysis alone cannot sustain ammonia production throughout the biofilm. This substrate stratification likely drives microbes in deeper layers to rely on alternative metabolic strategies for pH control via another substrate contained in the local proximity within biofilm (47,48). Therefore, other mechanisms for struvite precursor production are likely at play but remain under-investigated.

Traditionally, aerobic bacterial urine cultures (UC) have been considered the gold standard diagnostic for identifying bacteria in urine and stones (50,51). While UC provides information regarding bacterial species, studies suggest that discordant results between urine and stone cultures occurs (16,51). In more recent years, 16S rRNA sequencing has been widely used in urinary microbiome research in dogs (52,53). Unfortunately, both this technique and UC do not consistently provide detailed taxonomic and functional information, which limits our ability to fully understand the microbiome and reduces the usefulness of the data for elucidating disease pathophysiology (54,55). In contrast, shot-gun metatranscriptomics allow for comprehensive characterization of microbial communities, including unculturable and

low-abundance taxa that are often missed by conventional approaches, revealing bacterial names and some of the biochemical functions of the organisms that are alive, active, and expressing genes in a sample (56,57).

Research has highlighted a bidirectional relationship between the oral cavity and distant sites, including the urinary tract, which may contribute to urinary tract diseases such as urolithiasis in humans (26,58–60). *Porphyromonas*, a well-established oral organism, was found at significantly higher levels in the oral microbiome of individuals with uroliths composed of non-struvite compounds, suggesting a potential oral–stone link (59,60). Additionally, oral microbes can produce urease, raising the possibility that the oral cavity serves as a reservoir for organisms capable of contributing to struvite formation through urea-derived ammonia production (61,62).

Although the exact mechanisms of microbial transfer between organ systems remain unclear (63–67), individuals with periodontitis exhibit increased bacterial translocation, which has been associated with a higher risk of urinary stone formation (63,68–70). Disruption of epithelial barriers in periodontal disease may facilitate the spread of oral bacteria to distant sites, contributing to both local pathology and systemic physiological changes (65,71,72). Pregnancy, for example, in both dogs and humans is associated with increased oral inflammation and endothelial dysfunction—factors that may enhance microbial translocation from the oral cavity into circulation and distribution to distant tissues (73–77).

Hormonal fluctuations during pregnancy alter mucosal immunity and increase vascular permeability, reshaping the oral microenvironment (77). Elevated estrogen and progesterone concentrations enhance gingival vascularization, suppress immune

defenses, and promote inflammation, even in the absence of significant plaque (77). Progesterone, in particular, increases vascular permeability and impairs neutrophil function, potentially facilitating microbial translocation (77). As such, in this study comparisons were made between the urolith microbiome of struvite stones submitted to the laboratory that were removed from dogs and that of the oral microbiomes of dams that lacked evidence of oral disease. Their pregnancy status offered a relevant physiological context in which oral microbial translocation might be more likely, thereby strengthening their utility as a comparison group. Collectively, the gap in knowledge of how bacteria contribute to struvite formation coupled to high recurrence and source of microbes from the mouth brings about questions of microbiome membership and biochemical production of ammonia beyond current state of knowledge.

We hypothesized that a robust microbiome exists within struvite uroliths, comprising multiple organisms capable of producing ammonia through diverse metabolic routes contributing to struvite formation. The specific aims of this study were: 1) characterize the microbiome of struvite uroliths from dogs utilizing metatranscriptomics, 2) assess the transcriptional activity of microbial genes involved in ammonia production as well as other biochemical activities such as phosphatase and biofilm production, and 3) investigate the relationship between the microbiome in the oral cavity of pregnant dogs to that of the stone. Furthermore, we postulate that shared microbial taxa exist between the oral cavity and uroliths, with pregnancy increasing the likelihood of such translocation.

MATERIALS AND METHODS

Experimental Design and Specimen Collection

Stone Specimens

A selection of uroliths were submitted to, analyzed, and confirmed to be struvite at the Gerald V. Ling Urinary Stone Analysis Laboratory (University of California, Davis) between 2013-2020 (3) were used for this study. Stones composed of at least 70% struvite and ≤ 30% calcium apatite in each layer were used and large enough to provide enough material for all analyses.

Prior to RNA extraction each sample was disinfected with 70% ethanol, ground into a fine powder using a sterilized mortar and pestle, after which 0.4 g were added to 1.0 mL of LifeGuard™ (Qiagen, Germantown, MD, USA) (56,57).Specimens were immediately preserved in RNA Shield (Zymo Research Corporation, Irvine, CA) to ensure stabilization of microbial RNA at the time of collection, as previously described by the 100K Pathogen Genome Project (78) for downstream molecular analysis.

Oral Specimens

Oral specimens were collected from a different cohort of privately owned dogs undergoing Cesarean sections. All dams were deemed systemically healthy based on the absence of abnormalities on physical examination, complete blood count, and serum chemistry panel results. Pregnancy viability and litter size were confirmed via abdominal ultrasound prior to sample collection. Oral examinations of these dogs revealed only mild to moderate gingivitis, plaque, and calculus accumulation, without any clinical evidence of oral or maxillofacial trauma, neoplasia, or osteomyelitis. At the

time of Cesarean delivery, oral swabs were collected from each dam using sterile swabs (FlowQ, Copan, Murrieta, CA). Samples were obtained by gently swabbing the maxillary teeth from the canine tooth caudally to the carnassial tooth, avoiding contamination with other tissues andensuring consistent sampling of the supragingival biofilm. Specimens were immediately preserved in RNA Shield (Zymo Research Corporation, Irvine, CA) to ensure stabilization of microbial RNA at the time of collection, as previously described by the 100K Pathogen Genome Project (78) for downstream molecular analysis via total RNA extraction. Written informed consent was obtained from all owners.

RNA isolation

Total RNA extraction was performed on stone and oral specimens. The microbial portion of each specimen was collected by differential centrifugation prior to cell lysis and RNA extraction after addition to TRIzol LS (Ambion, Austin, TX, USA) following manufacturer instructions. Once the RNA was collected, purity was determined using the NanoDrop spectrophotometer (Thermo Scientific, Waltham, MA, USA) with $A_{260/230}$ and $A_{260/280}$ ratios ≥ 1.5, and the degradation was determined via TapeStation (Agilent Technologies Inc, Santa Clara, CA, USA) (78,79).

Library Preparation and Metagenome sequencing

RNA sequencing libraries were constructed using methods previously described (78–80). Briefly, KAPA HyperPlus library preparation kit (Roche Sequencing Solutions, Pleasanton, CA, USA) with a total cDNA (~100 ng) was enzymatically fragmented to

an average insert size of ~350-450 bp and the inserts were indexed using Weimer 384 TS-LT DNA barcodes (Integrated DNA Technologies, Coralville, IA, USA) and the library was size-selected by using KAPA Pure beads and dual-SPRI protocol to generate an average adapter-ligated gDNA insert molecule size of ~450-650 bp. Size-selected libraries were PCR (polymerase chain reaction) amplified for five cycles, and the average library molecular size was determined using the DNA High Sensitivity Assay kit with the Agilent 2100 Bioanalyzer (Agilent Technologies, Inc) (78–81). Libraries were sequenced on an Illumina NovaSeq S4 (Illumina, San Diego, CA, USA) using paired end 150 bp sequencing. (78–81)

Taxonomic Assignment

Using methods previously described (56,57) raw paired-end reads were trimmed to remove adapters and low-quality bases using Trimmomatic (version 0.39; command: trimmomatic PE [input] [output] ILLUMINACLIP:[adapters]:2:40:15 LEADING:2 TRAILING:2 SLIDINGWINDOW:4:15 MINLEN:50) (82). Read quality was assessed before and after trimming using FastQC (version 0.12.1), and summary reports were compiled using MultiQC (version 1.21) (83).

Trimmed reads were split into host (dog) and non-host reads using the --classified-out and --unclassified-out options in Kraken2 (version 2.1.3) (84), with a custom database built from four high-quality *Canis lupus familiaris* genomes including the reference genome for the species (*GCA_011100685.1*, German Shepherd) and three additional representatives from other breeds: *GCA_012044875.1* (Labrador Retriever), *GCA_013276365.2* (Basenji), and *GCA_031010295.1* (Cairn Terrier). Non-

host reads were subsequently classified using Kraken2, based on Kraken database of microbes from RefSeq, built on July 6, 2023. The --use-names, --report-zero-counts, and --minimum-hit-groups 3 flags were applied to enhance classification depth and specificity.

Microbial taxonomic abundances at the genus and species levels were calculated using Bracken (version 2.8) (84) with the database constructed from the same Kraken2 microbial database (k-mer size: 35; read length: 150 bp). Further analysis of relative abundance was done after normalizing the reads of each organism divided by the total reads in that specimen (85). To reduce noise, only organisms with >100 reads per sample and that were present in at least two-thirds of the samples within a given cohort were retained.

Overall, this study processed struvite stones from dogs to extract the total RNA after surface disinfection. Bucal swabs from pregnant dogs were also processed for total RNA extraction that were sequenced to on average ~22.35 million reads per sample. These sequences were examined for transcriptionally active microbial community in stones and the mouth after informatic removal of dog transcripts. This approach provided the microbiome membership expressed metabolic genes that were focused on ammonia producing routes. Because naming the organism using these methods is 98-99% accurate for genus and species, respectively (84,85), it allowed specific comparison of species/strains found in oral and stone samples.

Functional Annotation and Analysis

Quality-trimmed and adapter-removed reads were classified using Kraken2 (v2.1.3; standard database built on 2023, Jul06) (85). The --classified-out option was applied during Kraken2 classification to retain only reads assigned to a taxonomic identifier (taxid), which was included in each read header. Reads belonging to *Bacillus*, *Enterococcus*, *Porphyromonas*, and *Staphylococcus* were retrieved by matching the corresponding taxids. A custom Bash script was developed to automate the extraction, using 'grep' command to filter and separate genus-specific reads into paired FASTQ files for each taxid (zcat "$FASTQ" | grep -A 3 -w "kraken:taxid|${TAXID}" --no-group-separator | pigz -p 64 > "$OUTPUT"). Each set of genus-specific reads was independently assembled using Trinity v2.15.1 (86), with strand-specific libraries (RF orientation), 100 GB of maximum memory, and 16 CPUs per assembly. Assemblies were done separately for each genus to generate *de novo* transcriptomes representing the extracted reads.

Transcript quantification was subsequently done using Salmon v1.10.2 (87). For each genus-specific assembly, a Salmon index was created, and the extracted reads were mapped back to the corresponding assembly to obtain transcript abundance estimates. Abundance values were reported in transcripts per million (TPM) to normalize for gene length and sequencing depth across samples. Coding sequences (CDSs) were predicted and extracted from each Trinity assembly using Prokka v1.14.6 (88), using Prodigal for gene prediction. The resulting protein sequences (.faa files) were functionally annotated using EggNOG-mapper v2.1.12 (89), based on EggNOG 5.0.2 (90). Lastly, the functional annotations were integrated with the TPM abundance values, generating a genus-specific, functionally annotated abundance table that linked

predicted genes with the normalized expression levels across all samples for use in statistical analysis and graphical display.

Statistical Analysis and Plotting of Microbiome Taxonomy

Diversity Metrics

The Shannon diversity index and Bray-Curtis dissimilarity values were calculated for each specimen after grouping them into their respective cohorts (oral and stone) using the *vegan* package (Version 2.7.0) in R (Version 4.3.1) and visualized as box-and-whisker plots using *ggplot2* (Version 3.5.1) and *ggpubr* (Version 0.6.0). Differences in Shannon diversity and Bray-Curtis dissimilarity between cohorts were evaluated using a Wilcoxon rank-sum test; normality was assessed beforehand using the Shapiro–Wilk test (91).

Comparison of metranscriptomic findings to stone and urine cultures and to isolates from reported in scientific literature

UC were performed at the time of stone removal using standard culture media (3). Statistical comparisons were performed using a Wilcoxon signed-rank test to evaluate differences in average relative activity between stone and oral cohorts for genera previously associated with struvite urolithiasis in dogs, based on published literature.

Taxonomic Structure and Co-occurrence Patterns in Oral and Stone Microbiomes

To further explore the link between the oral cavity and stone microbiome a detailed assessment of the relative activity between each location was done, which was focused on the most active members of the stone microbiome.

Microbiome member distributions were visualized using alluvial plots generated with the *ggplot2* package and the *ggalluvial* package (Version 0.12.5) in R (56,57). Genera contributing <1.0% of total transcripts for a given cohort (oral or stone) were grouped as 'low activity' within that cohort.

Organisms were compared by sample type using correlation plots that were constructed using TPM values and as previously described (92). Log_2-transformed scatter plots were generated using *ggplot2* in R, with final labeling performed manually in Inkscape (Version 1.4), accessed via GitHub (https://githubcom/inkscape/inkscape) (92).

Microbial taxa co-occurrence networks within each cohort were assessed using Spearman rank correlation coefficients that were calculated with the *Hmisc* package (Version 5.2.2) in R (91). For all networks, only statistically significant ($p < 0.05$) correlations were displayed. The networks were constructed in Python (Version 3.11.5) using the *networkx* library (Version 3.1), visualized with *matplotlib* (Version 3.7.1) (93), and final color coding and labeling was done manually in Inkscape (Version 1.4) accessed via GitHub https://githubcom/inkscape/inkscape) (91).

Statistical Analysis and Visualization of Ammonia, Phosphatase, and Biofilm-Related Gene Expression in the Stone Microbiome

Differential gene expression abundance was quantified using normalized TPM values. Assessment of possible biochemical routes that produce ammonia was done and a specific list of genes associated with single steps and routes were defined (Supplemental Table 1) for use in ammonia production analyses.

One-way ANOVA was done using R to determine statistical significance in the stone cohort for deamination expression by *Staphylococcus, Enterococcus,* and *Porphyromonas*. The normality of distribution assumption was tested (Shapiro-Wilk $p > 0.05$) was met for *Enterococcus* and *Staphylococcus*, which led to the use of paired *t*-tests for pairwise comparisons to compare their respective ammonia, phosphpatase, and biofilm pathway expression. For *Porphyromonas*, the normality of distribution assumption was not met ($p < 0.05$), so a paired Wilcoxon signed-rank test was done to assess signficance between its ammonia-producing routes. Box-and-whisker plots were generated using *ggplot2* and *ggpubr*.

Metabolic capacity was visualized using radar charts and a radial tree that were generated with Flourish Studio (Canva UK Operations Ltd, https://flourishstudio/). Stacked bar charts illustrating the percentage of expression abundance were generated with GraphPad Prism (Version 10.4.2) (GraphPad, Boston, MA, USA).

RESULTS

Dog Demographics

Eleven stone specimens were met the inclusion criteria and were submitted to the laboratorie from dogs that ranged in age from 3 to 12 years and included the following breeds: Bichon Frise (n=2), Belgian Malinois (n=1, MI), Cairn Terrier cross

(n=1), Cavalier King Charles Spaniel (n=1), Dachshund cross (n=1), Miniature Poodle-Maltese cross (n=1), Terrier-Maltese cross (n=1, FS), Vizsla (n=1), and Yorkshire Terrier (n=1). Additional dog demographics can be found in Table 1, with the majority (91%) removed from spayed female dogs. The following breeds were included in the oral cohort: French Bulldog (n=4), Welsh Corgi (n=1), Newfoundland (n=1), and Boston Terrier (n=1), and additional patient demographics are provided in Table 1, with the overwhelming majority being intact pregnant female dogs.

Table 1. Mean age, weight and sex of dogs that had struvite uroliths submitted for analysis and of pregnant female dogs from which oral cavity specimens were collected. FS= Female, spayed, MI= Male intact, FI= Female Intact.

	Stone (n= 11)	**Oral (n=7)**
Mean Age ± SD (years)	6.5 ± 2.7	2.4 ± 0.8
Mean Weight ± SD (kg)	11.3 ± 9.8	16.8 ± 17.9
Sex	10 FS, 1 MI	7 FI

Overlap in community membership: oral-stone axis

Using shot gun metatranscriptomics, we observed a robustly active and diverse microbiome in stones that contained 481 genera and 693 different species/strains. Approximately 74% (356/481) of the total genera in the stone were shared with the oral cavity (Figure 1A, B, respectively). There were 1,613 total species/strains identified in the oral cavity compared to 693 in the stone (Figure 1B), of which 46.5% (322/693) were shared between stone-associated species/strains with the oral microbiome.

With nearly 47% shared community members between the stone and oral microbiomes, we examined community diversity using α-diversity of species/strains to

examine the richness and abundance of the species in the communities. A significantly ($P < 0.001$) lower richness and abundance was found in the stone samples compared to the oral samples (Figure 1C). β-diversity analysis, revealed significantly ($P < 0.01$) greater species-level diversity within the oral cohort compared to the stone cohort.

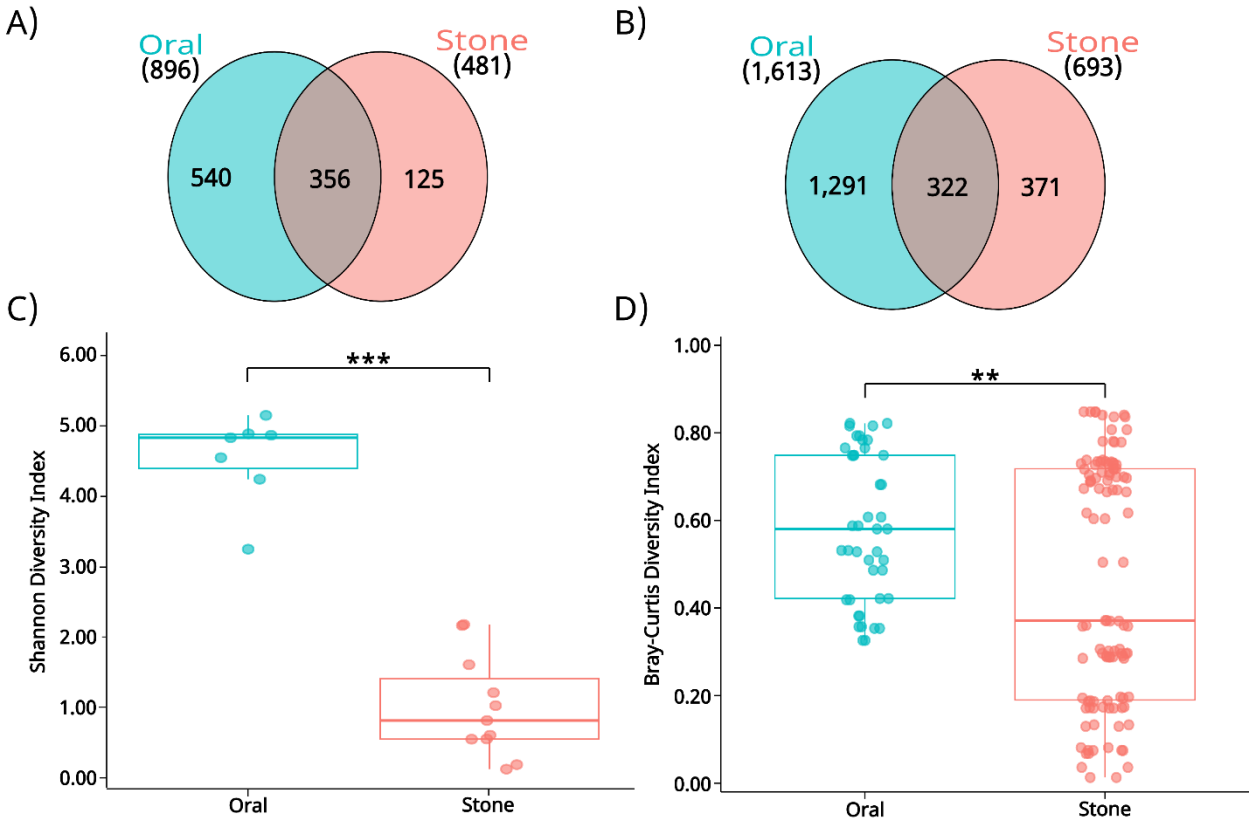

Figure 1. Comparison in the taxonomy of the dog oral microbiome and the struvite urolith microbiome. (A) Venn diagram of the unique and shared genera between the oral and stone cohorts. (B) Venn diagram of the unique and shared species/strains between the oral and stone cohorts. (C) a-diversity of the cohorts of species/strains as measured by the Shannon Index. (D) b-diversity of the oral and stone microbiomes of species/strains as measured by the Bray-Curtis dissimilarity.

Urine culture agreement between uroliths and urine specimens obtained at stone removal

Urine cultures obtained at the time of urolith removal were positive for growth in 60% (6/10) of the dogs while 73% (8/11) of stones yielded bacterial growth (Table 2).

Only *Staphylococcus* and *Enterococcus* were isolated, both of which were detected in the stone microbiomes using shotgun metatranscriptomics. Additionally, culture negative stones contained RNA from hundreds of additional genera that were active using metatranscriptomicss. All 18 previously identified genera associated with struvite uroliths in dogs and humans ??? were transcriptionally active in the stones (Table 3).

Table 2. Urine culture results and isolates obtained from struvite uroliths and urine obtained at the time of struvite stone removal in dogs. Antibiotics were to seven of the dogs at the time of urine culture and stone removal.

Organism	**Urine Cultures (n= 10)**	**Urolith Cultures (n= 11)**
Positive	6	8
Staphylococcus	4	6
Enterococcus	1	1
Both organisms found in sample	1	1
Negative	4	3

Table 3. Organisms identified from aerobic bacterial urine cultures (UC) from urine and stones of dogs and humans with struvite urolithiasis from scientific literature and detected via metatranscriptomics in this study.

Genus	**Isolation Species (Reference)**
Achromobacter spp.	Dog (11)
Candida spp.	Dog (37,38) Human (24,94)
Citrobacter spp.	Dog (20,35) Human (15)
Corynebacterium spp.	Dog (3,18,95) Human (23,24)
Enterobacter spp.	Dog (16,20) Human (24)
Enterococcus spp.	Dog (3,16,21,25) Human (24)
Escherichia spp.	Dog (16,21,25,39,96) Human (24,26,29)
Klebsiella spp.	Dog (16,21,39) Human (24,26,29)

Moraxella spp.	Dog (20) Human (24)
Mycoplasma spp.	Dog (20)
Pasteurella spp.	Dog (21) Human (24)
Proteus spp.	Dog (10,20) Human (26,28)
Providencia spp.	Dog (3,25) Human (19,30)
Pseudomonas spp.	Dog (10,18,20) Human (24,30,31,34)
Serratia spp.	Dog (36) Human (26)
Staphylococcus spp.	Dog (3,10,39) Human (24,97)
Streptococcus spp.	Dog (20,39) Human (24,97)
Ureaplasma spp.	Dog (18,39) Human (28,31,33)
Yersinia spp.	Dog (20) Human (28,32,36)

Since all of these organisms reported in Table 3 were contained in the microbiome of struvite stones in this study, and at differential activity, we proceeded to evaluate the relative microbial activity in each cohort to find that only *Staphylococcus* ($P < 0.001$) and *Enterococcus* ($P < 0.05$) were more active in the stones as compared to the oral microbiome (Figure 2). All previously reported stone-derived genera were found not only in the microbiome of the stone but also in the oral microbiome.

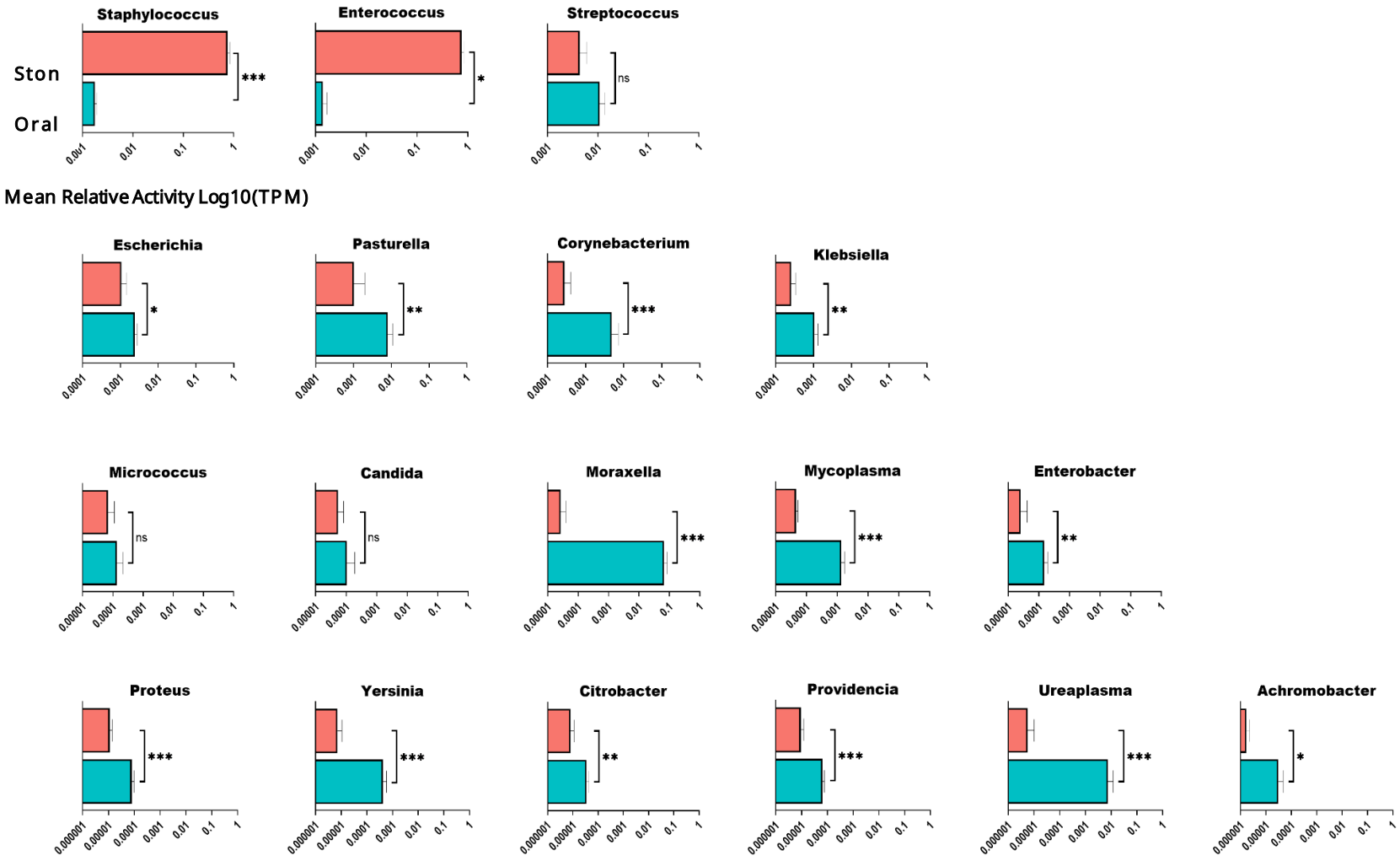

Figure 2. The mean relative activity (Log_{10}) of genera reported from the literature using AUC in comparison to those found in this study using shotgun metatranscriptomics. Error bars represent standard error of the mean (SEM). See Table 3 for citations for organisms.

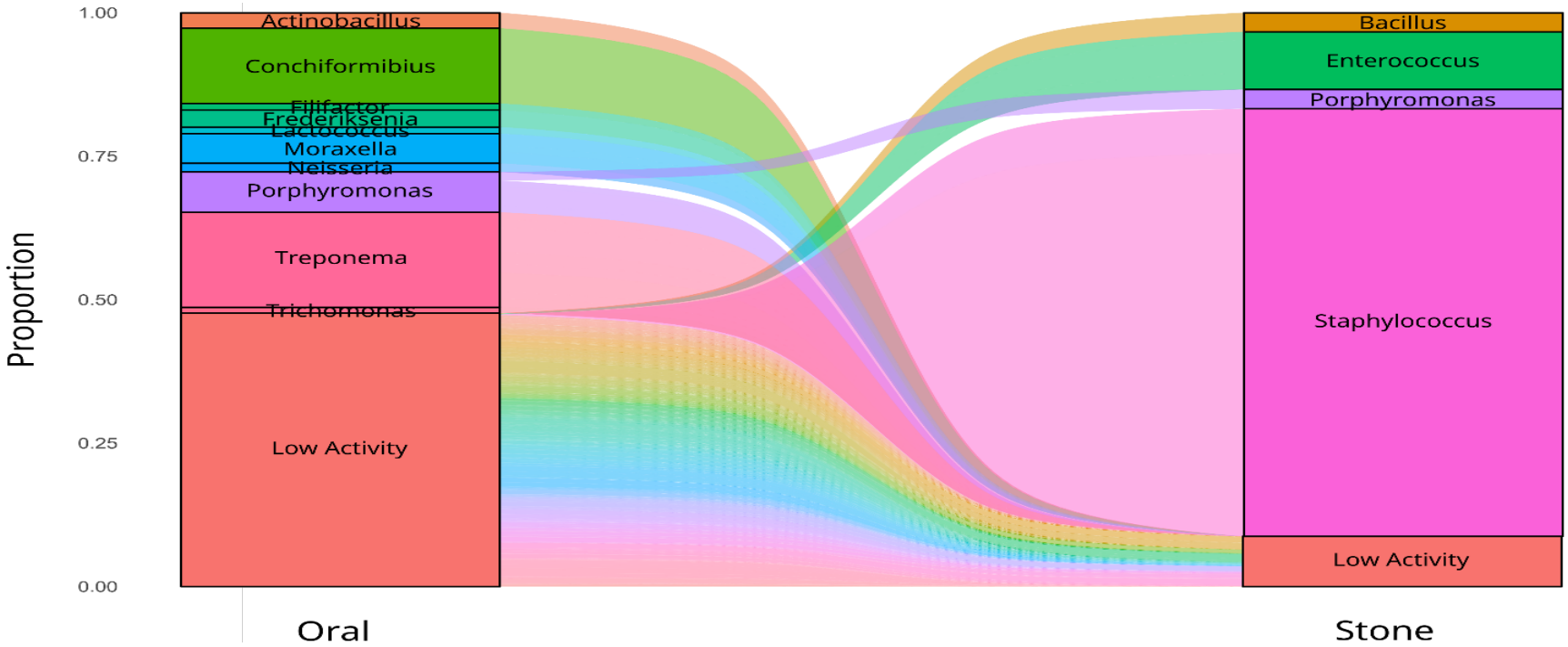

Figure 3. Taxonomic shift between the oral and stone microbiomes. Organisms with less than 0.1 of the total proportion of reads in the respective microbiome were collapsed into the 'Low Activity' category in both sample sets.

Dominant taxa in the oral and stone microbiomes

The oral microbiome contained 10 predominantly active genera that included known oral pathogens such as *Moraxella*, *Porphyromonas*, *Treponema*, and *Trichomonas*, which together accounted for 38.9% of the most transcriptionally active genera within the oral cavity (Figure 3). The most active organisms in the oral samples showed markedly reduced activity in the stone samples. Four genera—*Staphylococcus, Enterococcus*, *Porphyromonas*, and *Bacillus*—dominated the stone microbial community, accounting for 89.8% of the total active microbial population. *Bacillus* has not been previously associated with struvite urolithiasis, yet it comprised a large portion of the active organisms in the stone. *Porphyromonas,* which was found to be highly active in both the oral cavity and the stone, but different species were active in each location. This genus also exhibited species-specific shifts in activity between the cohorts, with *Porphyromonas gingivalis* dominating in the oral cavity (proportion = 0.43) but decreasing substantially in the stone cohort to become represented within the mixed group (proportion < 0.01). In contrast, *Porphyromonas cangingivalis* comprised nearly all (99.95%) of the *Porphyromonas* species detected in stones but only 0.20% of the total *Porphyromonas* species/strains present in the oral microbiome (Supplemental Figure 1).

Considering that some species exhibited niche-specific activity and switched their level of activity depending on location, we further examined species/strain changes in both sample locations. This analysis revealed that numerous genera consisting of multiple species or strains, were unique and shared between the oral cavity and stone samples (Figure 4). Multiple *Treponema* species, a well-established oral pathogen in

dogs (98–100), comprised 70% (7/10) of the most active oral-exclusive species/strains but were not found in stones. Conversely, *Staphylococcus pseudintermedius* that was previously isolated from the dog oral cavity (101), was found in the oral samples but it's abundance was more enriched in stone samples. *Proteus mirabilis* and *Klebsiella pneumoniae*, organisms commonly associated with struvite urolithiasis, were shared in both sample locations and were significantly ($P < 0.001$) more active in the oral cavity compared to the stone (Figure 4).

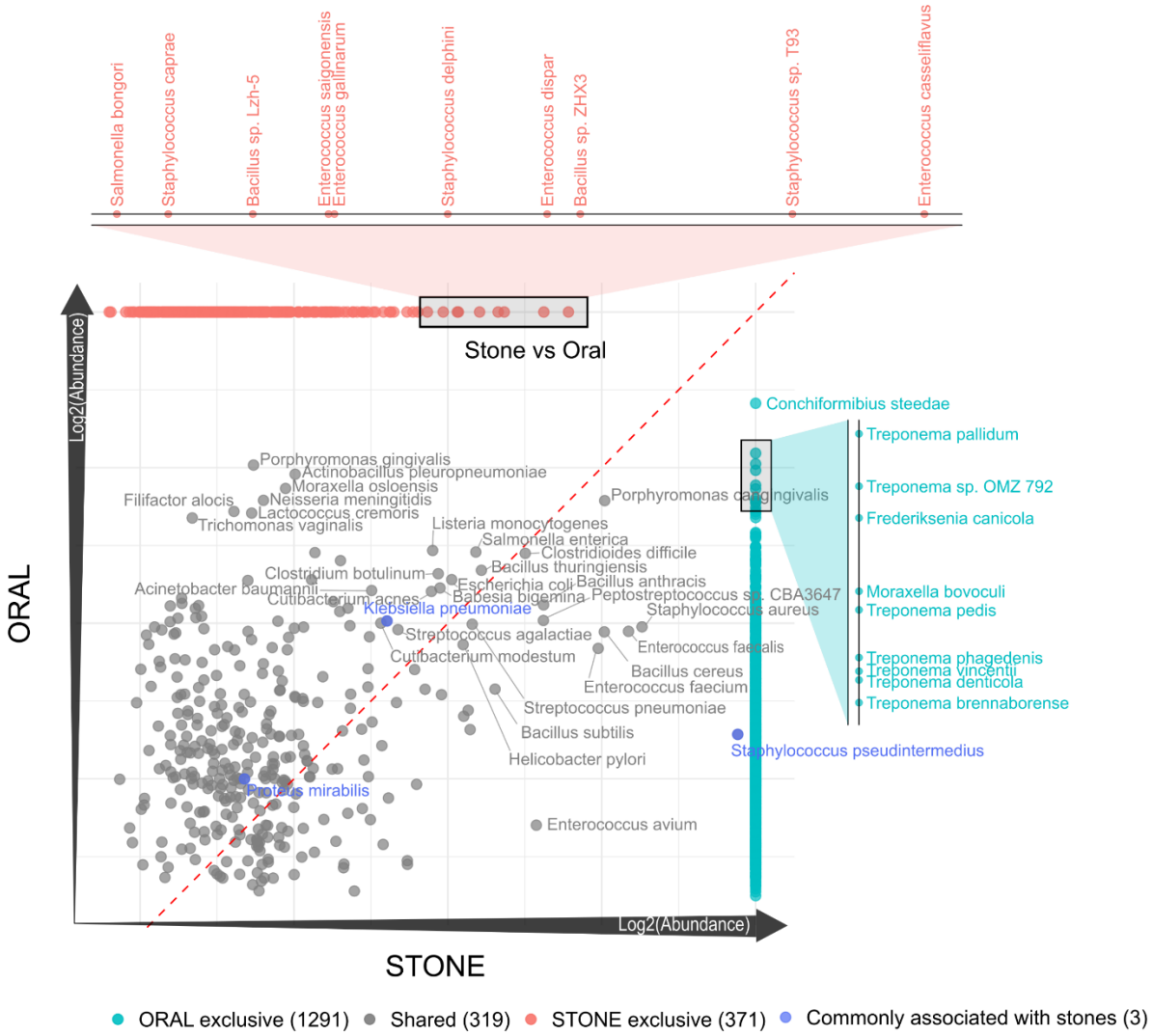

Figure 4. Correlation of the oral and stone microbiome species/strains. Each data point represents a single organism, with the diagonal line indicating equal abundance in the two cohorts. Each grey data point represents a single microbial species/strain that is present in both the oral cavity and stone. Species/strains above the dotted line are enriched in the oral cavity compared to the stone, while those below the line are enriched in the stone. The clustering pattern of data points with organisms around the center indicate a similar abundance/activity in each location. Microbes found exclusively in the stone are displayed along the top horizontal axis, parallel to the x-axis. Similarly, organisms exclusive to the oral cavity are positioned along the far-right vertical axis, parallel to the y-axis. The boxes on each of the exclusive populations are expansions to provide names of top 10 organisms.

Co-occurrence of sub-communities

The ecological metrics (Figure 1) indicate that the local environment changes the active organisms in the mouth vs the stone that creates an ecosystem specific to that

tissue. This often leads to ‘sub-communities’ of organisms that are compatible together with specific metabolic compatibility (102). In the stone, microbial sub-communities exhibited distinct co-occurrence patterns. *S. pseudintermedius* displayed very strong negative correlations with other organisms, including the lactic acid bacteria *Loigolactobacillus backii* and *Lactobacillus acidophilus* ($\rho = -0.94$, $P < 0.001$ for both) (Figure 5A). *Enterococcus faecalis* displayed a significant strong association observed with *Staphylococcus hyicus* ($\rho = -0.75$, $P = 0.008$) (Figure 5C). *P. gingivalis* exhibited very strong positive associations with multiple co-occurring taxa including *Bacillus stercoris* ($\rho = 0.98$, $P < 0.001$) (Figure 6A). In contrast, *P. cangingivalis* showed limited connectivity, with only *Peptostreptococcus* sp. CBA3647 having a very strong positive correlation ($\rho = 0.94$, $P < 0.001$) (Figure 6C).

In the oral microbiome, *S. pseudintermedius* exhibited positive correlations with all but two organisms, in stark contrast to its exclusively negative associations in the stone environment (Figure 5B). A very strong correlation was observed with *Capnocytophaga stomatis* ($\rho = 0.96$, $P < 0.001$), a dominant oral taxon, and with *Bacillus thuringiensis* ($\rho = 0.89$, $P = 0.0068$), the most abundant *Bacillus* species in the oral microbiome (Supplemental Figure 1). *E. faecalis* also formed more extensive networks in the oral cavity compared to the stone, with correlations ranging from $|\rho| = 0.75$ to 0.96 (Figure 5D), including a strong negative correlation with *Ureaplasma urealyticum* ($\rho = -0.86$, $P = 0.014$), an organism associated with struvite uroliths and encrusting cystitis (33,103). *P. cangingivalis* showed robust associations with diverse oral taxa including a very strong positive correlation with *Treponema peruense* ($\rho = 0.96$, $P < 0.001$) (Figure 6B), and a very strong negative correlation with *C. steedae* ($\rho =$

–0.93, P = 0.003). *P. gingivalis* showed very strong correlations (|ρ| = 0.96, P < 0.001) with multiple organisms—positive with *Acetoanaerobium sticklandii* and *Staphylococcus haemolyticus,* and negative with *Alysiella crassa* and *Moraxella sp. ZY190618* (Figure 6D).

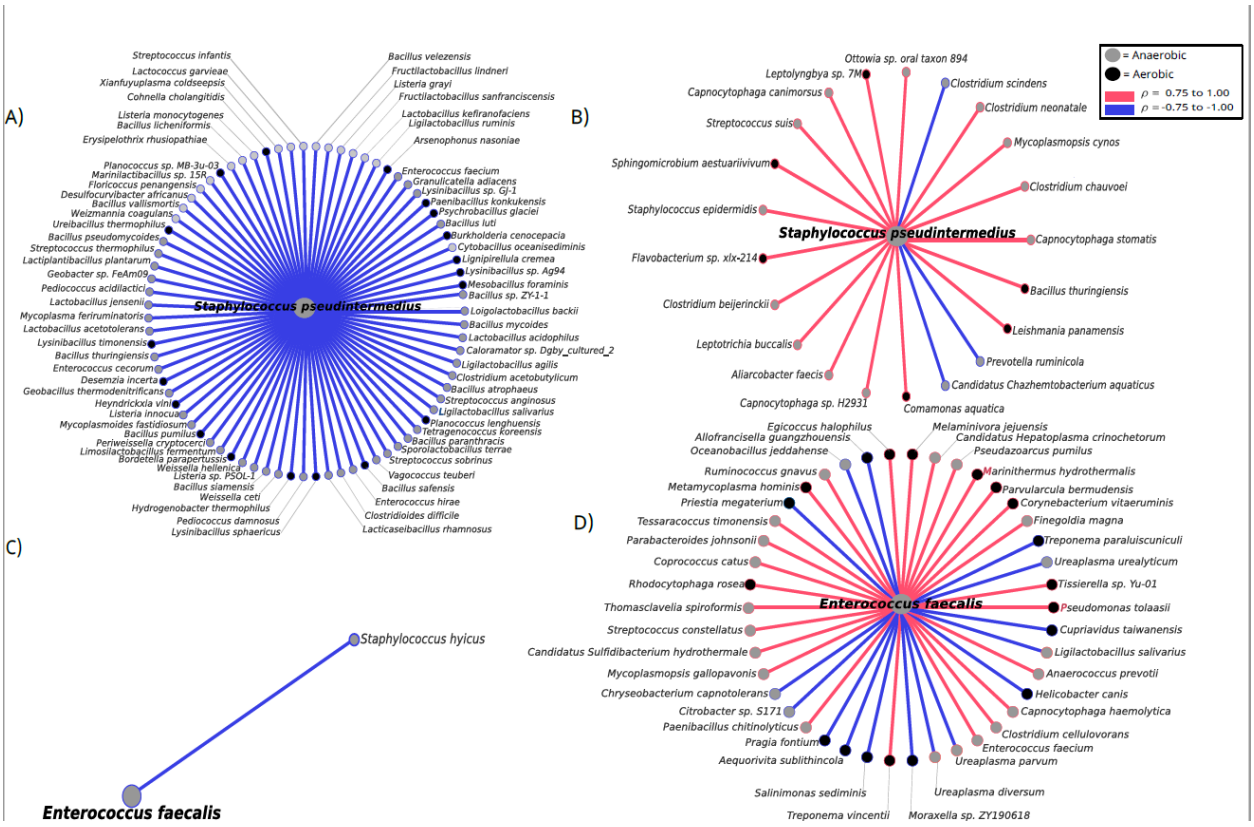

Figure 5. Co-occurrence plots at the strain- and species-level in organisms typically associated with struvite urolithiasis in the dog, identified in both the stone (A, C) and the oral (B,D) cohorts. Pink edges represent positive correlations, while blue edges represent negative correlations. Node colors reflect the oxygen requirements of organisms, classified at the strain or species level when available, or otherwise inferred from genus-level taxonomy based on published literature. A threshold of $\rho \geq 0.79$ was applied for *S. pseudintermedius.* A threshold of $\rho \geq 0.75$ was applied for *E. faecalis.* Co-occurrences shown were found to be statistically significant ($p<0.05$). Spearman rank correlation coefficients showing as follows: A) ($|\rho| = 0.79$ to 0.94), B) ($|\rho| = 0.79$ to 0.96), C) ($|\rho| = 0.75$), D) ($|\rho| = 0.75$ to 0.96).

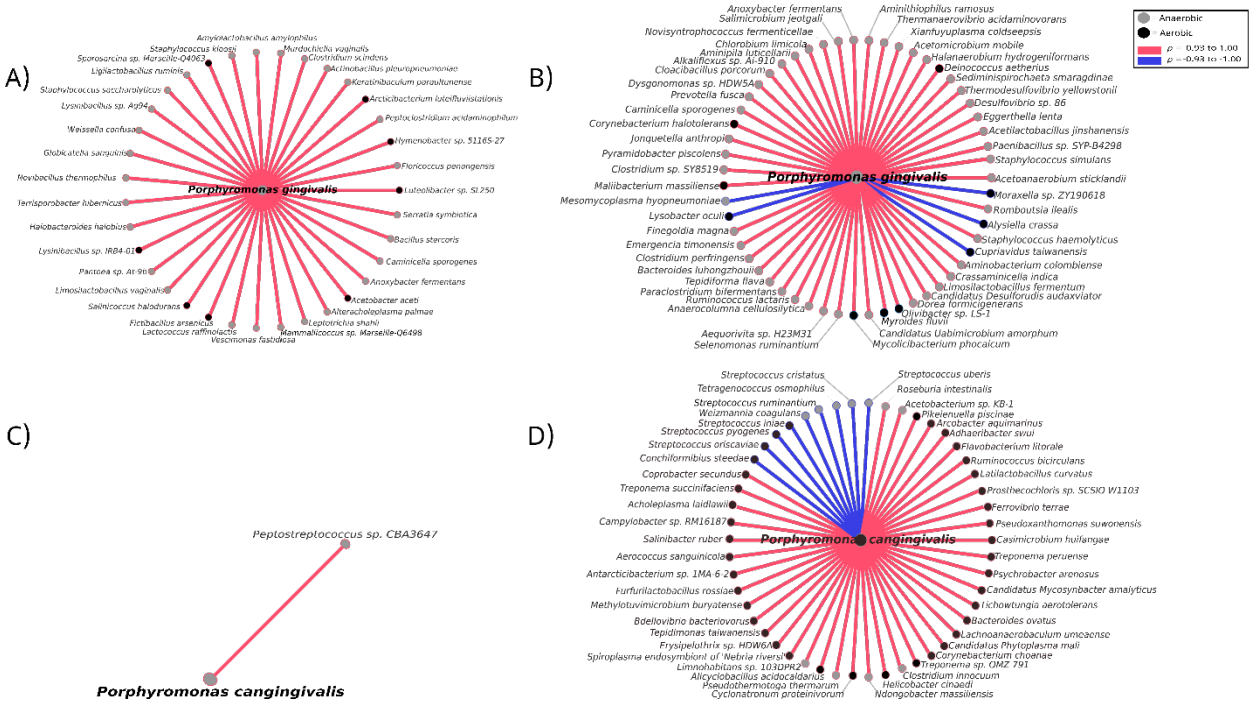

Figure 6. Co-occurrence plots at the strain- and species-level in organisms previously associated with struvite urolithiasis in the stone cohort (A, C) and the oral (B,D) cohorts. Porphyromonas species which are typically considered oral pathogens, *P. gingivalis* and *P. cangingivalis* were chosen as they were the most abundant species of *Porphyromonas* in the oral and stone cohorts, respectively (Supplemental Figure 1). Pink edges represent positive correlations, while blue edges represent negative correlations. Node colors reflect the oxygen requirements of organisms, classified at the strain or species level when available, or otherwise inferred from genus-level taxonomy based on published literature. Co-occurrences shown were found to be statistically significant ($P<0.05$). Spearman's rank correlation coefficients are as follows: A) ($|\rho|= 0.90$ to 0.98), B) ($|\rho|= 0.90$ to 0.96) C) ($|\rho|= 0.95$, $R^2= 0.90$), D) ($|\rho|= 0.92$ to 0.99)

Expression of ammonia producing routes in the stones: Urease and beyond

Use of metatranscriptomics allowed examination of gene expression directly in stone and oral samples to identify genes involved in the four major routes that yield ammonia release (Figure 7). This analysis also includes genes that sense nutrients (i.e. two component systems) as well as nutrient transporters that are difficult to assess using other techniques (104). This was particularly useful in measuring expression of route regulatory mechanisms. Specifically, *nreABC*, a nitrate-responsive two-component system that senses nitrate pool and changes metabolite pools was expressed by *Staphylococcus* presumably *to* regulates nitrate and nitrite reductase expression in response to oxygen and nitrate levels in the stone (105).

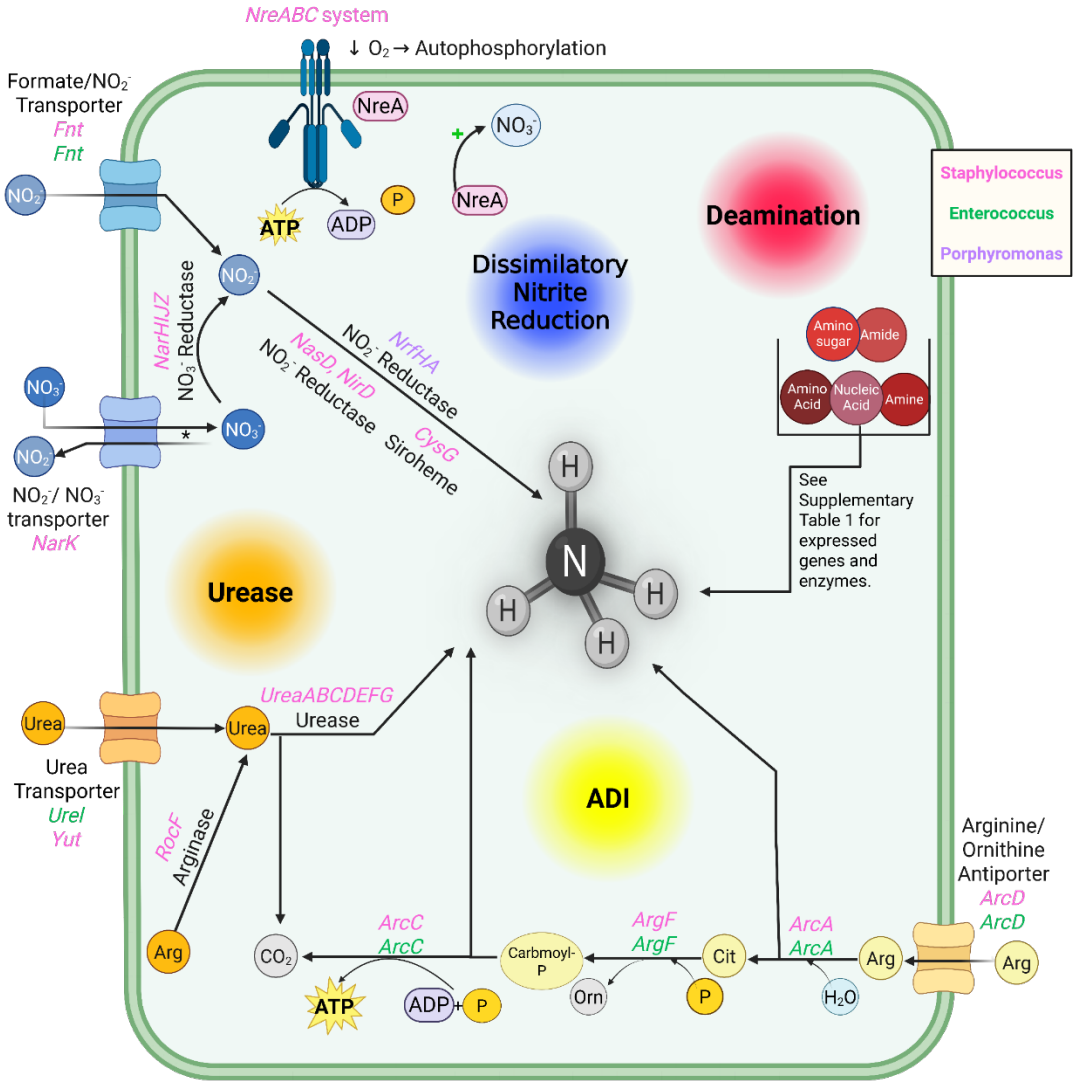

Figure 7. Routes that produce ammonia in bacteria. Expression in *Staphylococcus*, *Enterococcus*, and *Porphyromonas* within the microbiome of the dog struvite urolith are listed in specific route and step of pathways to produce ammonia. Deamination is a summation of multiple routes using multiple substrates (see Supplemental Table 1).CK= carbamate kinase, OTC= Ornithine carbmoyltransferase, ADI= Arginine Deiminase. *= During DNRA, nitrite (NO_2^-) may be exported if nitrite reductase capacity is exceeded to avoid excessive NO_2^- accumulation which can be toxic to the cell. During our analysis, it was discovered that Staphylococcus and Porphyramonas both contained sections of the DNRA (Dissimilatory Nitrate Reduction to Ammonia), nitrate reduction to nitrite and nitrite reduction to ammonia, respectively. Created using Biorender.com.

Genes involved in multiple ammonia producing routes in *Staphylococcus*, *Enterococcus*, and *Porphyromonas* were found in varying relative amounts, confirming the concurrent activity of multiple stone-promoting routes by the stone microbiome. In *Staphylococcus*, three of the four ammonia-producing routes (deamination, urease, ADI) were simultaneously expressed within the stone microbiome (Figure 8A). Expression of the three active routes differed significantly ($P < 0.001$; Figure 8A), with deamination having the highest ammonia production potential. Each route produces different amounts of ammonia. Therefore, considering the molar amount of ammonia produced by each of the routes led to deamination, urease, and the ADI pathway accounting for approximately 54.3%, 28.3%, and 17.5% of the total expression, respectively (Supplemental Figure 4A). *Staphylococcus* expressed nitrate reduction genes (*narHIJZK*) and the genes that encode for the two component regulatory system *nreB/nreC*, which controls DNRA gene expression in response to oxygen (Figure 7). However, in *Staphylococcus*, canonical genes for dissimilatory nitrite reduction to ammonia were not detected; therefore, this route was excluded from ammonia quantification in our analysis in this organism.

In *Enterococcus*, urease was not expressed but the collective ADI and deamination routes were found (Figure 8B). The ADI pathway was transcriptionally active with the expression of *arcA*, *argF*, *arcC,* and *arcD* (Figure 8B, Supplemental Figure 4A), this pathway produces two moles of ammonia per mole of Arg along with one mole of carbon dioxide. Deamination reactions showed significantly higher expression than the ADI pathway ($P < 0.01$; Figure 8B), accounting for approximately 67.0% of the total ammonia-yield–adjusted expression, while the ADI pathway

contributed the remaining 33.0% (Supplemental Figure 4A). *Enterococcus* expressed the full ethanolamine utilization (eut) operon (*eutA, eutB, eutC, eutH, eutN, eutP, eutQ*), which enables ethanolamine catabolism via deamination. The key enzyme, ethanolamine ammonia-lyase (*eutBC*), releases free ammonia from ethanolamine with 1 mole of ammonia per ethanolamine (106,107).

While *Porphyromonas* is known to contain urease in the genome, urease-associated gene expression was not observed. Experssion of the ADI pathway was also not detected. Rather, ammonia production was observed via deamination and DNRA but the two component regulator system was not expressed in this organism (Figure 8C). As in *Staphylococcus* and *Enterococcus*, deamination was also the predominant ammonia-producing route in *Porphyromonas*, accounting for 85.3% of its ammonia-adjusted yield (Supplemental Figure 4A). In addition, *Porphyromonas* expressed cytochrome c nitrite reductase (*nrfA*) that reduces nitrite to ammonia anaerobicly (108,109). Deamination expression was found to be significantly higher than nitrite reduction ($P < .001$; Figure 8D), with deamination accounting for approximately 85.3% of the total ammonia-yield-adjusted expression and nitrite reduction contributing the remaining 14.7% (Supplemental Figure 4A). When comparing expression of the ammonia producing routes among the three most abundantly active genera in the stone microbiome, *Staphylococcus* exhibited significantly higher expression of the ADI pathway compared to *Enterococcus* ($P < .001$; Figure 8D). Expression of deamination routes was observed to be higher in *Staphylococcus* compared to both *Enterococcus* and *Porphyromonas* ($P < 0.001$; Figure 8E).

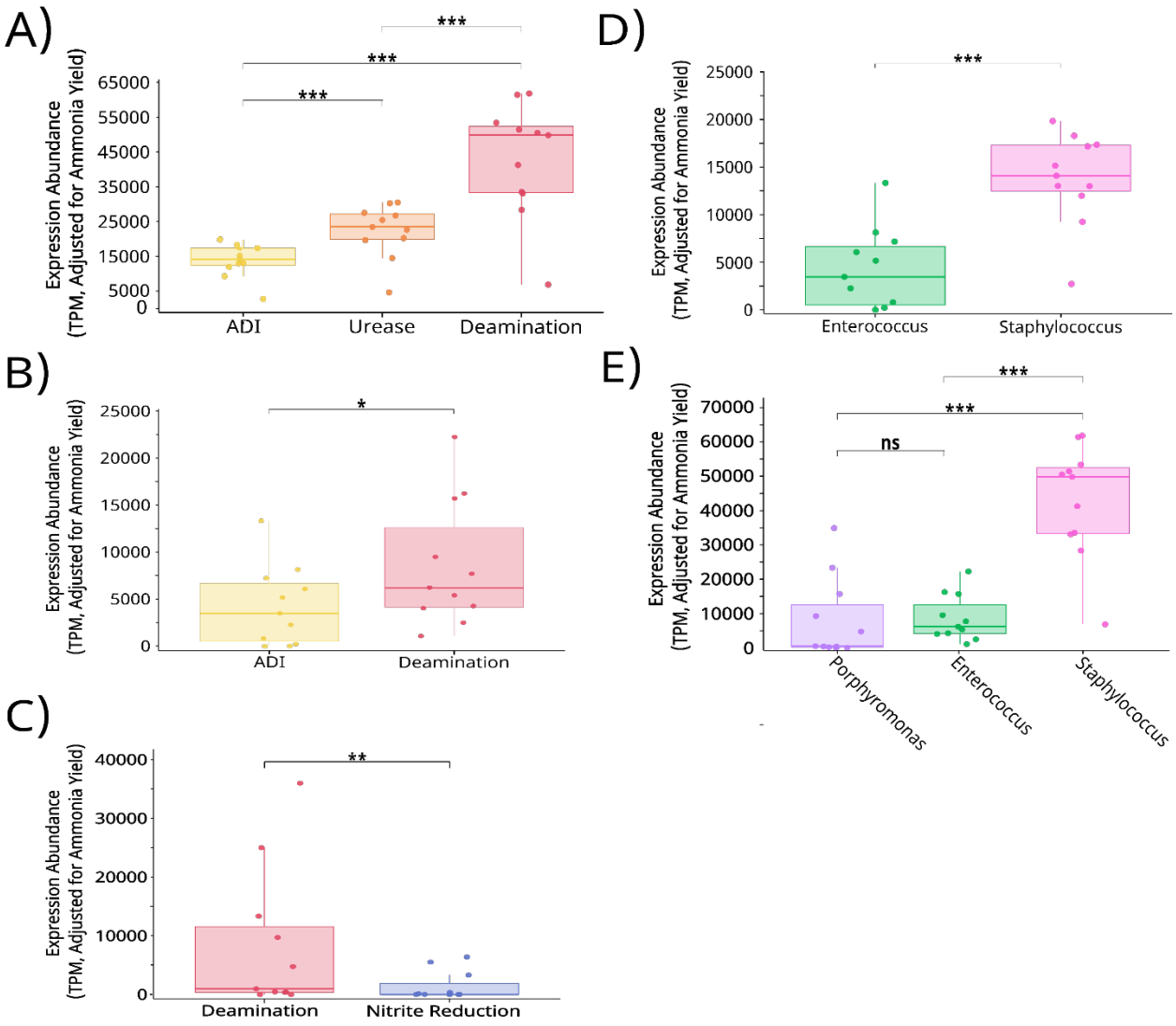

Figure 8. Expression Abundance of Ammonia Producing Routes. Panels A–C display expression abundance of ADI, urease, and deamination routes in panel A is *Staphylococcus*, B is *Enterococcus*, and C is *Porphyromonas* after adjusting for the ammonia yield per route. The urease route includes *rocF, yut*, and *ureABCDEFG*. Deamination includes genes detailed in Supp Table 1. Panels D and E show differences in expression abundance of (D) ADI and (E) deamination by genus.

Phosphate mobilization in the stone

Experssion of multipole ammonia producting routes was found and confirmed (i.e. urease) within specific members of the microbiome, we theorized that these same microbes may also express genes needed for mobilization of phosphate and biofilm production. We examined phosphatase gene expression to determine the potential for

PO_4^{3-} mobilization by the most active organisms (Supplemental Figure 4). Each organism expressed phosphatase genes with *Staphylococcus* producing ~2-fold more than *Enterococcus*, and ~3-fold more than *Porphyromonas* (Figure 9; Supplemental Figure 4B; Supplemental Table 2).

All three genera expressed both alkaline phosphatases (*phoB* or homologs of alkaline phosphatase) and acid phosphatases (*yodY* in *Enterococcus* and *pgpB3* in *Staphylococcus*), highlighting the functional importance of PO_4^{3-} release across a range of pH conditions in the struvite stone environment. Such overlapping expression profiles illustrate adaptive strategies for PO_4^{3-} mobilization across different pH environments in stones (Supplemental Table 2).

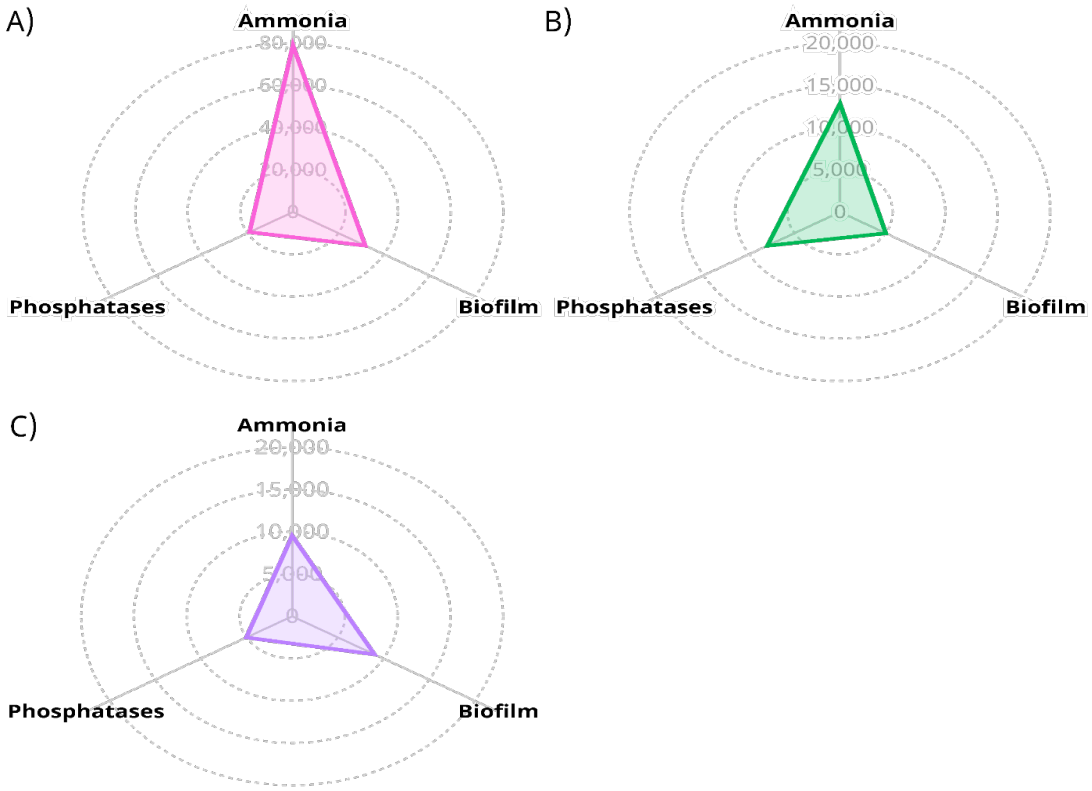

Figure 9. The relative activity of ammonia, phosphatase and biofilm associated genes in the most active organisms in stones. Each plot displays the mean expression level of each functional pathway categories. Average TPM-normalized expression adjusted for estimated ammonia yield per route: *Staphylococcus* (A), *Enterococcus* (B), and *Porphyromonas* (C).

Staphylococcus had significantly higher average phosphatase expression (TPM) compared to both *Enterococcus* ($P < 0.001$) and *Porphyromonas* ($P < 0.01$) (Supplemental Figure 4). *Staphylococcus* also expressed several phosphatases not detected in the other genera including *ppx and ppaC*. Expression of *ppx* enables the stepwise degradation of intracellular polyphosphate chains, releasing free PO_4^{3-} with each cleavage (110). Expression of *ppaC* encodes for an inorganic pyrophosphatase

that converts pyrophosphate (PPi) into two PO_4^{3-} molecules, making it another efficient source of free PO_4^{3-} (111).

Enterococcus uniquely expressed *suhB,* an inositol monophosphatase, and *ltrC,* which encodes a phosphatase involved in phospholipid processing (112,113). Expression of *rdgB* by *Enterococcus* was also observed. Although rdgB, does not directly produce PO_4^{3-}, it catalyzes the conversion of non-canonical purine nucleotides into monophosphate products and releases PPi which can then be rapidly hydrolyzed by PpaC to yield additional PO_4^{3-} (114). Together, the coordinated action of RdgB and PpaC effectively converts a single nucleotide substrate into multiple PO_4^{3-} ions, amplifying the amount of PO_4^{3-} available for release and sequestration into struvite crystals.

Although overall phosphatase expression in *Porphyromonas* was lower than that of *Staphylococcus*, the expression levels of phosphate-liberating enzymes were comparable to those observed in *Enterococcus* (Supplemental Figure 4B). *Porphyromonas* expressed several phosphatases that were not detected in *Staphylococcus* or *Enterococcus.* Notably, *Porphyromonas expressed kdsC, which* encodes a KDO 8-phosphate phosphatase, to catalyze the dephosphorylation of an intermediate in lipopolysaccharide (LPS) biosynthesis, releasing free PO_4^{3-} in the process (115,116). Additionally, *Porphyromonas* expressed *serB*, an enzyme that hydrolyzes O-phospho-L-serine to yield L-serine and free PO_4^{3-} (117). These enzyme activities highlight a distinct capacity of *Porphyromonas* to liberate PO_4^{3-} using multiple substrates associated with cell wall formation.

Biofilm production in the stone

Biofilm-associated genes were highest in *Staphylococcus* accounting for >70% of the total biofilm-related transcriptional activity among the three most active genera. Average biofilm-associated gene expression was significantly higher in *Staphylococcus* compared to both *Enterococcus* ($P < 0.001$) and *Porphyromonas* ($P < 0.01$) (Supplemental Figure 4C). *Staphylococcus* expressed the complete *icaADBC* operon that encodes enzymes responsible for the synthesis of polysaccharide intercellular adhesin (PIA), a key component of the biofilm matrix (118) (Supplemental Table 3, Supplemental Table 4). It also expressed *sarA*, a global regulator of biofilm and virulence genes, and the *agrA*, *agrB*, and *agrD* quorum sensing system components. Additional transcripts included *veg* and the *cidABC* operon. Capsule biosynthesis genes *capA, capD*, and *capO* were also expressed (119), along with *srtA* (sortase A).

Enterococcus accounted for approximately 11% of total biofilm-associated transcript abundance by the three dominant genera in the stone microbiome (Supplemental Figure 4C). Expression of *veg, srtA, srtC*, and capsule biosynthesis genes *(capA, capD, capO)* was detected (Supplemental Table 3). Additionally, *Enterococcus* uniquely expressed gelatinase, *gelE,* a crucial virulence factor that degrades host structural proteins such as collagen and fibrin while also facilitating eDNA release (120,121). A transglutaminase homologue was also expressed by *Enterococcus* (Supplemental Table 1).

Porphyromonas contributed approximately 18% of total biofilm-associated gene expression. It expressed *fimA* (major fimbrial subunit), *mmdC* (involved in poly-γ-glutamic acid (PGA)-dependent biofilm synthesis), and capsule-related genes (*cap,*

capA) (Supplemental Table 3). Like *Enterococcus*, *Porphyromonas* also expressed a transglutaminase gene.

DISCUSSION

Traditional urine and urolith cultures emphasize urease-positive bacteria such as *Staphylococcus* as primary etiological agents of canine struvite stones, but they underestimate both the taxonomic and functional diversity of stone-associated microbiota. Our metatranscriptomic approach not only confirmed the presence of all culture-reported taxa but also revealed hundreds of additional transcriptionally active genera. Importantly, this method captured the active metabolic functions of these microbes, demonstrating that diverse taxa contribute to ammonia generation, phosphate mobilization, and biofilm formation within struvite stones. These findings underscore the limitations of culture-based diagnostics and highlight the value of functional profiling in defining the microbial ecology of urolithiasis.

Overlap in community membership: oral-stone axis

The extensive overlap between stone and oral microbiome, 74% of genera and 46.5% of species/strains shared, supports the concept of an oral–stone microbial axis (Figure 1). Given our pipeline's high classification accuracy, this overlap likely reflects true ecological connectivity rather than artifact (84,85). Furthermore, genera that had been reported in the literature from dogs with struvite urolithiasis were identified not only in the stones in our dataset but also in the oral specimens (Figure 2). These findings suggest that the oral cavity might serve as a reservoir for stone-associated microbes,

though the exact routes of transmission remain unclear. Potential pathways include grooming behaviors or hematogenous spread, mechanisms already documented for oral pathogens colonizing distant organ systems (122–124). Notably, parallels between the oral cavity and urinary tract—such as biofilm formation, ureolytic activity, and localized pH elevation—point to common ecological mechanisms shaping microbial communities in both niches (15,125).

Despite broad overlap, presumptive selective pressures within the stone such as elevated pH, hypoxia, and nutrient limitation are likely contributing to the distinct community composition (48,49). Stones were dominated by facultative and strict anaerobes such as *Staphylococcus*, *Enterococcus*, *Porphyromonas*, and *Bacillus*, which accounted for nearly 90% of transcriptional activity (Figures 3 and 4). In contrast, oral samples were dominated by a broader array of genera, with aerobic and microaerophilic taxa such as *Moraxella, Treponema*, and *Trichomonas* together comprising nearly 40% of the active community (Figure 4 and 5). The constrained community composition reflects survival of organisms adapted to the stone environment, and the metabolic traits they carry such as anaerobic growth and tolerance of alkaline conditions.

Co-occurrence of sub-communities

Correlation analyses revealed that *S. pseudintermedius* is strongly negatively correlated with acid-tolerant taxa in stones (Figure 5A), suggesting that it may play a pivotal role in shaping the stone microbiome. This pattern implies that *S. pseudintermedius* could suppress acidogenic organisms either through pH modulation

or competitive exclusion, acting as a keystone species that helps structure microbial community composition within the stone. While *S. pseudintermedius* has been previously detected in the dog oral cavity (126), its transcriptional activity in oral samples was low, and it displayed predominantly positive associations with other taxa. This contrast indicates that its ecological role is context-dependent, potentially shifting from a regulatory or inhibitory function within stones to a more cooperative or neutral role in the oral environment.

Porphyromonas formed specific associations in stones that appear to support cooperative metabolism and biofilm development (Figure 6). *P. gingivalis* was strongly associated with *B. stercoris*, a surfactin-producing species that promotes biofilm matrix development and colony spreading (127,128), and with *A. sticklandii*, a strict anaerobe capable of high ammonia production via Stickland fermentation (129). Notably, *A. sticklandii* has also been detected in subgingival plaque from dogs using 16S rRNA sequencing (130), suggesting its presence across oral and stone niches. Such interactions facilitate the formation of complex, multispecies biofilms, enhancing microbial survival and pathogenicity (14,131). These interactions may include nutrient cross-feeding, co-aggregation within the biofilm matrix, or shared resistance to environmental stressors (132–134). The cooperative interactions observed, particularly among strict or facultative anaerobes, not only challenge the long-standing paradigm of single-organism causality in struvite urolithiasis but also highlight the limitations of using aerobic urine cultures as the diagnostic gold standard. These findings instead support a polymicrobial, synergistic process shaped by selective pressures and ecological interdependence.

Expression of ammonia producing routes in the stones: Urease and beyond

In addition to urease-mediated hydrolysis, multiple microbial pathways, including deamination, the ADI pathway, and dissimilatory nitrite reduction to ammonia, were actively expressed in the stone microbiome (Figures 7-9, Supplemental Table 1). *Staphylococcus* dominated ammonia production, yet only ~28% was urease-associated, with deamination (~54%) and ADI (~18%) contributing more substantial (Supplemental Figure 4). This expanded repertoire indicates that focusing solely on urease underestimates the stone microbiome's biochemical potential for ammonia production.

Staphylococcus also expressed genes indicative of an alternative DNRA pathway. The narKHIJZ operon, which facilitates nitrate uptake (NarK) and reduction to nitrite (NarGHI), was co-expressed with the nitrate sensor nreA and the two-component regulatory system nreB/nreC (Figure 7, Supplemental Table 1) (135). This regulatory system likely allows *Staphylococcus* to sense environmental nitrate levels and dynamically adjust gene expression to optimize nitrite production under anaerobic or nutrient-limited conditions, providing metabolic flexibility for ammonia generation in the stone (105,136). Although canonical dissimilatory nitrite reductases such as nrfA were absent, expression of siroheme-dependent reductases nasD and nirD, along with cysG and the fnt transporter, suggests functional nitrite reduction under anaerobic conditions (136,137). This added functionality would increase its metabolic versatility for anaerobic ammonia production in the stone.

While *Enterococcus* lacked urease expression, the notable activity of the ADI pathway suggests that arginine catabolism plays a central role in ammonia production by *Enterococcus* in the stone (Figure 7 and 8). Additionally, the expression of

transglutaminase further supports ammonia release via glutamine deamidation, offering yet another non-urease mediated ammonia-producing route (Supplemental Table 1). Further, the complete ethanolamine utilization (eut) operon was expressed by Enterococcus, enabling the breakdown of ethanolamine into acetaldehyde and free ammonia via ethanolamine ammonia-lyase (EutBC) (138). This enzymatic activity releases ammonia, raising local pH and creating conditions favorable for struvite crystallization. Ethanolamine is a degradation product of host membrane phospholipids and might accumulate in damaged or inflamed uroepithelial tissues, an anticipated consequence of struvite stone pathology (138,139). Such metabolic flexibility likely enhances local alkalinization, favoring struvite crystallization.

Porphyromonas, while lacking nitrate reduction genes, expressed *nrfA* and *nrfH* that convert nitrite to ammonia under anaerobic conditions (135). Concurrent expression of hybrid cluster protein (HCP) suggests that *Porphyromonas* can detoxify reactive nitrogen intermediates generated during nitrite reduction (140,141). *Porphyromonas* likely depends on external sources of nitrite in the stone, such as that produced by nitrate-reducing bacteria cohabiting the microbiome, including Staphylococcus
(109,140). This reliance underscores a metabolic interdependence within the community. *Porphyromonas* also expressed a broad suite of deaminases, collectively producing more ammonia per substrate than Staphylococcus or Enterococcus (Supplemental Table 1), highlighting its versatility in utilizing diverse nitrogen sources.

Collectively, these findings reveal a complex network of complementary ammonia-generating pathways across taxa, underscoring metabolic interdependence and the importance of considering non-urease routes in struvite stone formation.

Phosphate mobilization in the stone

All dominant genera in the stone microbiome employ complementary phosphate mobilization strategies, collectively ensuring a continuous supply of PO_4^{3-} under varying pH conditions (Figure 9, Supplemental Table 2). The co-expression of both acid and alkaline phosphatases, including *phoB, yodM,* and *pgpB3* homologs, reflects a shared approach to phosphate acquisition across *Staphylococcus, Enterococcus,* and *Porphyromonas*. *Staphylococcus* had the highest phosphatase activity (Figure 9) and expressed genes for unique enzymes such as Ppx and PpaC for efficient phosphate release (110,111). The coordinated action of these enzymes amplifies phosphate availability, supporting struvite crystallization and influencing the biochemical environment for other microbial community members. In contrast, *Enterococcus* uniquely expressed *suhB* which liberates PO_4^{3-} from sugar-derived signaling intermediates, and LtrC which facilitates phosphate liberation from membrane lipid precursors (112,113). *Porphyromonas* on the other hand, expressed *serB*, encoding phosphoserine phosphatase, which produces L-serine and PO_4^{3-} (117). This reaction is particularly noteworthy for its dual contribution to struvite-promoting conditions: the liberated PO_4^{3-} increases the availability of a key struvite precursor, while the resulting L-serine may serve as a substrate for ammonia production. This is supported by the expression of *sdhB*, encoding L-serine dehydratase, in both *Staphylococcus* and *Enterococcus* (Supplemental Table 1). Additionally, Porphyromonas expressed *kdsC* for LPS biosynthesis, which supports phosphate release and engages TLR4-mediated bladder responses, transiently altering urinary parameters (142,143). Despite host defenses, the persistence of struvite suggests that the host defense is insufficient to

overcome bacterial strategies such as continued release of struvite precursors. These findings underscore the metabolic versatility of dominant stone microbiome genera and highlight their interdependence, where complementary phosphate mobilization strategies collectively sustain PO_4^{3-} availability, driving struvite formation even in the face of host defenses.

Biofilm production in the stone

The three dominant genera also expressed distinct sets of biofilm-associated genes (Supplemental Tables 4). *Staphylococcus* expressed the icaADBC operon which enables synthesis of PIA, a critical biofilm matrix component (Supplemental Table 3 and 4) (118). Research demonstrates that genes involved in the ADI pathway are essential for optimal PIA production, creating a functional link between arginine catabolism (ammonia formation) and biofilm architecture (144). *Staphylococcus* within biofilm has been found to upregulate genes involved in the ADI pathway, with early biofilm formation marked by upregulation of ADI and urease gene clusters (144,145). This reflects a metabolic shift toward anaerobic pathways that sustain growth and viability within the stone's biofilm scaffolding, aligns with our observation that organisms with anaerobic capacity are dominant contributors to stone formation. formation.

It has been proposed that *Enterococcus* can increase biofilm formation in other bacteria and in mixed biofilms they may aid in matrix stabilization and support the persistence of more lithogenic species (121,146) In our study, Enterococcus expressed *srtA*, *srtC*, *veg*, and capsule biosynthesis genes (*capA*, *capD*, *capO*) (Supplemental Table 3). These findings indicate that Enterococcus likely plays a role in surface

attachment and matrix development of the biofilm while its expression of *gelE* that encodes for a matrix-degrading enzyme, likely contributes to biofilm remodeling and structural adaptation (120).

Both *Enterococcus* and *Porphyromonas* were found to express the enzyme transglutaminase (Supplemental Table 1). This enzyme plays a dual role that is highly relevant to struvite stone formation. Not only does it produce ammonia, it promotes the formation of highly cross-linked protein matrices that act as structural scaffolds for biofilm development, increasing the strength and structure (147). Additionally, transglutaminase expression in *Porphyromonas* has been shown to play a critical role in adherence of the microbe to host cells (15,148), which could further support stone development by enhancing its adherence to the uroepithelium. Together, these activities suggest that transglutaminase expression by *Enterococcus* and *Porphyromonas* may enhance both the biochemical and structural processes necessary for struvite precipitation, further emphasizing the complex microbial contributions to stone pathogenesis.

Porphyromonas also expressed unique biofilm-associated genes like that for FimA, a glycan-binding adhesin, mediates both auto-aggregation and co-aggregation with other species, promoting early biofilm organization and anchoring *Porphyromonas* within established mixed-species biofilms (Supplemental Table 3) (149–151). In struvite stones, these interactions likely occur alongside matrix components produced by *Staphylococcus* and *Enterococcus,* including PIA, exopolysaccharides, and eDNA, which contribute to biofilm stability and structural integrity (152). *Porphyromonas* also expressed genes (*mmdC*) for involved in PGA synthesis (Supplemental Table 3 and 4).

PGA-based biofilms are structurally distinct in that the compound forms a dense, gel-like matrixes that are highly hydrated and cohesive and offer superior resistance to desiccation, host defenses, and antimicrobial penetration (152–154). Together, these features suggest that Porphyromonas enhances stone biofilm resilience both through its own matrix production and by integrating into the structural networks formed by other taxa.

CONCLUSION

Through high-resolution transcriptomic profiling, we defined the taxonomic and functional profiles of the canine struvite stone microbiome and uncovered extensive overlap with the healthy canine oral microbiome. Interestingly, new microbes not previously reported in the stone like *Porphyromonas* and *Bacillus* were highly active. Although the oral microbiome was more diverse, the extensive overlap in community membership between the microbiomes suggests the existence of a functional oral-stone microbial axis.

Metatranscriptomics revealed not only canonical urease activity but also underappreciated mechanisms—including the ADI pathway, deamination of nitrogenous compounds, and dissimilatory nitrite reduction to ammonia—highlighting functional activities that would remain undetected by metagenomics or culture-dependent approaches. Rather than being driven by a single urease-positive organism, struvite stone formation appears to result from a metabolically coordinated microbial community, predominantly composed of *Staphylococcus, Enterococcus,* and *Porphyromonas,* each contributing to ammonia production, phosphate mobilization, and biofilm formation.

These metabolic routes were distributed across taxa, indicating cooperative functionality within a structured microbial consortium. This cooperative activity ensures the sustained release of ammonia and phosphate under varying environmental conditions, while biofilm-associated genes support microbial persistence and provide a scaffolding for continued mineral crystallization.

Together, these findings offer a new perspective of a polymicrobial model of struvite stone pathogenesis in dogs. This shifts the paradigm from a model centered on individual pathogens to a community-level perspective, where microbial sub-communities collectively drive the conditions required for struvite formation. This work underscores the value of functional metatranscriptomics in elucidating complex microbial interactions with real world, clinical applications and has important implications for improving future diagnostics and therapies in the clinical setting.

Acknowledgments: The authors would like to thank B. Carol Huang from the UC Davis School of Veterinary Medicine for their technical expertise.

Funding: This work was supported by UCD School of Veterinary Medicine, The Center for Companion Animal Health at the UC Davis School of Veterinary Medicine and Soltero-Rivera startup funds. Financial support for AMF was supported by the Students Training in Advanced Research (STAR) Program through a UC Davis School of Veterinary Medicine Endowment Fund, MSTP T32 (NIH Grant T32GM136559), NIH TL1 Training Grant (5TL1DK139565-02) through the LAUNCH Program, UCSF.
The funding sources were not involved in the study design, collection, analysis and interpretation of the data, in writing the report, or in the decision to submit this article for publication.

Data Availability Statement: Please contact the corresponding authors for data presented in this study.

Conflicts of Interest: The authors declare no conflicts of interest.

References

1. Perry JF. Diseases of The Urinary Organs. In: Dogs Their Management and Treatment in Disease: A Study of the Theory and Practice of Canine Medicine. 2nd ed. J. Loring Thayer; 1891. p. 89–104.

2. Robinson MR, Norris RD, Sur RL, Preminger GM. Urolithiasis: Not Just a 2-Legged Animal Disease. Vol. 179, Journal of Urology. 2008. p. 46–52.

3. Kopecny L, Palm CA, Segev G, Westropp JL. Urolithiasis in dogs: Evaluation of trends in urolith composition and risk factors (2006-2018). J Vet Intern Med. 2021 May;35(3):1406–15.

4. Mendoza-López CI, Del-Angel-Caraza J, Aké-Chiñas MA, Quijano-Hernández IA, Barbosa-Mireles MA. Epidemiology of urolithiasis in dogs from Guadalajara City, Mexico. Vet México OA. 2019 Mar;6(1).

5. Stavroulaki EM, Ortega C, Lawlor A, Lulich J, Cuq B. Trends in urolith composition and factors associated with different urolith types in dogs from the Republic of Ireland and Northern Ireland between 2010 and 2020. J Small Anim Pract. 2024 Jan;65(1):30–8.

6. Hunprasit V, Osborne CA, Schreiner PJ, Bender JB, Lulich JP. Epidemiologic evaluation of canine urolithiasis in Thailand from 2009 to 2015. Res Vet Sci. 2017 Dec;115:366–70.

7. Bende B, Kovács KB, Solymosi N, Németh T. Characteristics of Urolithiasis in the dog population of Hungary from 2001 to 2012. Vol. 63, Acta Veterinaria Hungarica. Akademiai Kiado ZRt.; 2015. p. 323–36.

8. Blavier A, Sulter A, Bogey A, Novelli K, Billiemaz B. Résultats des analyses par spectrométrie infrarouge de 1131 calculs urinaires canins prélevés de 2007 à 2010, en France. Prat Medicale Chir Anim Cie. 2012 Jan;47(1):7–16.

9. DiBartola SP, Chew DJ. Canine Urolithiasis. Compend Contin Educ Pract Vet. 1981 Mar;3(3):226–34.

10. Osborne CA, Klausner JS, Polzin DJ, Griffith DP. Etiopathogenesis of canine struvite urolithiasis. Am J Vet Res. 1986 Jan;16(1):67–86.

11. Brown NO, Parks JL, Greene RW. Recurrence of Canine Uroliths 1974. J Am Vet Med Assoc. 1977 Feb;170(4):419–22.

12. Jummai T, Boonyayatra S, Tangjitjaroen W, Akatvipat A. View of Factors affecting the recurrence of canine urolithiasis in the lower urinary tract after surgical removal. Vet Integr Sci. 2018;3(17):197–210.

13. Manoharan SA, Berent AC, Weisse CW, Purdon K, Bagley D. Medical dissolution of presumptive upper urinary tract struvite uroliths in 6 dogs (2012-2018). J Vet Intern Med. 2024 Nov;38(6):3095–104.

14. Nickel JC, Costerton JW, Mclean' RJC, Olson M. Bacterial biofilms: influence on the pathogenesis, diagnosis and treatment of urinary tract infections [Internet]. Vol. 33, Journal of Antimicrobial Chemotherapy. 1994 p. 31–41. Available from: https://academic.oup.com/jac/article/33/suppl_A/31/723390

15. Flannigan R, Choy WH, Chew B, Lange D. Renal struvite stones - Pathogenesis, microbiology, and management strategies. Nat Rev Urol. 2014;11(6):333–41.

16. Pridsadangbud N, Chantarasiri C, Visitkitjakarn N, Tantivimonkajor P, Yindee J, Mehl NS. Inconsistent and multiple bacterial species from different sample types of dogs with urolithiasis and bacterial cystitis. Thai J Vet Med. 2022 Jun;52(2):331–6.

17. Mohankumar A, Ganesh R, Shanmugam P. Exploring the Connection Between Bacterial Biofilms and Renal Calculi: A Comprehensive Review. Vol. 18, Journal of Pure and Applied Microbiology. Journal of Pure and Applied Microbiology; 2024. p. 2262–83.

18. Defarges A, Evason M, Dunn M, Berent A. Urolithiasis in Small Animals. In: Clinical Small Animal Internal Medicine. Wiley; 2020. p. 1123–56.

19. Flannigan RK, Battison A, De S, Humphreys MR, Bader M, Lellig E, et al. Evaluating factors that dictate struvite stone composition: A multi institutional clinical experience from the EDGE Research Consortium. Can Urol Assoc J. 2018 Apr;12(4):131–6.

20. Ling GV, Ruby AL, Johnson DL, Thurmond M, Franti CE. Renal calculi in dogs and cats: prevalence, mineral type, breed, age, and gender interrelationships (1981-1993). J Vet Intern Med Am Coll Vet Intern Med. 1998;12(1):11–21.

21. Ling GV, Ruby AL. Canine Uroliths Analysis of Data Derived from 813 Specimens. Vet Clin North Am Small Anim Pract. 1986 Mar;16(2):303–16.

22. Ling GV. Urinary Stone Disease. In: Lower Urinary Tract Diseases of Dogs and Cats: Diagnosis, Medical Management, Prevention [Internet]. Mosby-Year Book, Inc.; 1995. p. 144–77. Available from: https://uc-nrlf.caiasoft.com/reports/caiasoftBRW.php

23. Olender A, Bogut A, Bańska A. The role of opportunistic Corynebacterium spp. in human infections. Vol. 17, European Journal of Clinical and Experimental Medicine. Publishing Office of the University of Rzeszow; 2019. p. 157–61.

24. Parkhomenko E, Fazio AD, Tran T, Thai J, Blum K, Gupta M. A Multi-Institutional Study of Struvite Stones: Patterns of Infection and Colonization. J Endourol. 2017 May;31(5):533–7.

25. Houston DM, Moore A, Elliott DA, Biourge VC. Stone disease in animals. In: Urinary Tract Stone Disease. Springer London; 2011. p. 131–50.

26. Bostanghadiri N, Ziaeefar P, Sameni F, Mahmoudi M, Hashemi A, Darban-Sarokhalil D. The controversial association of gut and urinary microbiota with kidney stone formation. Microb Pathog. 2021 Dec;161.

27. Prywer J, Torzewska A, Cichomski M, Michałowski PP. Insights into the physical and chemical properties of struvite crystal surfaces in terms of the effectiveness of bacterial adhesion. Sci Rep. 2023 Dec;13(1).

28. Pahira J, Pevzner M. Nephrolithiasis. In: Hanno PM, Malkowicz SB, Wein AJ, editors. Penn clinical manual of urology. 1st ed. 2007.

29. Ishwarya R, Leela KV, Manjula SR. Urinary Calculi: A Study On Bacteriological Profile And Its Association Between Patients With Co-Morbidities At A Tertiary Care Hospital. J Pharm Negat Results ¦. 2022;13.

30. Griffith DP. Struvite stones. Kidney Int. 1978 May;13(5):372–82.

31. Perre EV de, Reichman G, Geyter DD, Geers C, Wissing KM, Letavernier E. Encrusted Uropathy: A Comprehensive Overview—To the Bottom of the Crust. Vol. 7, Frontiers in Medicine. Frontiers Media S.A.; 2021.

32. Bose A, Bushinsky DA. Nephrolithiasis, Nephrocalcinosis, and Hypercalciuria. In: Chronic Renal Disease. Elsevier; 2019. p. 1103–22.

33. Grenabo L, Hedelin H, Pettersson S. Urinary Infection Stones Caused by Ureaplasma urealyticum: A Review. Scand J Infect Dis. 1988;53:46–9.

34. Machado J da C, Renteria JM, Nascimento MM do, Cunha ACA, Vieira GM, Manso JEF. Association between urinary lithiasis, other than struvite by crystallography and non-ureolytic bacteria. Urolithiasis. 2024 Dec;52(1).

35. Pereira J, Pereira JDA, Bonci MM, Makita MT, Botteon RDCCM, Souza MMS de, et al. Urinary infection by Citrobacter koseri (C. diversus) in a dog affected by nephrolithiasis. Pubvet. 2021 Jan;15(02):1–6.

36. Mariano AD, Penninck DG, Sutherland-Smith J, Kudej RK. Ultrasonographic evaluation of the canine urinary bladder following cystotomy for treatment of urolithiasis. J Am Vet Med Assoc. 2018 May;252(9):1090–6.

37. Kumar M, Tufani N, Singh JL, Rajora VS. Diagnostic evaluation of renal failure in canine with special reference to urinalysis. 2354 J Entomol Zool Stud. 2017;5(6).

38. Lim BSTW. Isolation of Torulopsis Glabrata from a Urine Specimen of a Labrador Bitch with Urolithiasis. Vol. 133. 1977 p. 324.

39. Obsborne CA, Polzin DJ, Abdullahi SU, Leininger JR, Clinton CW, Griffith DP. Struvite Urolithiasis in Animals and Man: Formation, Detection, and Dissolution. Adv Vet Sci Comp Med. 1985;29:2–95.

40. Kim YJ, Kim TH, Yun SJ, Kim ME, Kim WJ, Lee SC. Renal Phosphate Control as a Reliable Predictive Factor of Stone Recurrence. J Urol. 2009 Jun;181(6):2566–72.

41. Danikowski KM, Cheng T. Alkaline Phosphatase Activity of Staphylococcus aureus Grown in Biofilm and Suspension Cultures. Curr Microbiol. 2018 Sep;75(9):1226–30.

42. Salikhova ZZ, Sokolova RB, Yusupova DV. Phosphatase from Proteus mirabilis. 2001;37(2).

43. McLean RJ, Nickel JC, Noakes VC, Costerton JW. An In Vitro Ultrastructural Study of Infectious Kidney Stone Genesis. Am Soc Microbiol. 1985;49(3):805–11.

44. Nickel JC, Emtage J, Costerton JW. Ultrastructural Microbial Ecology of Infection Induced Urinary Stones. J Urol. 1985;133(4):622–7.

45. Nickel JC, Curtis J. Biofilm Mediated Calculus Formation in the Urinary Tract. Vol. 6, Cells and Materials. 1996.

46. McLean RJC, Nickel JC. Glycosaminoglycans and struvite calculi. World J Urol. 1994 Feb;12(1):49–51.

47. Espinosa-Ortiz EJ, Gerlach R. Struvite Stone Formation by Ureolytic Biofilms. In: The Role of Bacteria in Urology. Springer International Publishing; 2019. p. 61–70.

48. Connolly JM, Jackson B, Rothman AP, Klapper I, Gerlach R. Estimation of a biofilm-specific reaction rate: Kinetics of bacterial urea hydrolysis in a biofilm. Npj Biofilms Microbiomes. 2015 Sep;1.

49. Stewart PS. Diffusion in biofilms. J Bacteriol. 2003 Mar;185(5):1485–91.

50. Brubaker L, Chai TC, Horsley H, Khasriya R, Moreland RB, Wolfe AJ. Tarnished gold—the “standard” urine culture: reassessing the characteristics of a criterion standard for detecting urinary microbes. Vol. 3, Frontiers in Urology. Frontiers Media SA; 2023.

51. Perry LA, Kass PH, Johnson DL, Ruby AL, Shiraki R, Westropp JL. Evaluation of culture techniques and bacterial cultures from uroliths. J Vet Diagn Invest. 2013 Mar;25(2):199–202.

52. Burton EN, Cohn LA, Reinero CN, Rindt H, Moore SG, Ericsson AC. Characterization of the urinary microbiome in healthy dogs. PLoS ONE. 2017 May;12(5).

53. Coffey EL, Gomez AM, Burton EN, Granick JL, Lulich JP, Furrow E. Characterization of the urogenital microbiome in Miniature Schnauzers with and without calcium oxalate urolithiasis. J Vet Intern Med. 2022 Jul;36(4):1341–52.

54. Matchado MS, Rühlemann M, Reitmeier S, Kacprowski T, Frost F, Haller D, et al. On the limits of 16S rRNA gene-based metagenome prediction and functional profiling. Microb Genomics. 2024 Feb;10(2).

55. Aguiar-Pulido V, Huang W, Suarez-Ulloa V, Cickovski T, Mathee K, Narasimhan G. Metagenomics, metatranscriptomics, and metabolomics approaches for microbiome analysis. Vol. 12, Evolutionary Bioinformatics. Libertas Academica Ltd.; 2016. p. 5–16.

56. Shaw CA, Soltero-Rivera M, Profeta R, Weimer BC. Case Report: Inflammation-Driven Species-Level Shifts in the Oral Microbiome of Refractory Feline Chronic Gingivostomatitis. Bacteria. 2025 Mar;4(1):1–0.

57. Shaw CA, Soltero-Rivera M, Profeta R, Weimer BC. Case Report: Shift from Aggressive Periodontitis to Feline Chronic Gingivostomatitis Is Linked to Increased Microbial Diversity. Pathogens. 2025 Mar;14(3).

58. Guo S, Wu G, Liu W, Fan Y, Song W, Wu J, et al. Characteristics of human oral microbiome and its non-invasive diagnostic value in chronic kidney disease. Biosci Rep. 2022 May;42(5).

59. Xu JZ, Sun JX, Miao LT, Zhang SH, Wang WJ, Liu CQ, et al. Interconnections between urolithiasis and oral health: a cross-sectional and bidirectional Mendelian randomization study. Front Med. 2023;10.

60. Xu ZJ, Chen L, Tang QL, Li D, He CJ, Xu CL, et al. Differential oral and gut microbial structure related to systemic metabolism in kidney stone patients. World J Urol. 2024 Dec;42(1).

61. Morou-Bermudez E, Elias-Boneta A, Billings RJ, Burne RA, Garcia-Rivas V, Brignoni-Nazario V, et al. Urease activity in dental plaque and saliva of children during a three-year study period and its relationship with other caries risk factors. Arch Oral Biol. 2011;56(11):1282–9.

62. Dahlén G, Hassan H, Blomqvist S, Carlén A. Rapid urease test (RUT) for evaluation of urease activity in oral bacteria in vitro and in supragingival dental plaque ex vivo. BMC Oral Health. 2018 May;18(1).

63. Britos M, Hernández M, Fernández A, Pellegrini E, Chaparro L, Chaparro A, et al. Bacterial translocation signatures and subgingival microbiome in individuals with periodontitis. Clin Oral Investig. 2025 Jun;29(6).

64. Farrugia C, Stafford GP, Potempa J, Wilkinson RN, Chen Y, Murdoch C, et al. Mechanisms of vascular damage by systemic dissemination of the oral pathogen Porphyromonas gingivalis. FEBS J. 2021 Mar;288(5):1479–95.

65. Li Q, Ouyang X, Lin J. The impact of periodontitis on vascular endothelial dysfunction. Vol. 12, Frontiers in Cellular and Infection Microbiology. Frontiers Media S.A.; 2022.

66. Tonelli A, Lumngwena EN, Ntusi NAB. The oral microbiome in the pathophysiology of cardiovascular disease. Vol. 20, Nature Reviews Cardiology. Nature Research; 2023. p. 386–403.

67. Liu L, Wei L, Mou FX, Zhang W, Wang RF, Wang Q, et al. Oral microbiome dysbiosis in women with a history of pregnancy loss: a metagenomic cross-sectional study. Sci Rep. 2025 Dec;15(1).

68. Sanchez C, Chile S, Miller A, Arroyave JS, Larenas F, Fulla J. IP15-22 MICROBIAL INTERACTIONS BETWEEN THE GUT AND URINARY TRACT: INSIGHTS INTO BACTERIAL TRANSLOCATION AND ITS ROLE IN STONE FORMATION AND STENT ENCRUSTATION. J Urol [Internet]. 2025 May [cited 2025 Aug 1];213(5S). Available from: http://www.auajournals.org/doi/10.1097/01.JU.0001109984.67114.74.22

69. Huang IS, Huang SE, Kao WT, Chiang CY, Chang T, Lin CI, et al. Patients with chronic periodontitis are more likely to develop upper urinary tract stone: A nation-wide populationbased eight-year follow up study. PeerJ. 2018;2018(7).

70. Shariff A, Patil S, Bhandi S, Licari FW. Periodontitis linked with Urinary Tract Infections- Coincidence or Causality? In: Annual Research Symposium. Roseman University of Health Sciences, College of Dental Medicine; 2025. p. 37.

71. Sudhakara P, Gupta A, Bhardwaj A, Wilson A. Oral dysbiotic communities and their implications in systemic diseases. Dent J. 2018 Jun;6(2).

72. Lee DB, Verstraete FJM, Arzi B. An Update on Feline Chronic Gingivostomatitis. Vet Clin N Am - Small Anim Pract. 2020 Sep;50(5):973–82.

73. Jennifer R, Williana B, Chad L, Richard W, Ben P. Evaluation of Gingivitis in Pregnant Beagle Dogs. J Vet Dent. 2019 Sep;36(3):179–85.

74. Kornacki J, Gutaj P, Kalantarova A, Sibiak R, Jankowski M, Wender-Ozegowska E. Endothelial dysfunction in pregnancy complications. Biomedicines. 2021 Dec;9(12).

75. Yang P, Ma G, Lu T, Zhou J, Fan H, Zhang X, et al. The influence of the oral microbiota in full-term pregnant women on immune regulation during pregnancy. Vol. 165, Journal of Reproductive Immunology. Elsevier Ireland Ltd; 2024.

76. Marcickiewicz J, Jamka M, Walkowiak J. A Potential Link Between Oral Microbiota and Female Reproductive Health. Vol. 13, Microorganisms. Multidisciplinary Digital Publishing Institute (MDPI); 2025.

77. Jawed STM, Tul Kubra Jawed K. Understanding the Link Between Hormonal Changes and Gingival Health in Women: A Review. Cureus. 2025 Jun 3;17(6):1–11.

78. Kong N, Ng W, Vivan L, Weimer BC. Production and Analysis of High Molecular Weight Genomic DNA for NGS Pipelines Using Agilent DNA Extraction Kit (p/n 200600) [Internet]. Agilent Technologies; 2014. Available from: http://100kgenome.

79. Kong N, Ng W, Foutouhi A, Huang BC, Weimer BC, Kelly L. Quality Control of High-Throughput Library Construction Pipeline for KAPA HTP Library Using an Agilent 2200 TapeStation [Internet]. 2014 Jan p. 1–8. Available from: http://100kgenome.vetmed.ucdavis.edu/

80. Beck KL, Haiminen N, Chambliss D, Edlund S, Kunitomi M, Huang BC, et al. Monitoring the microbiome for food safety and quality using deep shotgun sequencing. Npj Sci Food. 2021 Dec;5(1).

81. Haiminen N, Edlund S, Chambliss D, Kunitomi M, Weimer BC, Ganesan B, et al. Food authentication from shotgun sequencing reads with an application on high protein powders. Npj Sci Food 2019 31. 2019 Nov;3(1):1–11.

82. Bolger AM, Lohse M, Usadel B. Trimmomatic: A flexible trimmer for Illumina sequence data. Bioinformatics. 2014 Aug;30(15):2114–20.

83. Ewels P, Magnusson M, Lundin S, Käller M. MultiQC: Summarize analysis results for multiple tools and samples in a single report. Bioinformatics. 2016 Oct;32(19):3047–8.

84. Wood DE, Lu J, Langmead B. Improved metagenomic analysis with Kraken 2. Genome Biol. 2019 Nov;20(1).

85. Lu J, Breitwieser FP, Thielen P, Salzberg SL. Bracken: Estimating species abundance in metagenomics data. PeerJ Comput Sci. 2017;2017(1).

86. Grabherr MG, Haas BJ, Yassour M, Levin JZ, Thompson DA, Amit I, et al. Full-length transcriptome assembly from RNA-Seq data without a reference genome. Nat Biotechnol. 2011 Jul;29(7):644–52.

87. Patro R, Duggal G, Love MI, Irizarry RA, Kingsford C. Salmon provides fast and bias-aware quantification of transcript expression. Nat Methods. 2017;14(4):417–9.

88. Seemann T. Prokka: Rapid prokaryotic genome annotation. Bioinformatics. 2014 Jul;30(14):2068–9.

89. Cantalapiedra CP, Herṇandez-Plaza A, Letunic I, Bork P, Huerta-Cepas J. eggNOG-mapper v2: Functional Annotation, Orthology Assignments, and Domain Prediction at the Metagenomic Scale. Mol Biol Evol. 2021;38(12):5825–9.

90. Huerta-Cepas J, Szklarczyk D, Heller D, Hernández-Plaza A, Forslund SK, Cook H, et al. EggNOG 5.0: A hierarchical, functionally and phylogenetically annotated orthology resource based on 5090 organisms and 2502 viruses. Nucleic Acids Res. 2019 Jan;47(D1):D309–14.

91. Wen T, Niu G, Chen T, Shen Q, Yuan J, Liu YX. The best practice for microbiome analysis using R. Protein Cell. 2023 Oct;14(10):713–25.

92. Basbas C, Garzon A, Schlesener C, Heule M van, Profeta R, Weimer BC, et al. Unveiling the microbiome during post-partum uterine infection: a deep shotgun sequencing approach to characterize the dairy cow uterine microbiome. Anim Microbiome. 2023 Dec;5(1).

93. Batagelj V. Python Packages for Networks. In: Encyclopedia of Social Network Analysis and Mining. Springer New York; 2018. p. 1–10.

94. Lee MS, Soyster M, Woloshuk A, Assmus M, Agarwal D, Large T, et al. Comparison of Perioperative Outcomes and Clinical Characteristics of Calcium, Matrix and Struvite Stones From a Single Institution. Urology. 2022 Mar;161:25–30.

95. Bailiff NL, Westropp JL, Jang SS, Ling GV. Corynebacterium urealyticum urinary tract infection in dogs and cats: 7 cases (1996-2003). Sci Rep Retrosp Study JAVMA. 2005 May;226(10):1676–80.

96. Lulich JP, Berent AC, Adams LG, Westropp JL, Bartges JW, Osborne CA. ACVIM Small Animal Consensus Recommendations on the Treatment and Prevention of Uroliths in Dogs and Cats. J Vet Intern Med. 2016 Sep;30(5):1564–74.

97. Thompson RB, Stamey TA. Bacteriology of Infected Stones*. Urology. 1973 Dec;2(6):627–33.

98. Kwon D, Bae K, Kim HJ, Kim SH, Lee D, Lee JH. Treponema denticola as a prognostic biomarker for periodontitis in dogs. PLoS ONE. 2022 Jan;17(1 January).

99. Kwon D, Bae K, Jang K, Jo HM, Kang SS, Byun J, et al. Fusobacterium nucleatum and Treponema denticola are robust biomarkers for gingivitis and periodontitis in small dogs. Front Vet Sci. 2024;11.

100. Nises J, Rosander A, Pettersson A, Backhans A. The occurrence of Treponema spp. in gingival plaque from dogs with varying degree of periodontal disease. PLoS ONE. 2018 Aug;13(8).

101. Bailie WE, Stowe EC, Schmitt AM. Aerobic Bacterial Flora of Oral and Nasal Fluids of Canines with Reference to Bacteria Associated with Bites. J Clin Microbiol. 1978 Feb;7(2):223–31.

102. Cao Y, Wang Y, Zheng X, Li F, Bo X. RevEcoR: an R package for the reverse ecology analysis of microbiomes. BMC Bioinformatics. 2016 Jul 29;17(1):294.

103. Grenabo L, Brorson JE, Hedelin H, Pettersson S. Ureaplasma Urealyticum-Induced Crystallization of Magnesium Ammonium Phosphate and Calcium Phosphates in Synthetic Urine. J Urol. 1984 Oct;132(4):795–9.

104. Hasan MS, Feugang JM, Liao SF. A Nutrigenomics Approach Using RNA Sequencing Technology to Study Nutrient–Gene Interactions in Agricultural Animals. Curr Dev Nutr. 2019 Aug;3(8):nzz082.

105. Nilkens S, Koch-Singenstreu M, Niemann V, Götz F, Stehle T, Unden G. Nitrate/oxygen co-sensing by an NreA / NreB sensor complex of *S taphylococcus carnosus* . Mol Microbiol. 2014 Jan;91(2):381–93.

106. Dadswell K, Creagh S, McCullagh E, Liang M, Brown IR, Warren MJ, et al. Bacterial microcompartment-mediated ethanolamine metabolism in Escherichia coli urinary tract infection. Infect Immun. 2019;87(8).

107. Garsin DA. Ethanolamine utilization in bacterial pathogens: Roles and regulation. Vol. 8, Nature Reviews Microbiology. 2010. p. 290–5.

108. Welsh A, Chee-Sanford JC, Connor LM, Löffler FE, Sanford RA. Refined NrfA phylogeny improves PCR-based nrfA gene detection. Appl Environ Microbiol. 2014;80(7):2110–9.

109. Belvin BR, Gui Q, Hutcherson JA, Lewisa JP. The porphyromonas gingivalis hybrid cluster protein Hcp is required for growth with nitrite and survival with host cells. Infect Immun. 2019 Apr;87(4).

110. Dai S, Wang B, Ye R, Zhang D, Xie Z, Yu N, et al. Structural Evolution of Bacterial Polyphosphate Degradation Enzyme for Phosphorus Cycling. Adv Sci. 2024 Jul;11(26).

111. Gajadeera CS, Zhang X, Wei Y, Tsodikov OV. Structure of inorganic pyrophosphatase from Staphylococcus aureus reveals conformational flexibility of the active site. J Struct Biol. 2015 Feb;189(2):81–6.

112. Yano R, Nagai H, Shiba K, Yura T, Chang ; S., Ng D, et al. Inositol Monophosphatase Activity from the Escherichia coli suhB Gene Product. Vol. 177, JOURNAL OF BACTERIOLOGY. 1995 p. 3654–60.

113. Kumaran D, Bonanno JB, Burley SK, Swaminathan S. Crystal structure of phosphatidylglycerophosphatase (PGPase), a putative membrane-bound lipid

phosphatase, reveals a novel binuclear metal binding site and two “proton wires.” Proteins Struct Funct Genet. 2006 Sep;64(4):851–62.

114. Davies O, Mendes P, Smallbone K, Malys N. Characterisation of multiple substrate-specific (d)ITP/(d)XTPase and modelling of deaminated purine nucleotide metabolism. BMB Rep. 2012 Apr;45(4):259–64.

115. Biswas T, Yi L, Aggarwal P, Wu J, Rubin JR, Stuckey JA, et al. The tail of KdsC. Conformational changes control the activity of a haloacid dehalogenase superfamily phosphatase. J Biol Chem. 2009 Oct;284(44):30594–603.

116. Yi L, Velasquez MS, Holler TP, Woodard RW. A simple assay for 3-deoxy-D-manno-octulosonate cytidylyltransferase and its use as a pathway screen. Anal Biochem. 2011 Sep;416(2):152–8.

117. Bainbridge B, Verma RK, Eastman C, Yehia B, Rivera M, Moffatt C, et al. Role of Porphyromonas gingivalis phosphoserine phosphatase enzyme SerB in inflammation, immune response, and induction of alveolar bone resorption in rats. Infect Immun. 2010 Nov;78(11):4560–9.

118. Peng Q, Tang X, Dong W, Sun N, Yuan W. A Review of Biofilm Formation of Staphylococcus aureus and Its Regulation Mechanism. Vol. 12, Antibiotics. MDPI; 2023.

119. Wang H, Shen J, Ma K, Zhu C, Fang M, Hou X, et al. Transcriptome analysis revealed the role of capsular polysaccharides in desiccation tolerance of foodborne Staphylococcus aureus. Food Res Int. 2022 Sep;159.

120. Mohamed JA, Huang DB. Biofilm formation by enterococci. J Med Microbiol. 2007 Dec;56(12):1581–8.

121. Yang S, Meng X, Zhen Y, Baima Q, Wang Y, Jiang X, et al. Strategies and mechanisms targeting Enterococcus faecalis biofilms associated with endodontic infections: a comprehensive review. Vol. 14, Frontiers in Cellular and Infection Microbiology. Frontiers Media SA; 2024.

122. Kozak M, Pawlik A. The Role of the Oral Microbiome in the Development of Diseases. Vol. 24, International Journal of Molecular Sciences. Multidisciplinary Digital Publishing Institute (MDPI); 2023.

123. Chopra A, Franco-Duarte R, Rajagopal A, Choowong P, Soares P, Rito T, et al. Exploring the presence of oral bacteria in non-oral sites of patients with cardiovascular diseases using whole metagenomic data. Sci Rep. 2024 Dec;14(1).

124. Pisano M, Giordano F, Sangiovanni G, Capuano N, Acerra A, D’Ambrosio F. The Interaction between the Oral Microbiome and Systemic Diseases: A Narrative Review. Vol. 14, Microbiology Research. Multidisciplinary Digital Publishing Institute (MDPI); 2023. p. 1862–78.

125. D’souza LL, Lawande SA, Samuel J, Pinto MJW. Effect of salivary urea, pH and ureolytic microflora on dental calculus formation and its correlation with periodontal status. J Oral Biol Craniofacial Res. 2023 Jan;13(1):8–12.

126. Portilho FVR, Nóbrega J, Almeida BO de, Mota AR, Paula CL de, Listoni FJP, et al. Microbial Complexity of Oral Cavity of Healthy Dogs Identified by Mass Spectrometry and Next-Generation Sequencing. Animals. 2023 Aug;13(15).

127. Chouaia B, Dittmer J. A 2000-Year-Old Bacillus stercoris Strain Sheds Light on the Evolution of Cyclic Antimicrobial Lipopeptide Synthesis. Microorganisms. 2024 Feb;12(2).

128. Zhang Y, Qi J, Wang Y, Wen J, Zhao X, Qi G. Comparative study of the role of surfactin-triggered signalling in biofilm formation among different Bacillus species. Microbiol Res. 2022 Jan;254.

129. Fonknechten N, Chaussonnerie S, Tricot S, Lajus A, Andreesen JR, Perchat N, et al. Clostridium sticklandii, a specialist in amino acid degradation:Revisiting its metabolism through its genome sequence. BMC Genomics. 2010 Oct;11(1).

130. Dewhirst FE, Klein EA, Thompson EC, Blanton JM, Chen T, Milella L, et al. The canine oral microbiome. PLoS ONE. 2012 Apr;7(4).

131. Armbruster CE, Smith SN, Johnson AO, DeOrnellas V, Eaton KA, Yep A, et al. The pathogenic potential of Proteus mirabilis is enhanced by other uropathogens during polymicrobial urinary tract infection. Infect Immun. 2017;85(2).

132. Fritts RK, McCully AL, McKinlay JB. Extracellular Metabolism Sets the Table for Microbial Cross-Feeding. Microbiol Mol Biol Rev. 2021 Feb;85(1).

133. Smith NW, Shorten PR, Altermann E, Roy NC, McNabb WC. The Classification and Evolution of Bacterial Cross-Feeding. Front Ecol Evol. 2019 May;7.

134. Valiei A, Dickson A, Aminian-Dehkordi J, Mofrad MRK. Metabolic interactions shape emergent biofilm structures in a conceptual model of gut mucosal bacterial communities. NPJ Biofilms Microbiomes. 2024 Dec;10(1):99.

135. Wang C, He T, Zhang M, Zheng C, Yang L, Yang L. Review of the mechanisms involved in dissimilatory nitrate reduction to ammonium and the efficacies of these mechanisms in the environment. Vol. 345, Environmental Pollution. Elsevier Ltd; 2024.

136. Durand S, Guillier M. Transcriptional and Post-transcriptional Control of the Nitrate Respiration in Bacteria. Vol. 8, Frontiers in Molecular Biosciences. Frontiers Media S.A.; 2021.

137. Nakano MM, Hoffmann T, Zhu YI, †, Jahn and D. Nitrogen and Oxygen Regulation of Bacillus subtilis nasDEF Encoding NADH-Dependent Nitrite Reductase by TnrA and ResDE. J Bacteriol. 1998;180(20):5344–50.

138. Sintsova A, Smith S, Subashchandrabose S, Mobley HL. Role of Ethanolamine Utilization Genes in Host Colonization during Urinary Tract Infection. Infect Immun. 2018 Mar;86(3):1–10.

139. Reyes L, Reinhard M, Brown MB. Different inflammatory responses are associated with Ureaplasma parvum-induced UTI and urolith formation. BMC Infect Dis. 2009 Jan;9.

140. Lewis JP, Yanamandra SS, Anaya-Bergman C. HcpR of Porphyromonas gingivalis is required for growth under nitrosative stress and survival within host cells. Infect Immun. 2012 Sep;80(9):3319–31.

141. Lewis AJ, Richards AC, Mulvey MA. Invasion of Host Cells and Tissues by Uropathogenic Bacteria. Microbiol Spectr. 2016 Dec;4(6).

142. Aguiniga LM, Yaggie RE, Schaeffer AJ, Klumpp DJ, Klumpp J, Weiser AC, et al. Lipopolysaccharide Domains Modulate Urovirulence Uropathogenic Escherichia coli (UPEC) accounts for 80 to 90% of urinary tract infections (UTI), and the increasing rate of anti-biotic resistance among UPEC isolates reinforces the need for vaccines to prevent UTIs and recurrent infections. Previous stud-ies have shown that UPEC isolate NU14 suppresses proinflammatory NF-B-dependent cytokines (D. 2016; Available from: http://dx.doi.org/10.1128/IAI.69.11

143. Ueda N, Kondo M, Takezawa K, Kiuchi H, Sekii Y, Inagaki Y, et al. Bladder urothelium converts bacterial lipopolysaccharide information into neural signaling via an ATP-mediated pathway to enhance the micturition reflex for rapid defense. Sci Rep. 2020 Dec;10(1).

144. Vandecandelaere I, Nieuwerburgh FV, Deforce D, Coenye T. Metabolic activity, urease production, antibiotic resistance and virulence in dual species biofilms of Staphylococcus epidermidis and Staphylococcus aureus. PLoS ONE. 2017 Mar;12(3).

145. Vlaeminck J, Lin Q, Xavier BB, Backer SD, Berkell M, Greve HD, et al. The dynamic transcriptome during maturation of biofilms formed by methicillin-resistant Staphylococcus aureus. Front Microbiol. 2022 Jul;13.

146. Hatt JK, Rather PN. Role of Bacterial Biofilms in Urinary Tract Infections. In: Romeo T, editor. Current Topics in Microbiology and Immunology: Bacterial Biofilms. Springer-Verlag; 2008. p. 163–92.

147. Kolotylo V, Piwowarek K, Kieliszek M. Microbiological transglutaminase: Biotechnological application in the food industry. Vol. 18, Open Life Sciences. Walter de Gruyter GmbH; 2023.

148. Boisvert H, Lorand L, Duncan MJ. Transglutaminase 2 is essential for adherence of Porphyromonas gingivalis to host cells. Proc Natl Acad Sci U S A. 2014;111(14):5355–60.

149. Sakanaka A, Takeuchi H, Kuboniwa M, Amano A. Dual lifestyle of Porphyromonas gingivalis in biofilm and gingival cells. Microb Pathog. 2016;94:42–7.

150. Gerits E, Verstraeten N, Michiels J. New approaches to combat Porphyromonas gingivalis biofilms. J Oral Microbiol. 2017;9(1).

151. Wu J, Lin X, Xie H. Porphyromonas gingivalis short fimbriae are regulated by a FimS/FimR two-component system. FEMS Microbiol Lett. 2007 Jun;271(2):214–21.

152. Balducci E, Papi F, Capialbi DE, Bino LD. Polysaccharides' Structures and Functions in Biofilm Architecture of Antimicrobial-Resistant (AMR) Pathogens. Vol. 24, International Journal of Molecular Sciences. Multidisciplinary Digital Publishing Institute (MDPI); 2023.

153. Elbanna K, Alsulami FS, Neyaz LA, Abulreesh HH. Poly (γ) glutamic acid: a unique microbial biopolymer with diverse commercial applicability. Vol. 15, Frontiers in Microbiology. Frontiers Media SA; 2024.

154. Morris RJ, Stevenson D, Sukhodub T, Stanley-Wall NR, MacPhee CE. Density and temperature controlled fluid extraction in a bacterial biofilm is determined by poly-γ-glutamic acid production. Npj Biofilms Microbiomes. 2022 Dec;8(1).

155. Mcgee DJ, Radcliff FJ, Mendz GL, Ferrero RL, Mobley HLT. Helicobacter pylori rocF Is Required for Arginase Activity and Acid Protection In Vitro but Is Not Essential for Colonization of Mice or for Urease Activity. Vol. 181, JOURNAL OF BACTERIOLOGY. 1999 p. 7314–22.

156. Manna AC, Leo S, Girel S, González-Ruiz V, Rudaz S, Francois P, et al. Teg58, a small regulatory RNA, is involved in regulating arginine biosynthesis and biofilm formation in Staphylococcus aureus. Sci Rep. 2022 Dec;12(1).

157. Sebbane F, Bury-Moné S, Cailliau K, Browaeys-Poly E, Reuse HD, Simonet M. The Yersinia pseudotuberculosis Yut protein, a new type of urea transporter homologous to eukaryotic channels and functionally interchangeable in vitro with the Helicobacter pylori Urel protein. Mol Microbiol. 2002;45(4):1165–74.

158. Krajewska B. Ureases I. Functional, catalytic and kinetic properties: A review. Vol. 59, Journal of Molecular Catalysis B: Enzymatic. Elsevier; 2009. p. 9–21.

159. Stuart MR, Chou LS, Weimer BC. Influence of Carbohydrate Starvation and Arginine on Culturability and Amino Acid Utilization of Lactococcus lactis subsp. lactis. Appl Environ Microbiol. 1999 Feb;65(2):665–73.

160. Zuniga M, Perez G, Gonzalez-Candelas F. Evolution of arginine deiminase (ADI) pathway genes. Mol Phylogenet Evol. 2002 May;25:429–44.

161. Aakra Å, Vebø H, Snipen L, Hirt H, Aastveit A, Kapur V, et al. Transcriptional response of Enterococcus faecalis V583 to erythromycin. Antimicrob Agents Chemother. 2005 Jun;49(6):2246–59.

162. Keogh D, Tay WH, Ho YY, Dale JL, Chen S, Umashankar S, et al. Enterococcal Metabolite Cues Facilitate Interspecies Niche Modulation and Polymicrobial Infection. Cell Host Microbe. 2016 Oct;20(4):493–503.

163. Reslane I, Halsey CR, Stastny A, Cabrera BJ, Ahn J, Shinde D, et al. Catabolic Ornithine Carbamoyltransferase Activity Facilitates Growth of Staphylococcus aureus in Defined Medium Lacking Glucose and Arginine. mBio. 2022 Jun;13(3).

164. Beenken KE, Dunman PM, McAleese F, Macapagal D, Murphy E, Projan SJ, et al. Global gene expression in Staphylococcus aureus biofilms. J Bacteriol. 2004 Jul;186(14):4665–84.

165. Aniba R, Dihmane A, Raqraq H, Ressmi A, Nayme K, Timinouni M, et al. Exploring staphylococcus in urinary tract infections: A systematic review and meta-analysis on the epidemiology, antibiotic resistance and biofilm formation. Vol. 110, Diagnostic Microbiology and Infectious Disease. Elsevier Inc.; 2024.

166. Dale JL, Nilson JL, Barnes AMT, Dunny GM. Restructuring of Enterococcus faecalis biofilm architecture in response to antibiotic-induced stress. Npj Biofilms Microbiomes. 2017 Jun 30;3(1):15.

167. Bao K, Belibasakis GN, Thurnheer T, Aduse-Opoku J, Curtis MA, Bostanci N. Role of Porphyromonas gingivalis gingipains in multi-species biofilm formation. BMC Microbiol. 2014 Oct;14(1).

SUPPLEMENTAL FIGURES

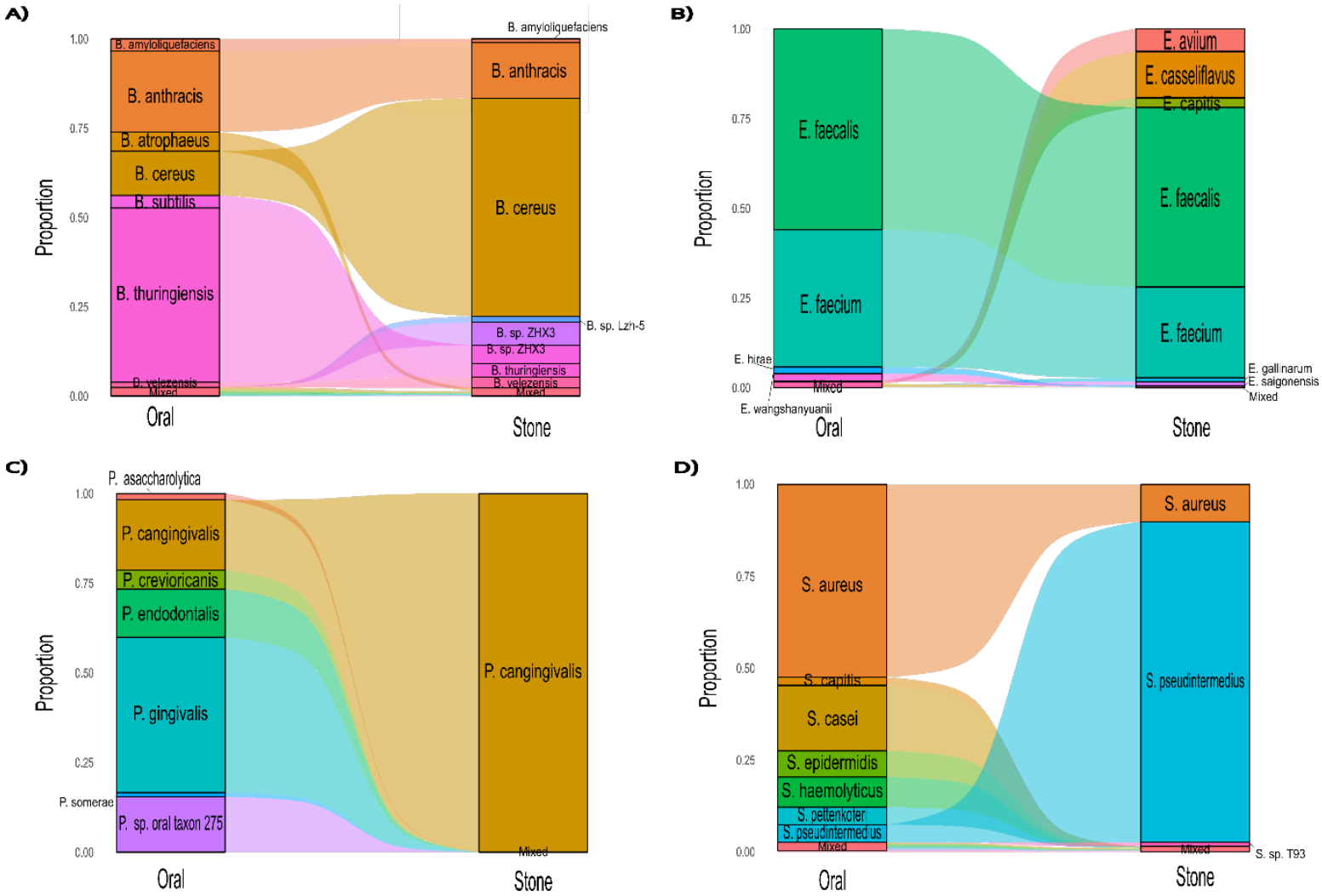

Supplementary Figure 1. Species- and strain-level shifts between keystone genera (proportion > 01; Fig 4). in the oral and stone microbiomes Alluvial plot displaying species/strain composition on the strata and species/strain shifts on the alluvia Organisms with less than 0.1 of the total proportion of reads in the microbiome were collapsed into the 'Mixed' category.

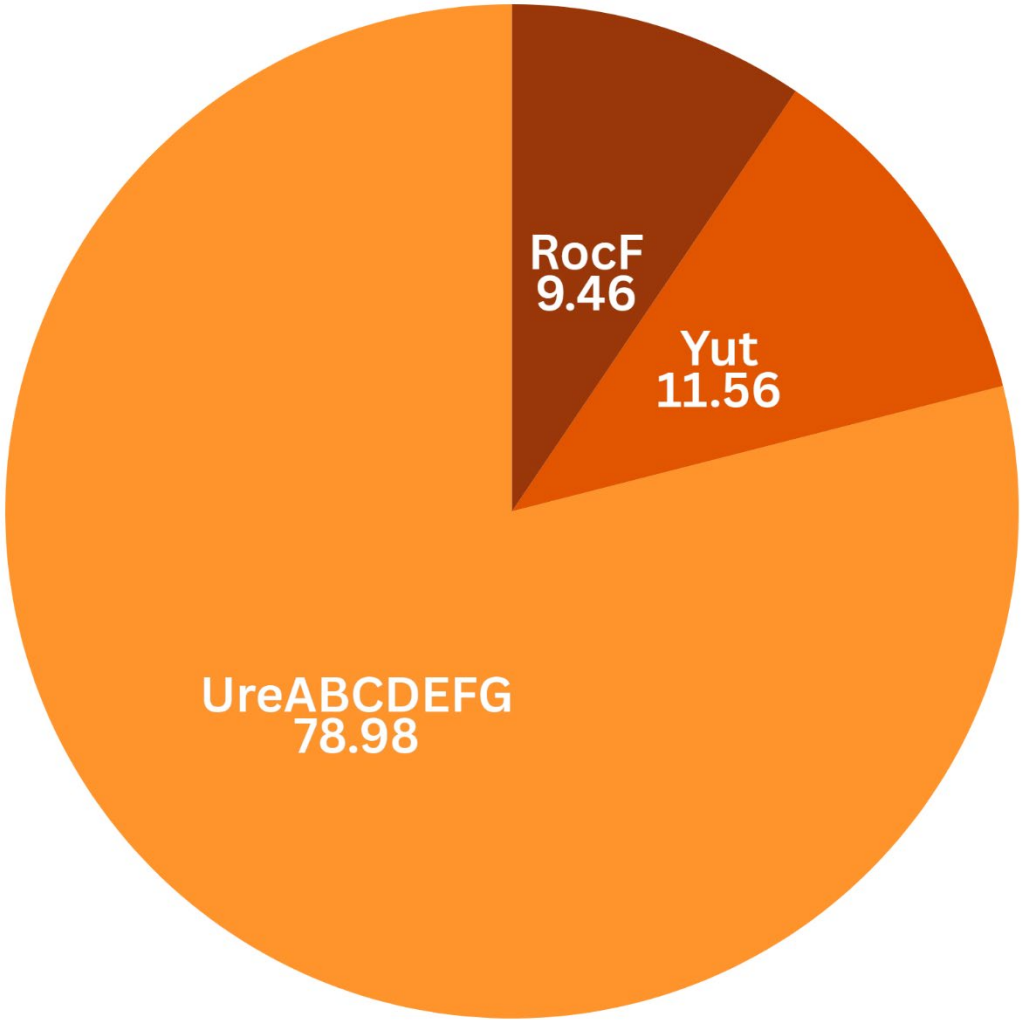

Supplementary Figure 2. Percentage of Average Expression Abundance related to Urease-associated expression in Staphylococcus. The category “urease” was defined as the combined expression of genes encoding intracellular urea production *(rocF),* urea transport *(yut),* and urea hydrolysis *(ureABCDEFG).*

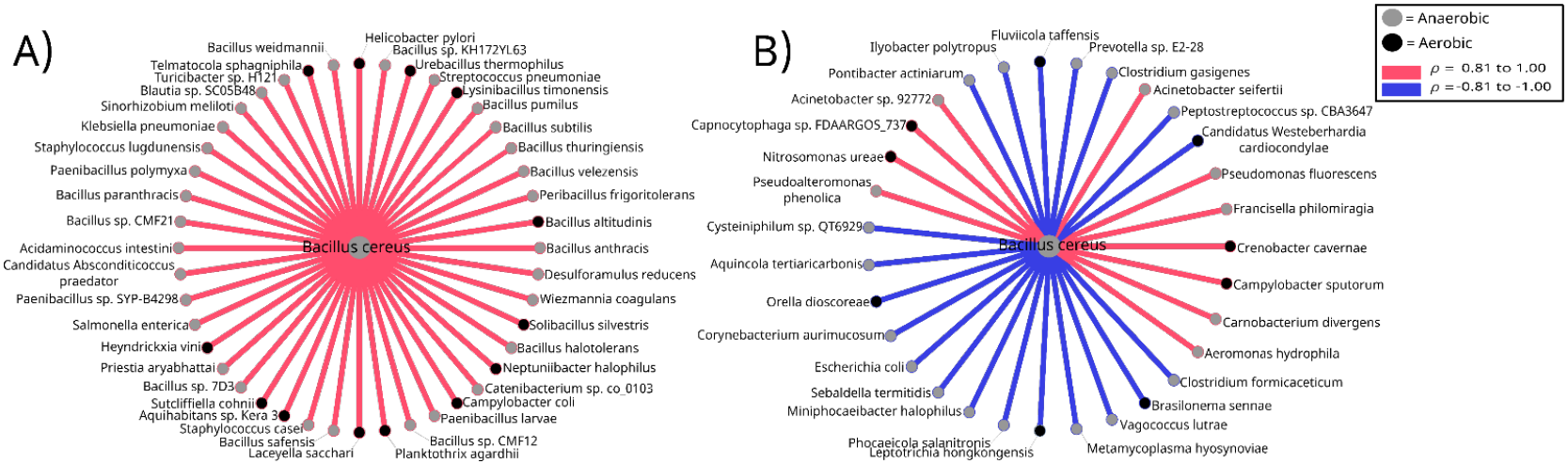

Supplementary Figure 3. Co-occurrence in Bacillus cereus in the Stone (A) and Oral (B) cohorts. Co-occurrences shown were found to be statistically significant (P<0.05). Spearman rank correlation coefficients= A) |ρ| = 0.90–0.99 (R^2 = 0.81–0.98) B) |ρ| = 0.90 to 0.99 (R^2 = 0.81–0.98). Shades of pink represent positive correlations (ρ = 0.90 to 1.00), while shades of blue indicate negative correlations (ρ = –0.90 to –1.00). Node colors reflect the oxygen requirements of organisms, classified at the strain or species level when available, or otherwise inferred from genus-level taxonomy based on published literature.

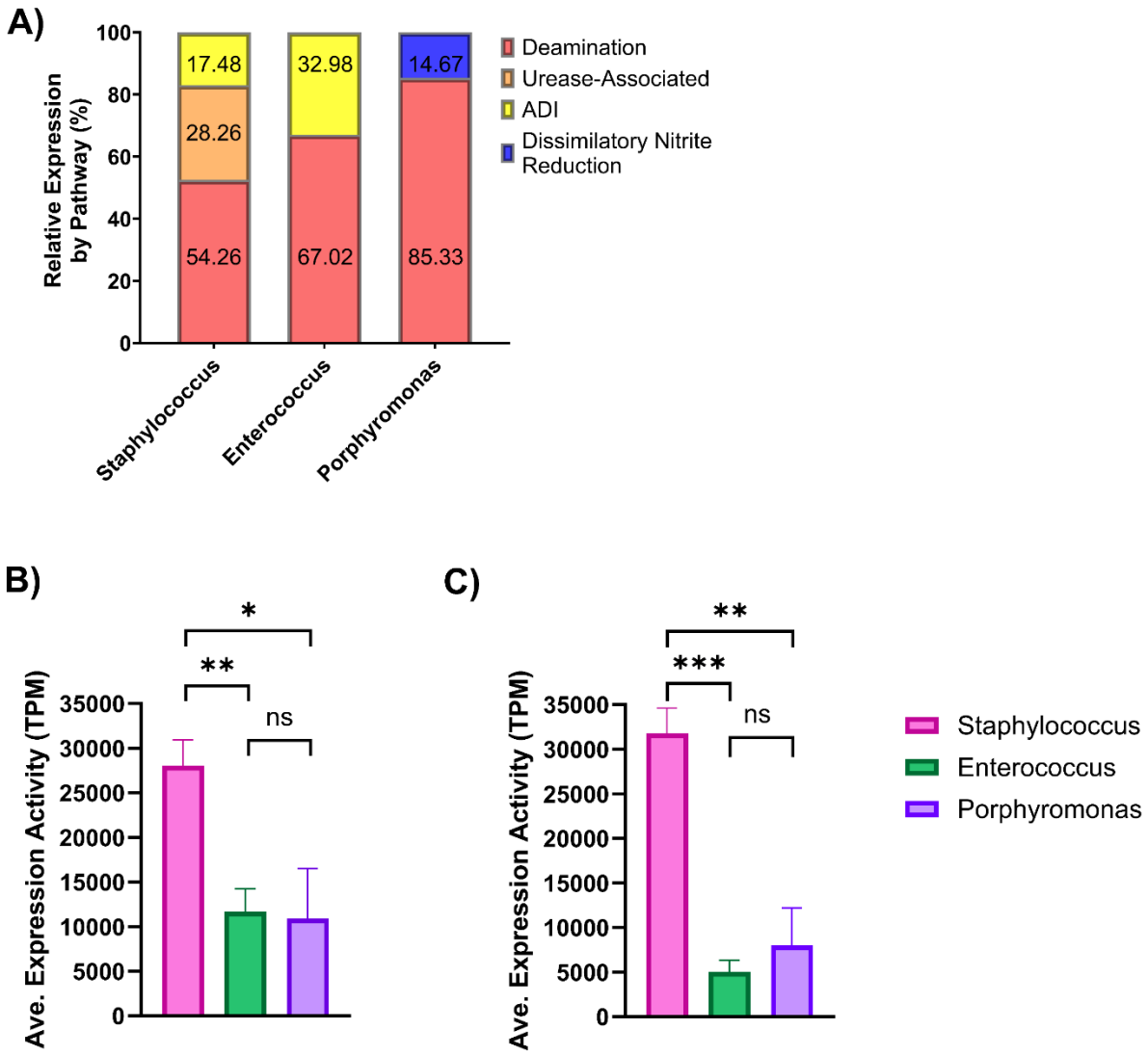

Supplemental Figure 4. Comparison of pathway expression profiles across the three dominant genera; A) Expression values adjusted for the moles of ammonia produced per pathway. B) Average phosphatase expression activity by genus. Shapiro–Wilk tests were used to assess normality. As the data were not normally distributed, Kruskal–Wallis tests were performed for both phosphatase and biofilm expression ($p < 0.0001$). C) Average biofilm expression activity by genus. Pairwise comparisons between organisms were conducted using Wilcoxon signed-rank tests. Asterisks indicate significance levels: ***($p < 0.001$), ** ($p < 0.01$), ns = not significant. Bars represent the mean expression activity, with error bars indicating SEM.

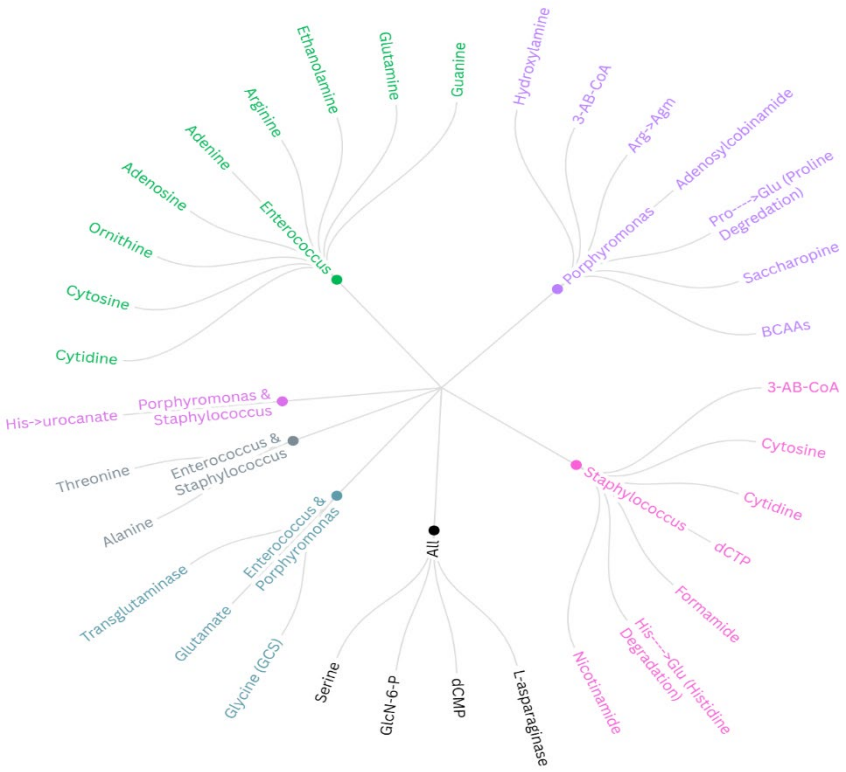

Supplemental Figure 5. Distribution of deamination pathway expression across keystone genera. “All” denotes that the pathway occurs in all 3 keystone genera.

Supplemental Table 1. Deamination Gene Expression by *Staphylococcus, Enterococcus,* and *Porphyromonas* in the Stone.

The urease-associated pathway included expression of *rocF* (155,156), *yut* (157), and *ureABCDEFG* (158). The ADI pathway was supported by expression of *arcA*, *argF*, *arcC*, and *arcD*, which mediate the conversion of arginine to citrulline and ammonia through a multi-step reaction often used by bacteria to produce energy and regulate pH (159,160). Although *arcB* encodes one of the enzymes involved in the ADI pathway, *argF* can serve a functionally redundant role (160–163). While DNRA was not quantified as a separate category due to incomplete gene expression, dissimilatory nitrite reduction was included in the analysis based on the presence of ammonia-producing *nrfA* in *Porphyromonas* (Figure 9). The TPM-normalized expression values were used for all analyses, and adjusted values were computed based on estimated ammonia yield per pathway as described follows: deamination:1-2 depending on substrate, urease: 2, ADI: 2, dissimilatory nitrite reduction: 1, which represents that total amount of ammonia produced by the reaction or pathway (Supplemental Table 2).

Enzyme	**EC Number**	***Stapylococcus***	***Enterococcus***	***Porphyromonas***	**Gene(s)**
1-pyrroline-5-carboxylate dehydrogenase	1.2.1.88	0	0	1	*pruA*
3-aminobutyryl-CoA ammonia lyase	4.3.1.14	1	0	1	-
Adenine deaminase	3.5.4.2	0	1	0	*ade*
Adenosine deaminase	3.5.4.4	0	1	0	*add*
Adenosylcobinamide amidohydrolase	3.5.1.90	0	0	1	*cbiZ*
Agmatine deiminase	3.5.3.12	0	0	1	-
Alanine dehydrogenase	1.4.1.1	1	0	0	*ald*
Arginine decarboxylase	4.1.1.19	0	0	1	-
Asparaginase	3.5.1.1	1	1	0	*ansB*
Branched-chain amino acid dehydrogenase	1.2.4.4	0	0	3	*scoA*
Cytidine deaminase	3.5.4.5	1	1	0	*cdd*
Cytosine deaminase	3.5.4.1	1	1	0	-
dCMP deaminase	3.5.4.12	1	1	1	*comEB*
dctp deaminase	3.5.4.13	1	0	0	*dcd*
Ethanolamine ammonia lyase	4.3.1.7	0	1	0	*eutA, eutB, eutC, eutH, eutN,*

					eutP, eutQ
Formiminoglutamase	3.5.3.8	1	0	1	*hutG*
glucosamine-6-phosphate deaminase	3.5.99.6	1	1	1	*nagB*
Glutamate Dehydrogenase	1.4.1.2	0	1	1	*gdh*
Glutaminase	3.5.1.2	0	1	0	*gls*
Glycine Cleavage System (GCS)	1.4.4.2, 2.1.2.10	0	0	1	*gcvH, gcvT*
Guanine deaminase	3.5.4.3	0	1	0	*guaD*
Histidine degradation (with formamide degradation): Histidine Ammonia lyase, Urocanate hydratase, Imidazolonepropionase,Formiminoglutamase, Formamidase	Present in Staphylococcus and Porphyromonas: 4.3.1.3 Staphylococcus only: 4.2.1.49, 3.5.2.7, 3.5.3.8, 3.5.1.49	2	0	1	*hutH, hutU, hutI, hutG, FmdA*
Hydroxylamine oxidoreductase (HAO)	1.7.99.1	0	0	1	*hcp*
L-asparaginase, type I	3.5.1.1	0	0	1	*ansA*
L-Serine dehydratase	4.3.1.17	1	1	1	*sdhB*
Nicotinamidase	3.5.1.19	1	0	0	*pncA*
Ornithine cyclodeaminase	4.3.1.12	0	1	0	-
Porphyromonas-type peptidyl-arginine deiminase	3.5.3.15	0	1	0	*aguA*
Proline dehydrogenase, 1-pyrroline-5-carboxylate dehydrogenase, Glutamate Dehydrogenase (Proline degredation pathway)	1.5.5.2, 1.2.1.88, 1.4.1.2	0	0	1	*proC, pruA, gdh*
Saccharopine dehydrogenase	1.5.1.7	0	0	1	*LYS1*
Siroheme synthase	2.1.1.107	1	0	0	*cysG*
Threonine deaminase	4.3.1.19	1	1	0	*ilvA*

Threonine dehydratase	4.3.1.17	1	1	0	*tdcB*
Transglutaminase	2.3.2.13	0	1	1	-
Total		**16**	**17**	**20**	

Supplemental Table 2. Phosphatase Gene Expression in *Staphylococcus, Enterococcus,* and *Porphyromonas*

Genus Expressing	**Description**	**Gene**
Staphylococcus	Type I phosphodiesterase / nucleotide pyrophosphatase	-
Staphylococcus	Histidine phosphatase superfamily (branch 1)	-
Staphylococcus	ATP diphosphatase activity	-
Staphylococcus	alpha-ribazole phosphatase activity	-
Porphyromonas	Acid phosphatase homologues	-
Porphyromonas	Belongs to the alkaline phosphatase family	-
Porphyromonas	alpha-ribazole phosphatase activity	-
Porphyromonas	Endonuclease/Exonuclease/phosphatase family	-
Porphyromonas	Ser Thr phosphatase family protein	-
Porphyromonas	Type I phosphodiesterase / nucleotide pyrophosphatase	-
Porphyromonas	Tyrosine phosphatase family	-
Enterococcus	COG1387 Histidinol phosphatase and related hydrolases of the PHP family	-
Enterococcus	endonuclease exonuclease phosphatase family protein	-
Enterococcus	phosphoprotein phosphatase activity	-
Enterococcus	Type I phosphodiesterase / nucleotide pyrophosphatase	-
Enterococcus	Tyrosine phosphatase family	-
Staphylococcus	Belongs to the acylphosphatase family	*acyP*
Enterococcus	Belongs to the acylphosphatase family	*acyP*
Enterococcus	Low molecular weight phosphatase family	*arsC*
Enterococcus	Chemotaxis phosphatase CheX	*cheC*
Enterococcus	Endonuclease/Exonuclease/phosphatase family	*exoA*
Enterococcus	Firmicute fructose-1,6-bisphosphatase	*fbp*
Enterococcus	Histidine phosphatase superfamily (branch 1)	*gpmB*
Enterococcus	Histidinol phosphatase and related hydrolases of the PHP family	*hisJ*

Staphylococcus	Endonuclease/Exonuclease/phosphatase family	*hlb*
Porphyromonas	3-deoxy-D-manno-octulosonate 8-phosphate phosphatase	*kdsC*
Enterococcus	Phosphatidylglycerophosphatase A	*ltrC*
Enterococcus	Endonuclease/Exonuclease/phosphatase family	*M1-449*
Staphylococcus	acid phosphatase family protein	*pgpB3*
Staphylococcus	Belongs to the alkaline phosphatase family	*phoB*
Enterococcus	Alkaline phosphatase	*phoB*
Staphylococcus *Enterococcus*	Alkaline phosphatase	*phoB*
Staphylococcus *Enterococcus* *Porphyromonas*	Phosphate starvation protein PhoH,	*phoH*
Staphylococcus *Enterococcus*	Alkaline phosphatase synthesis transcriptional regulatory protein	*phoP*
Staphylococcus *Enterococcus*	Histidine kinase	*phoR*
Staphylococcus *Enterococcus* *Porphyromonas*	Plays a role in the regulation of phosphate uptake	*phoU*
Enterococcus	bis(5'-adenosyl)-triphosphatase activity	*pkcI*
Staphylococcus	Inorganic pyrophosphatase	*ppaC*
Staphylococcus	Exopolyphosphatase	*ppx*
Staphylococcus *Enterococcus* *Porphyromonas*	phosphate transport system permease	*pstA*
Staphylococcus *Enterococcus* *Porphyromonas*	Part of the ABC transporter complex PstSACB involved in phosphate import. Responsible for energy coupling to the transport system	*pstB (Staphylococcus and Porphyromonas), pstB1,*

		pstB2 (Enterococcus)
Staphylococcus *Enterococcus* *Porphyromonas*	probably responsible for the translocation of the substrate across the membrane	*pstC*
Staphylococcus *Enterococcus* *Porphyromonas*	Phosphate ABC transporter substrate-binding protein	pstS
Enterococcus	Pfam:Y_phosphatase3C	*ptp3*
Porphyromonas	Belongs to the low molecular weight phosphotyrosine protein phosphatase family	*ptpA*
Enterococcus	Belongs to the low molecular weight phosphotyrosine protein phosphatase family	*ptpA*
Staphylococcus	Pyrophosphatase that catalyzes the hydrolysis of nucleoside triphosphates to their monophosphate derivatives, with a high preference for the non-canonical purine nucleotides XTP (xanthosine triphosphate), dITP (deoxyinosine triphosphate) and ITP.	*rdgB*
Porphyromonas	Pyrophosphatase that catalyzes the hydrolysis of nucleoside triphosphates to their monophosphate derivatives, with a high preference for the non-canonical purine nucleotides XTP (xanthosine triphosphate), dITP (deoxyinosine triphosphate) and ITP.	*rdgB*
Porphyromonas	phosphoserine phosphatase	*serB*
Staphylococcus	phosphatase	*stp*
Enterococcus	Sigma factor PP2C-like phosphatases	*stp*
Staphylococcus	Inositol monophosphatase	*suhB*
Enterococcus	Inositol monophosphatase family	*suhB*
Porphyromonas	Nucleotidase that shows phosphatase activity on nucleoside 5'-monophosphates	*surE*
Staphylococcus	endonuclease exonuclease phosphatase	*XK27_02140*
Staphylococcus	Belongs to the low molecular weight phosphotyrosine protein phosphatase family	*yfkJ*

Enterococcus	Acid phosphatase homologues	*yodM*
Staphylococcus	Mitochondrial PGP phosphatase	*yqeG*
Enterococcus	Mitochondrial PGP phosphatase	*yqeG*

Supplemental Table 3. Biofilm-Associated Gene Expression in *Staphylococcus* and *Enterococcus* in the Stone

Genus Expressing	**Description**	**Gene**
Staphylococcus	-	*icaD*
Staphylococcus	transferase activity, transferring acyl groups other than amino-acyl groups	*icaC*
Staphylococcus	Catalyzes the N-deacetylation of poly-beta-1,6-N-acetyl- D-glucosamine (PNAG, also referred to as PIA), a biofilm adhesin polysaccharide	*icaB*
Staphylococcus	N-acetylglucosaminyltransferase that catalyzes the polymerization of single monomer units of UDP-N-acetylglucosamine to produce the linear homopolymer PNAG, also referred to as PIA, a biofilm adhesin polysaccharide. Requires IcaD for full activity	*icaA*
Staphylococcus	transcriptional	*sarA*
Staphylococcus	Biofilm formation stimulator VEG	*veg*
Staphylococcus	Staphylococcal AgrD protein	*agrD*
Staphylococcus	Essential for the production of a quorum sensing system signal molecule, the autoinducing peptide (AIP).	*agrB*
Staphylococcus	Regulator	*agrA*
Staphylococcus	COG3764 Sortase (surface protein transpeptidase)	*srtA*
Staphylococcus	Lysin motif	*ebpS*
Staphylococcus	Catalyzes the reversible conversion of 2- phosphoglycerate into phosphoenolpyruvate. It is essential for the degradation of carbohydrates via glycolysis	*eno*
Staphylococcus	C-terminus of bacterial fibrinogen-binding adhesin	-
Staphylococcus	C-terminus of bacterial fibrinogen-binding adhesin	-
Staphylococcus	Putative adhesin	-
Staphylococcus	Capsular polysaccharide biosynthesis protein	*ywqE*
Staphylococcus	Belongs to the UDP-glucose GDP-mannose dehydrogenase family	*capO*
Staphylococcus	Belongs to the UDP-glucose GDP-mannose dehydrogenase family	*capL*

Staphylococcus	GDP-mannose 4,6 dehydratase	*capI*
Staphylococcus	Polysaccharide biosynthesis protein	*capD*
Staphylococcus	ATPase MipZ	*capB*
Staphylococcus	Chain length determinant protein	*capA*
Staphylococcus	Lysin motif	*ebpS*
Staphylococcus	Belongs to the TPP enzyme family	*cidC*
Staphylococcus	Increases the activity of extracellular murein hydrolases possibly by mediating their export via hole formation.	*cidB*
Staphylococcus	Increases the activity of extracellular murein hydrolases possibly by mediating their export via hole formation.	*cidA*
Porphyromonas	Major fimbrial subunit protein (FimA)	*fimA*
Porphyromonas	Major fimbrial subunit protein type IV, Fimbrillin, C-terminal	-
Porphyromonas	Biofilm PGA synthesis protein PgaD	*mmdC*
Porphyromonas	Fimbrillin-A associated anchor proteins Mfa1 and Mfa2	-
Porphyromonas	Fimbrillin-like	-
Porphyromonas	Transcriptional regulator, LuxR family	-
Porphyromonas	Belongs to the ompA family	-
Porphyromonas	OmpA family	-
Porphyromonas	Catalyzes the reversible conversion of 2- phosphoglycerate into phosphoenolpyruvate. It is essential for the degradation of carbohydrates via glycolysis	*eno*
Porphyromonas	Capsule biosynthesis protein CapA	-
Porphyromonas	COG COG4464 Capsular polysaccharide biosynthesis protein	-
Porphyromonas	Polysaccharide biosynthesis protein	*cap*
Porphyromonas	Polysaccharide biosynthesis protein	*cap*
Porphyromonas	Belongs to the UDP-glucose GDP-mannose dehydrogenase family	*capO*
Porphyromonas	Transglutaminase-like superfamily	-
Enterococcus	Transglutaminase/protease-like homologues	*yebA*
Enterococcus	Transglutaminase-like superfamily	-
Enterococcus	Biofilm formation stimulator VEG	*veg*
Enterococcus	COG3227 Zinc metalloprotease (elastase)	*gelE*
Enterococcus	Sortase family	*srtC*

Enterococcus	Catalyzes the reversible conversion of 2- phosphoglycerate into phosphoenolpyruvate. It is essential for the degradation of carbohydrates via glycolysis	*eno*
Enterococcus	Putative adhesin	*yvlB*
Enterococcus	Putative adhesin	-
Enterococcus	Bacterial capsule synthesis protein PGA_cap	*capA*
Enterococcus	CAP-associated N-terminal	-
Enterococcus	Capsular polysaccharide biosynthesis protein	*ywqE*
Enterococcus	CoA-binding domain	*capD*
Enterococcus	UDP-glucose/GDP-mannose dehydrogenase family, central domain	*capO*
Enterococcus	COG3764 Sortase (surface protein transpeptidase)	*srtA*
Enterococcus	Sortase family	*srtC*
Enterococcus	Sortase family	*srtA*
Enterococcus	Catalyzes the reversible conversion of 2- phosphoglycerate into phosphoenolpyruvate. It is essential for the degradation of carbohydrates via glycolysis	*eno*
Enterococcus	cell adhesion	-

Supplemental Table 4. Biofilm type and role in Struvite formation

Genus	**Primary Biofilm Matrix Component**
Staphylococcus	PNAG (poly-β-1, 6-N-acetylglucosamine), proteins (118,164,165)
Enterococcus	Capsular polysaccharides, rhamnose-glucose polymers (120,166)
Porphyromonas	Capsular polysaccharides, LPS and protein-rich matrix (150,167)

Chapter 4:

Oral and Stone Microbiomes of the Cat

Struvite Stones from Cats Are Not Sterile: Metatranscriptomic Insights into the Stone and Oral Microbiota in Health and Feline Chronic Gingivostomatitis

Ashleigh M Flores[1#], Rodrigo Profeta[1#], Jodi L Westropp[2*], Maria Soltero-Rivera[3*], Bart C Weimer[1*]

[1]Population Health and Reproduction, 100K Pathogen Genome Project, School of Veterinary Medicine, University of California, Davis, Davis, CA, USA

[2]Medicine and Epidemiology, School of Veterinary Medicine, University of California, Davis, Davis, CA, USA

[3]Surgical and Radiological Sciences, School of Veterinary Medicine, University of California, Davis, Davis, CA, USA

[#]authors contributed equally to this work

***Correspondence:**

bcweimer@ucdavis.edu

jlwestropp@ucdavis.edu

msoltero@ucdavis.edu

Keywords: urolith, urinary stone, calculi, dentistry, lithiasis, MAP, metatranscriptomics, feline, oral microbiome

Contributions:

AMF: project design, data analysis, visualization, data interpretation, writing and editing; RP: sequence analysis, bioinformatics, data analysis, visualization, editing; JLW: funding, project design, data interpretation, writing and editing, MSR: funding, project design, data interpretation, writing and editing; BCW: funding, project design, data interpretation, writing and editing

ABSTRACT

Struvite uroliths in cats have traditionally been regarded as sterile because urine cultures are rarely positive. Using metatranscriptomic analysis, we demonstrated that struvite stones in cats harbor a diverse and transcriptionally active microbiome comprising 762 genera and 781 species/strains. All stones, including those with negative aerobic cultures, showed microbial transcriptional activity. Comparative analysis of stone and oral microbiomes revealed substantial overlap, with greater compositional similarity between stones and the oral microbiomes of cats with Feline Chronic Gingivostomatitis (FCGS) than those of healthy cats, supporting an oral–stone microbial axis in the context of disease. Oral-associated taxa such as *Pasteurella* were present in both niches, and several taxa showed high transcriptional activity in stones, including *Staphylococcus*, *Enterococcus*, and *Klebsiella*. Ammonia-producing pathways contributing to stone pathogenesis included deamination of nitrogenous substrates, the arginine deiminase pathway, and urease expression; notably, urease was expressed only by *Staphylococcus* and accounted for 34.1% of its ammonia-related activity. Pathways involved in phosphate liberation and biofilm formation were also actively expressed, with *Enterococcus* showing stronger biofilm-associated gene expression than *Staphylococcus*. These findings demonstrate that feline struvite uroliths are not sterile but instead support a robust, metabolically active microbiome, and suggest that oral bacteria—particularly under conditions of mucosal barrier breakdown in FCGS—may contribute to stone formation and pathogenesis

INTRODUCTION

Urolithiasis in cats has been recognized as a clinical concern for over a century (1–3). This condition is associated with significant pain and remains the most common cause of urethral obstruction in cats which can be life-threatening if left untreated (4,5). Although the recurrence rate of struvite urolithiasis in cats is not well established, it has been reported to range from 2.7–19.1%, with an average time to recurrence of 20–29 months (6,7).

Struvite stones develop when magnesium, ammonium, and phosphate crystals precipitate within a microbial biofilm, which often adheres to the bladder mucosa and serves as a nidus for stone formation (8,9). Ammonia increases urinary pH, producing an alkaline environment that promotes the binding of magnesium and phosphate ions, leading to struvite crystallization (9). Ammonia production in the stone has been largely attributed to urease activity, primarily in dogs and humans (13). Yet, urease does not fully explain all instances of struvite formation. Studies demonstrate that weakly ureolytic or non-ureolytic microbes can also induce struvite precipitation in sterile urine (14), implicating alternative ammonia-generating pathways such as deamination, an ammonia-generating mechanisms recognized nearly a century ago as a source of urinary ammonia in cats (3). This and additional alternative microbial metabolic processes remain largely unexamined. While it has been recently postulated that struvite stones may result from multiple microbially encoded metabolic pathways, systematic investigation beyond urease production has yet to be widely pursued (15).

In cats, struvite uroliths differ in their proposed pathogenesis compared to those in dogs and humans, where bacterial urinary tract infections (UTIs) caused by urease-

producing organisms such as *Staphylococcus*, *Proteus*, and *Klebsiella* have been strongly implicated (16). In contrast, struvite stones from cats are widely considered to be sterile, as bacteria are rarely isolated by standard aerobic urine cultures (UCs) (13,17–19). This has reinforced the prevailing belief that UTIs play little to no role in struvite formation in cats, with stone development instead attributed primarily to dietary, metabolic, genetic factors, and urine pH—though their exact contributions remain unclear (20–22).

For decades, UCs have served as the gold standard for detecting bacteria in urine and stones (23,24). However, standard aerobic cultures detect only a subset of microbial contributors, potentially overlooking fastidious or unculturable organisms involved in stone formation (23). Kopecny et al. reported a culture-positive rate of only 10.9% in samples in cats (21), while a 2025 study found positive cultures in 62% of stone samples (25). In cats with urolithiasis, stones that contained urease-producing bacteria such as *Staphylococcus* or *Proteus* were nearly 12 times more likely to be struvite, whereas stones with non-urease-producing bacteria (e.g., *Enterococcus*, *Pasteurella*, *Acinetobacter*) were about 4 times more likely to be struvite compared to stones without bacteria (25). Despite advances in diagnostics and acidifying diets, the incidence of struvite urolithiasis in cats has risen in recent decades (21,26), highlighting the limitations of culture-based methods and the need for refined diagnostic and therapeutic strategies.

Culture-independent methods such as molecular sequencing have gained popularity for detecting bacterial genetic material that evades traditional culture, with the cat urinary microbiome studies emerging only recently in 2021 (27). While 16S rRNA

sequencing offers greater sensitivity than culture, it offers limited taxonomic resolution which can hinder accurate identification of closely related genera and species (28,29). This limitation has led to inconsistent findings in studies pertaining to cats: some failed to detect urinary microbes (30,31), possibly due to low biomass and detection limits. A 2025 study (32) on the other hand, identified microbes in all samples using 16s rRNA sequencing, despite negative UC results Furthermore, differences in urinary microbiome composition have been reported between cats with and without calcium oxalate stones (33) using this technique. These discrepancies highlight the need for more comprehensive, high-resolution methods to characterize the struvite stone microbiome of cats.

Using RNA-based approaches are suitable for studying microbial communities to define the community members that are active independent of their ability to grow in culture (28). Total RNA sequencing offers high taxonomic resolution and insight into transcriptional activity—enabling identification of metabolically active microbes and their functional potential (34,35). This makes metatranscriptomics a particularly powerful tool for investigating the active microbiome within struvite stones from cats and its potential role in disease.

A growing body of evidence supports a functional link between the oral cavity and urinary tract. The cat oral cavity harbors a complex microbiome that influences both oral and systemic health (36–38). Culture-based studies have identified *Staphylococcus pseudintermedius* as the most common isolate of the oral cavity of clinically healthy cats. (39,40). Its frequent colonization of both the oral cavity and

urogenital tract suggests a potential role in stone formation, warranting further investigation in struvite urolithiasis in cats.

Previous studies have noted that animals with periodontitis exhibit increased bacterial translocation, which is associated with a higher risk of urinary stone formation (41–44). A recent study (45) demonstrated that oral bacteria can translocate to the urinary tract under inflammatory conditions. Feline chronic gingivostomatitis (FCGS), a severe oral inflammatory disease affecting up to 26% of adult cats (46), and it is characterized by extensive mucosal barrier disruption and microbial dysbiosis (34,35,41,42,46–51). The etiology of this disease is multifactorial with some studies pointing to a combination of immune dysregulation and microbial dysbiosis (34,35,41,47–49). Cats with FCGS exhibit altered oral microbiomes with elevated levels of Gram-negative and anaerobic bacteria, some of which are capable of ammonia production (34,35,41,47,48,50). Inflammation likely damages the oral endothelial glycocalyx and disrupts tight junctions, facilitating microbial translocation into the bloodstream (51). Certain oral pathogens, such as *Porphyromonas gingivalis*, are thought to contribute to this process by producing enzymes that degrade endothelial tight junction proteins, further compromising the vascular barrier, thereby increasing vascular permeability and facilitating microbial translocation into the bloodstream (52).

Given the established microbial role in struvite formation in humans and dogs (53–56), we hypothesized that cat stones contain a robust and active microbiome. Our prior work in dogs demonstrated that culture and 16S rRNA methods dramatically underestimate microbial diversity, missing numerous metabolically active taxa. We hypothesize a similar under-detection occurs in cats, reinforcing the need for high-

resolution, RNA-based approaches like metatranscriptomics to define active microbial communities and their roles in stone pathogenesis. Further, we hypothesize that the microbial community in cats stones more closely resemble that of FCGS-affected cats than healthy controls. Comparing the oral microbiomes of healthy and FCGS-affected cats may help determine whether oral disease increases the likelihood of shared taxa between the oral cavity and struvite stones.

MATERIALS AND METHODS

Experimental Design

This study defined the microbiome composition and biochemical functions in three cohorts: healthy oral cavity (healthy), the oral cavity of patients with feline chronic gingivostomatitis (FCGS), and struvite stones (stone).

Stone Specimens

All uroliths were submitted to, analyzed, and confirmed to be struvite at the Gerald V. Ling Urinary Stone Analysis Laboratory (University of California, Davis) between 2013-2020 (57). Stones composed of at least 70% struvite and ≤ 30% calcium apatite in each layer were used (57–59).

Prior to RNA extraction each sample was disinfected with 70% ethanol, ground into a fine powder using a sterilized mortar and pestle, after which 0.4 g were added to 1.0 mL of LifeGuard™ (Qiagen, Germantown, MD, USA) (34,35). Specimens were immediately preserved in RNA Shield (Zymo Research Corporation, Irvine, CA) to

ensure stabilization of microbial RNA at the time of collection, as previously described by the 100K Pathogen Genome Project (60) for downstream molecular analysis.

Oral Specimens

Oral specimens were collected from a different cohort of privately owned cats. Healthy cats were considered systemically normal based on physical examination, complete blood count, and serum chemistry panel results. Oral examinations revealed no more than mild gingivitis, plaque, or calculus accumulation, and no clinical signs of periodontal breakdown, neoplasia, or oral/maxillofacial trauma. Written informed consent was obtained from all owners prior to enrollment.

Inclusion criteria for FCGS-affected cats required the presence of moderate-to-severe oral inflammation extending laterally to the palatoglossal folds, with concurrent gingivitis, and a histopathologic diagnosis consistent with FCGS. Cats were excluded if they had concurrent oral neoplasia, osteomyelitis, or systemic immune-mediated or immunocompromising conditions, such as diabetes mellitus, or those undergoing chemotherapy. Swabbing targeted the buccal mucosa in FCGS and supragingival biofilm from the region extending caudally from the maxillary canine to the premolars from healthy individuals. Specimens were immediately preserved in RNA Shield (Zymo Research Corporation, Irvine, CA) to ensure stabilization of microbial RNA at the time of collection, as previously described by the 100K Pathogen Genome Project (60) for downstream molecular analysis via total RNA extraction. Written informed consent was obtained from all owners.

RNA isolation

Total RNA extraction was performed on stone and oral (healthy and FCGS) specimens as previously described (34,35,47). The microbial portion of each specimen was collected by differential centrifugation prior to cell lysis and RNA extraction after addition to TRIzol LS (Ambion, Austin, TX, USA) following manufacturer instructions. Once the RNA was collected, purity was determined using the NanoDrop spectrophotometer (Thermo Scientific, Waltham, MA, USA) with $A_{260/230}$ and $A_{260/280}$ ratios ≥ 1.5, and the degradation was determined via TapeStation (Agilent Technologies Inc, Santa Clara, CA, USA) (60,61).

Library Preparation and Metagenome sequencing:

Sequencing libraries were constructed using methods previously described (60–62). Briefly, KAPA HyperPlus library preparation kit (Roche Sequencing Solutions, Pleasanton, CA, USA) with a total cDNA (~100 ng) was fragmented to an average insert size of ~350-450 bp and the inserts were indexed using Weimer 384 TS-LT DNA barcodes (Integrated DNA Technologies, Coralville, IA, USA) and the library is size-selected by using KAPA Pure beads and dual-SPRI protocol to generate an average adapter-ligated gDNA insert molecule size of ~450-650 bp Size-selected libraries were PCR (polymerase chain reaction) amplified for five cycles, and the average library molecular size was determined using the DNA High Sensitivity Assay kit with the Agilent 2100 Bioanalyzer (Agilent Technologies, Inc). Libraries were sequenced on an Illumina NovaSeq S4 using PE150 protocols to a depth of at least 150 million reads/specimen (Illumina, San Diego, CA, USA) (60–63).

Taxonomic Assignment

Using methods previously described (34,35) the raw paired-end reads were trimmed to remove adapters and low-quality bases using Trimmomatic (version 0.39; command: trimmomatic PE [input] [output] ILLUMINACLIP:[adapters]:2:40:15 LEADING:2 TRAILING:2 SLIDINGWINDOW:4:15 MINLEN:50) (64). Read quality was assessed before and after trimming using FastQC (version 0.12.1) (65), and summary reports were compiled using MultiQC (version 1.21) (66).

Trimmed reads were split into cat (host) and non-host reads using the --classified-out and --unclassified-out options in Kraken2 (version 2.1.3) (67), with a custom database built from four high-quality *Felis catus* genomes, including the reference genome for the species (GCF_018350175.1, unspecified; general domestic cat), and three additional representatives: GCA_000003115.1 (mixed breed), GCA_000181335.6 (Abyssinian), and GCA_016509815.2 (unspecified; general domestic cat). Non-host reads were subsequently classified using Kraken2, based on Kraken database of microbes from RefSeq, built on July 6, 2023. The --use-names, --report-zero-counts, and --minimum-hit-groups 3 flags were applied to enhance classification depth and specificity.

Microbial taxonomic abundances at the genus and species levels were calculated using Bracken (version 2.8) (68) with the database constructed from the same Kraken2 microbial database (k-mer size: 35; read length: 150 bp). Further analysis of relative abundance was done after normalizing the reads of each organism divided by the total reads in that specimen. Organism identification results were retained

if there were >100 reads and were present in at least two-thirds of the specimens within that cohort.

Functional Annotation and Analysis:

Quality-trimmed and adapter-removed reads were classified using Kraken2 (v2.1.3; standard database built on 2023Jul06) (67). The --classified-out option was applied during Kraken2 classification to retain only reads assigned to a taxonomic identifier (taxid), which was included in each read header. Reads belonging to 5 bacterial genera of interest (*Bacillus*, *Clostridium, Enterococcus*, *Klebsiella,* and *Staphylococcus*) were retrieved by matching the corresponding taxids. A custom Bash script was developed to automate the extraction, using 'grep' command to filter and separate genus-specific reads into paired FASTQ files for each taxid (zcat "$FASTQ" | grep -A 3 -w "kraken:taxid|${TAXID}" --no-group-separator | pigz -p 64 > "$OUTPUT"). Each set of genus-specific reads was independently assembled using Trinity v2.15.1 (69), with strand-specific libraries (RF orientation), 100 GB of maximum memory, and 16 CPUs per assembly. Assemblies were done separately for each genus to generate *de novo* transcriptomes representing the extracted reads.

Transcript quantification was subsequently done using Salmon v1.10.2 (70). For each genus-specific assembly, a Salmon index was created, and the extracted reads were mapped back to the corresponding assembly to obtain transcript abundance estimates. Abundance values were reported in transcripts per million (TPM) to normalize for gene length and sequencing depth across specimens. Coding sequences (CDSs) were predicted and extracted from each Trinity assembly using Prokka v1.14.6 (71), which employs Prodigal for gene prediction. The resulting protein sequences (.faa

files) were then functionally annotated using EggNOG-mapper v2.1.12 (72), based on the EggNOG 5.0.2 database (73). Lastly, the functional annotations were integrated with the TPM abundance data, generating a genus-specific, functionally annotated abundance table that links predicted genes with their normalized expression levels across all specimens for use in statistical analysis and graphical display.

Microbiome Taxonomy Diversity and Statistical Analysis

Diversity Metrics

The alpha (Shannon diversity index) and beta (Bray-Curtis dissimilarity) diversity were calculated for each specimen after grouping them into their respective sample specimans (healthy, stone, and FCGS). These diversity metrics were computed using the *vegan* package (Version 2.7.0) in R (Version 4.3.1) and visualized as box-and-whisker plots using GraphPad Prism (Version 10.4.2) (GraphPad, Boston, MA, USA). Statistical differences between the groups in alpha and beta diversity were done using the Kruskal–Wallis test (n = 6 per group). Pairwise Mann–Whitney U tests were performed post-hoc to identify specific group differences (74). Additionally, to verify that organisms in the dataset had been identified previously in the literature were present and compare the relative abundance of the three cohorts, grouped bar charts were generated with GraphPad Prism (Version 10.4.2) (GraphPad, Boston, MA, USA). Microbiome member distributions were separately visualized using alluvial plots generated with the *ggplot2* package and the *ggalluvial* package (Version 0.12.5) in R (34,35).

Taxonomic Structure and Co-occurrence Patterns in Oral and Stone Microbiomes

Microbiome member distributions were visualized using alluvial plots generated with the *ggplot2* package and the *ggalluvial* package (Version 0.12.5) in R (34,35). Genera contributing <1.5% of total transcripts for a given cohort (oral or stone) were grouped as 'low activity' within that cohort.

Organisms were compared by sample type using correlation plots that were constructed using TPM values and as previously described (75). Log_2-transformed scatter plots were generated using *ggplot2* in R, with final labeling performed manually in Inkscape (Version 1.4), accessed via GitHub (https://githubcom/inkscape/inkscape) (75).

Statistical association of microbial taxa co-occurrence networks within each specimen was assessed using Spearman rank correlation coefficients that were calculated with the *Hmisc* package (Version 5.2.2) in R (74) with significance considered to be $p < 0.05$. Diagrams were constructed in Python (Version 3.11.5) using the *networkx* library (Version 3.1), visualized with *matplotlib* (Version 3.7.1) (76), with color coding and labeling being done manually in Inkscape (Version 1.4) accessed via GitHub (https://githubcom/inkscape/inkscape) (74).

Analysis and Plotting of Stone Microbiome Functional Profile

Differential gene expression abundance was quantified using Transcripts Per Million (TPM) that were normalized for sequencing depth and gene length. The TPM-normalized expression values were used for all analyses, and adjusted values were computed based on estimated ammonia yield per pathway as described follows:

deamination:1-2 depending on substrate, urease: 2, and ADI: 2 which represents that total amount of ammonia produced by the reaction or pathway (Supp Table 2).

The amount of expression for the ADI, urease, deamination, and nitrate/nitrite pathways across the stone specimens (n= 6), were determined using TPM-normalized values. Subsequently, the values were adjusted based on the estimated amount of ammonia produced per pathway was done based on specific pathways (Supp Table 1). To visualize metabolic pathways of interest radar charts were generated using Flourish Studio (Canva UK Operations Ltd, https://flourishstudio/).

To compare gene expression levels across functional groups (arginine deiminase pathway (ADI), urease, and deamination), statistical testing was conducted using R (Version 4.3.1), and figures were generated using GraphPad Prism (Version 10). To compare expression of the ADI, urease, and deamination pathways within *Staphylococcus* from stone specimens, used the Kruskal–Wallis test to assess expression differences between pathways. Wilcoxon matched-pairs signed-rank tests were used for post-hoc pairwise comparisons between pathway expression magnitiude for the activity of each organism.

Box-and-whisker plots were created in GraphPad Prism using the same data, with significance annotations based on the R-derived test results.Ammonia-adjusted deamination pathway expression values were $\log_2$-transformed before comparing stone and oral specimens using a non-parametric Mann-Whitney U Test (Wilcoxon rank-sum test), normality of $\log_2$-transformed normalized TPM values was assessed using the Shapiro–Wilk test prior. Rank-biserial correlation was used as the effect size measure

for the Mann-Whitney U Test Results were visualized using the *ggplot2* and *ggpubr* packages in R.

RESULTS

Stones from cats were processed to extract the total RNA after surface disinfection. Bucal swabs were taken from cats without oral disease (healthy) and from FCGS-affected individuals and were also processed for total RNA extraction that were sequenced to on average ~22.35 million reads per sample. These sequences were examined for transcriptionally active microbial community in stones and the two oral cohorts after informatic removal of cat transcripts. This approach provided the microbiome membership expressed metabolic genes that were focused on ammonia producing routes. Because naming the organism using these methods is 98-99% accurate for genus and species, respectively (67,68), it allowed specific comparison of species/strains found in oral and stone samples.

Patient Demographics

Signalment information can be found in Table 1.

Table 1. Mean age, weight and sex of cats that had struvite uroliths submitted for analysis and of cats from which oral cavity specimens were collected. *FS= Female spayed, MC= Male castrated, MI= Male intact.*

	Stone *(n= 6)*	**Healthy** *(n=6)*	**FCGS** *(n=6)*
Mean Age ± SD (years)	5.0 ± 2.6	1.6 ± 1.4	5.3 ± 2.7
Mean Weight ± SD (kg)	6.2 ± 2.5	4.0 ± 1.8	5.1 ± 1.3
Sex	2 FS, 4 MC	3 FS, 3 MC	2 FS, 3 MC, 1 MI

Overlap in Community Membership Reveals an Oral/Stone Axis

The struvite stones of the cat harbor a taxonomically rich microbiome, comprising 762 (Supplemental Figure 1) genera and 781 distinct species/strains (Fig 1A, 1B). With taxonomic assignments achieving approximately 98–99% accuracy at the genus and species levels (67,68), we were able to confidently compare microbial profiles between stone and oral specimens.

Considering the reported connections between oral health and urinary disease, including urolithiasis in humans (77–79), we hypothesized the existence of an oral/stone microbial axis, that would be observed in part by substantially overlapping microbiome members between the locations. The stone microbiome displayed a notable amount of overlap at both the genus (Supplemental Figure 1) and species/strain levels (Figure 1A, 1B) with both healthy and FCGS microbiomes. Stones and healthy oral microbiomes shared 505 species/strains, accounting for 64.7% and 15.4% of each community, respectively (Figure 1A). By comparison, 298 species/strains were shared between the microbiomes of the stones and FCGS-affected cats, accounting for 61.7% and 46.0% of each microbial community, respectively (Figure 1B).

Alpha diversity, measured by the Shannon Diversity Index, was determined to be significantly lower in stone specimens compared to both FCGS ($P < 0.05$) and healthy oral specimens ($P < 0.01$) (Figure 1C). β diversity was evaluated among the species/strains revealing a statistically significant difference between the stone and healthy oral cohorts ($P < 0.001$). No significant difference was observed between the stone and FCGS cohorts (Figure 1D), indicating that the overall microbial community

structure of the stone microbiome is not identical to but more closely resembles that of the FCGS cohort than the healthy cohort.

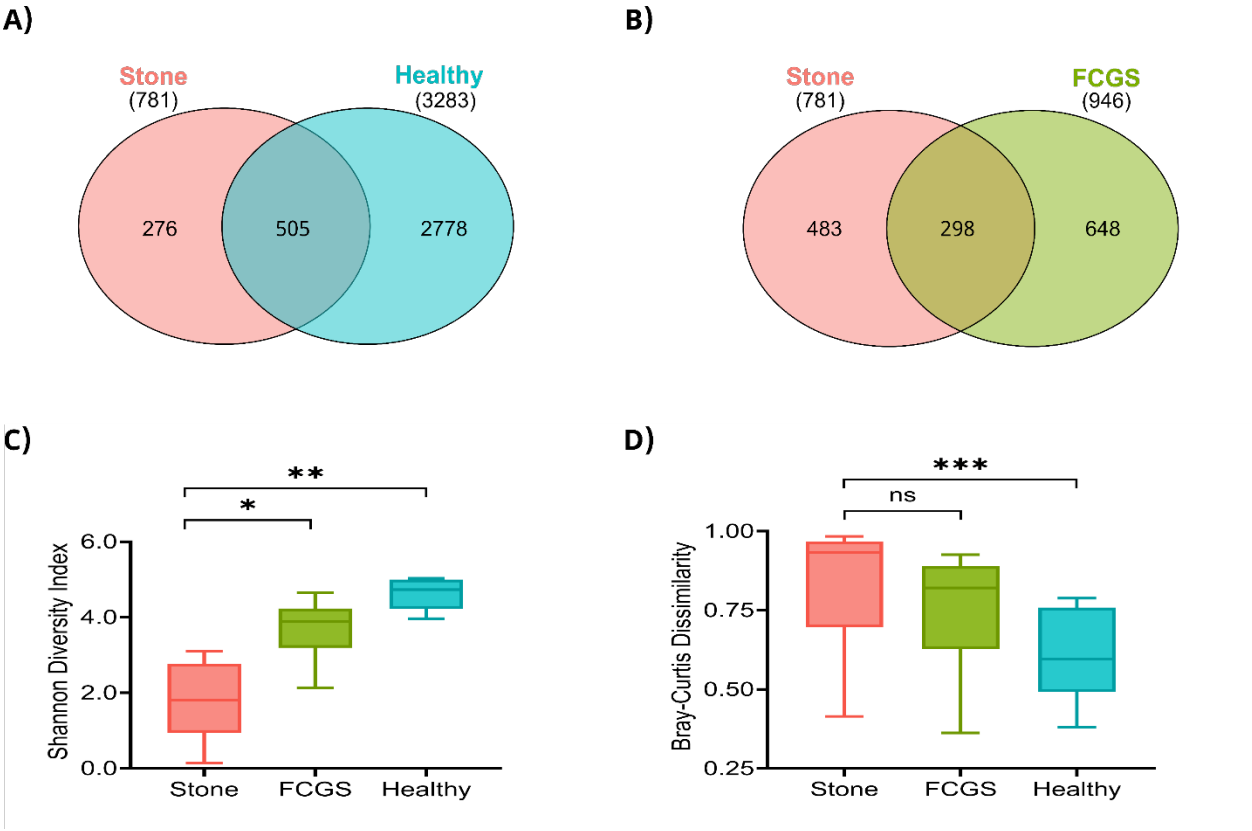

Figure 1. Comparison in the taxonomy of the struvite stone, healthy, and FCGS oral cavity microbiomes (A) Unique and overlapping species- and strain-level between the stone and healthy cohorts (B) Unique and overlapping species- and strain-level between the stone and FCGS cohorts. (C) Alpha diversity of the stone, FCGS, and healthy cohorts at the species- and strain-level as measured by the Shannon Index (D). Beta diversity of the stone, FCGS, and healthy microbiomes at the species- and strain-level as measured by the Bray-Curtis dissimilarity.

Comparison with Prior Literature and UCs

Stone cultures were positive in 50% (3/6) of specimens, with *Staphylococcus* as the sole isolate in all cases (Table 2). Our analysis found *Staphylococcus* to be part of the microbiome in stones, healthy, and FCGS specimens. Even the culture-negative stones contained RNA from numerous genera that were transcriptionally active within the stone, prompting us to compare our findings to isolates reported in previous studies.

Table 2. UC and stone culture results. Urine cultures conducted prior to stone removal. The cats did not receive antibiotics.

Organism	**Urine Cultures (n= 3)**	**Urolith Cultures (n= 6)**
Positive (*Staphylococcus* isolated)	1	3
Negative	2	3

To evaluate whether our findings aligned with previous reports, we compared the bacterial genera identified by shotgun metatranscriptomics to those previously isolated by UC from the urine and stones of cats with struvite urolithiasis and reported in the literature. All reported genera were found to be present and active in not only the stone but in the two oral cohorts (Table 3). Our analysis uncovered a much broader range of transcriptionally active organisms, including genera not commonly considered clinically within the stone (Figure 2). Among the literature-reported genera, *Staphylococcus*, *Enterococcus*, and *Candida* exhibited significantly higher activity in stone specimens compared to one or more oral cohorts. *Staphylococcus* showed significantly elevated activity in the stone relative to both the FCGS and healthy groups ($P < 0.01$ for each). In contrast, *Enterococcus* and *Candida* were significantly higher in the stone compared only to the healthy group ($P < 0.01$ and $P < 0.05$, respectively).

Table 3. Organisms identified from urine and stones of cats with struvite urolithiasis according to the scientific literature and detected via RNAseq.

Genus	Isolation Species (Reference)
Acinetobacter spp.	Cat (25) Human (80)
Candida spp.	Cat (81) Human (80)
Corynebacterium spp.	Cat (21,82,83) Human (80,84)
Enterococcus spp.	Cat (21,25,85) Human (80,86)
Escherichia spp.	Cat (21,25,85,87) Human (2–4)
Klebsiella spp.	Cat (7,25) Human (80,86)
Pasteurella spp.	Cat (7,25) Human (80)
Proteus spp.	Cat (7,21,25,85,88) Human (80,86,89)
Pseudomonas spp.	Cat (7) Human (80,86,89)
Staphylococcus spp.	Cat (21,25,87) Human (80,86)
Streptococcus spp.	Cat (7,85,87,88) Human (80,86)

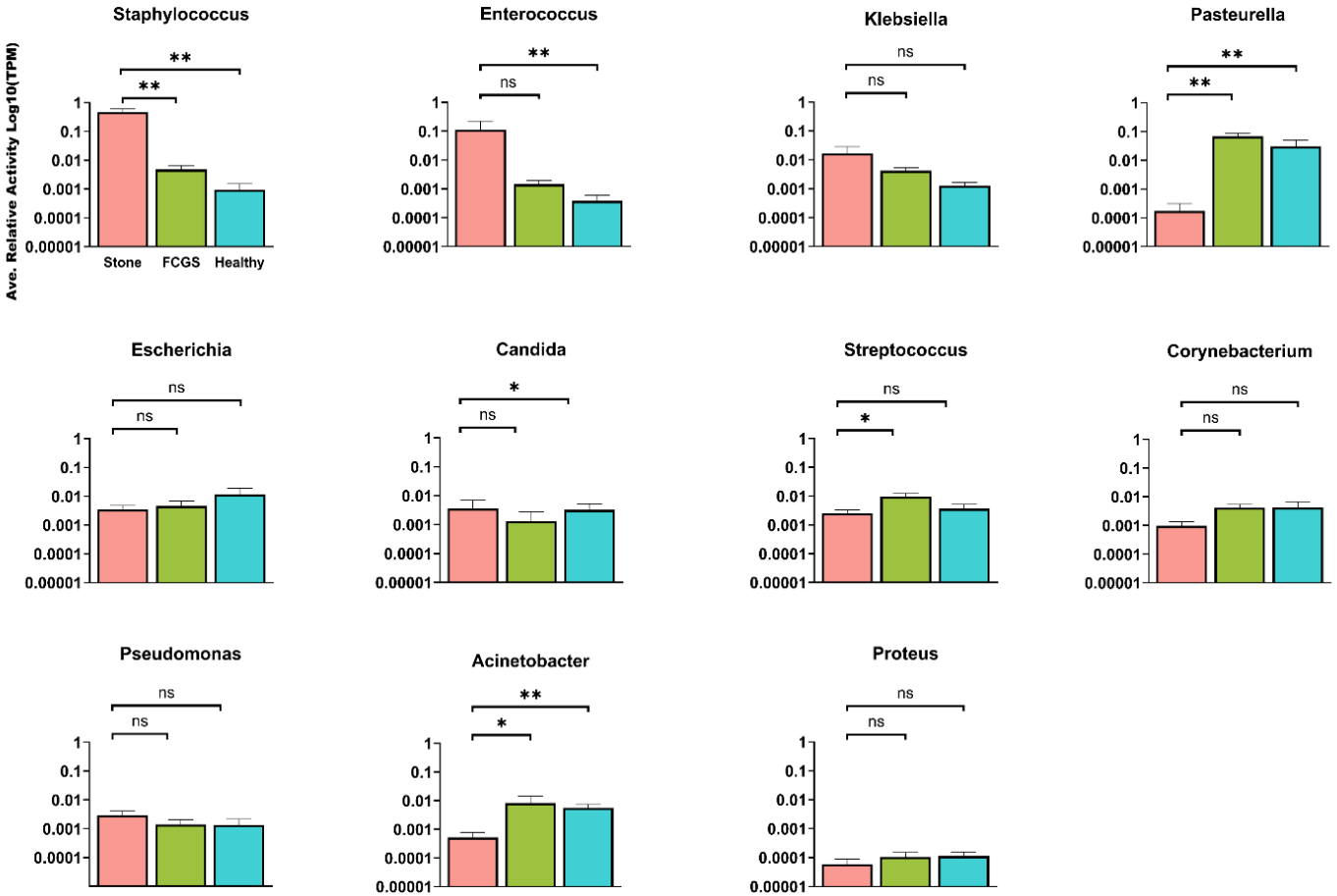

Figure 2. The average relative activity (Log10) of genera previously reported from the literature using SUC in comparison to those found in this study using shotgun RNAseq. The error bar represents standard error of the mean. See Table 3 for organisms and citations. Pairwise comparisons using the Mann–Whitney test were performed for each organism to assess differences in transcriptional activity between Stone and FCGS cohorts and between the Stone and Healthy cohorts. $P \leq 0.01$ (**), $P \leq 0.05$ (*), $P > 0.05$ (ns).

Abundant and Active Organisms in Each Microbiome

The healthy group contained a large group of lowly active genera (1,346, 64.9%) compared to the stone (754, 53.6%), or the FCGS microbiomes (639, 55.4%). Among the 10 most transcriptionally active genera in the healthy group were pathogens previously identified in both healthly and diseased oral cavities in cats, including *Moraxella, Frederiksenia, Pasteurella, Porphyromonas,* and *Treponema* (34,35,50,90,91). The most transcriptionally active genera in the stone microbiome included a mix of bacterial, fungal, and protozoal taxa: *Staphylococcus*, *Klebsiella*, *Enterococcus*, *Clostridium*, *Bacillus*, *Aspergillus*, *Plasmodium*, and *Babesia*. Together, these genera accounted for 84.6% of the total transcriptionally active stone microbiome.

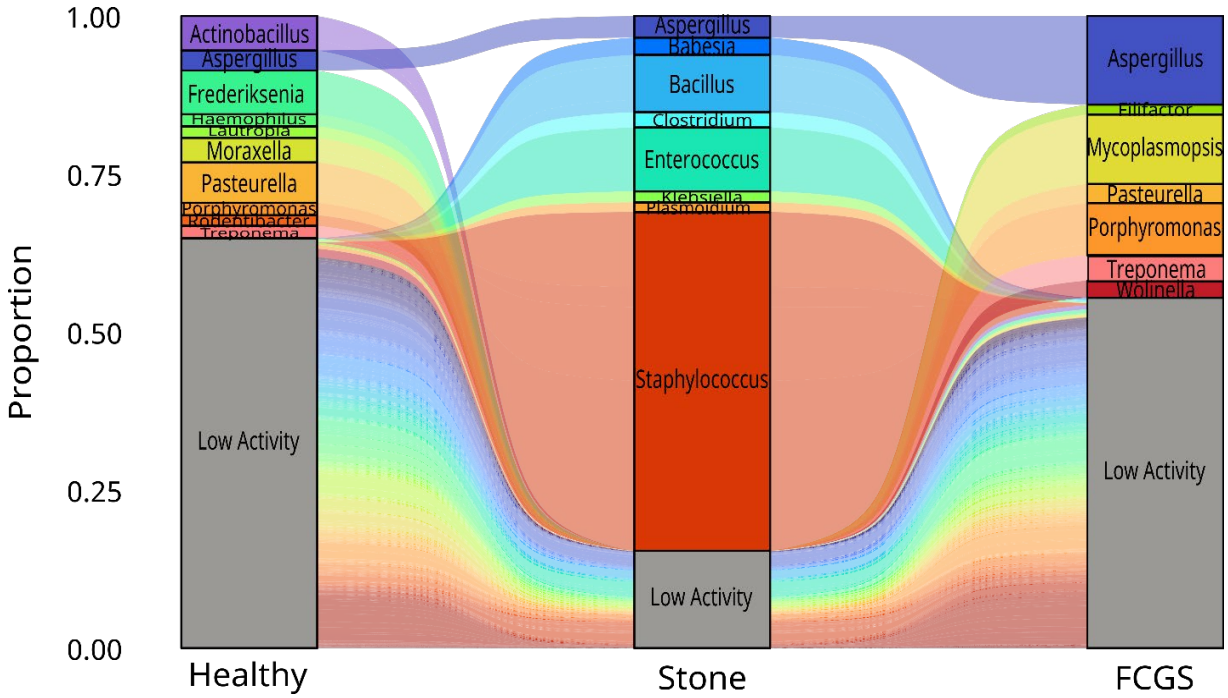

Figure 3. Taxonomic shift between Healthy, Stone, and FCGS microbiomes. Organisms with less than 0.15 of the total proportion of reads in the microbiome were collapsed into the 'Mixed' category in both cohorts.

While this analysis revealed clear differences in dominant taxa across groups, it

did not resolve whether the same species or strains were contributing to activity in each niche. To address this, we assessed their species/strain level abundance and distribution across specimens (Figure 4). Overall, many organisms were shared with enrichment in one microbiome over the other. We also identified several organisms unique to the stone microbiome that were absent from all oral specimens.

Microbes previously identified in cases of struvite urolithiasis including *S. pseudintermedius*, *K. pneumoniae*, and *E. faecalis* (25) were shared between the healthy oral and stone microbiomes but were more enriched in that of the stone. Conversely, known oral-associated species such as *Porphyromonas gingivalis*, *Porphyromonas cangingivalis*, *Treponema denticola*, and *P. multocida* were shared between the healthy oral and stone microbiomes, but were enriched in activity in the healthy oral cavity (Figure 4A). *S. felis* was detected in both healthy oral and stone specimens, with higher abundance in the stone.

When comparing the stone to the FCGS cohort (Figure 4B), 60% of the most abundant stone-exclusive species belonged to *Staphylococcus* or *Enterococcus* (Figure 4A). As in the healthy cohort, *T. denticola* was shared between the FCGS and stone microbiomes, but it was enriched in the FCGS group, where its activity surpassed that in both the stone and healthy oral microbiomes. *Fusobacterium nucleatum* and *Fusobacterium gastrosuis*, both previously implicated in FCGS (35), were highly active in FCGS-affected oral specimens but absent in stones (Figure 4B). Although *S. felis* was present in healthy and stone microbiomes, it was absent from FCGS specimens.

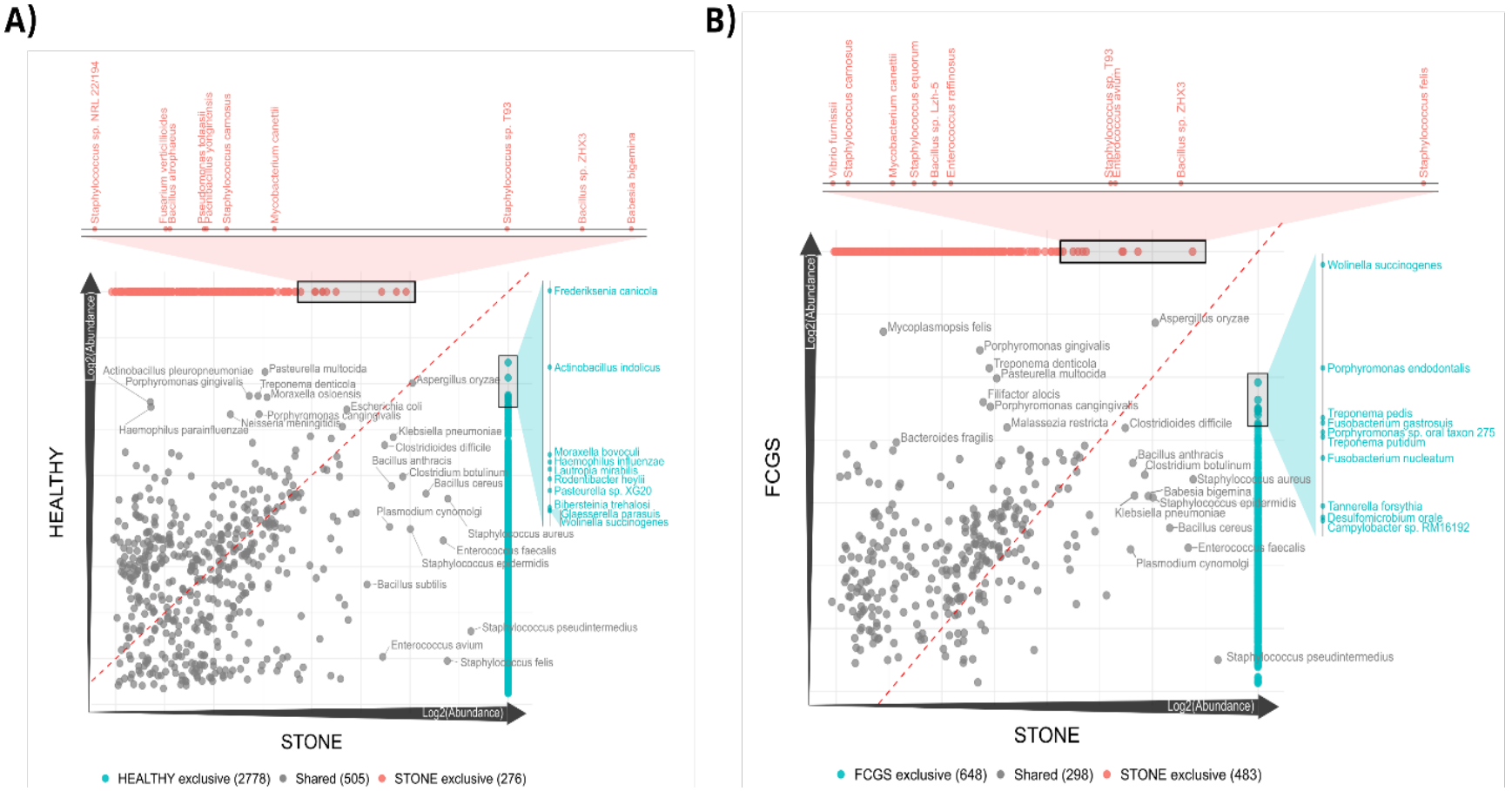

Figure 4. A) Healthy vs Stone, B) FCGS vs Stone. Correlation of the oral and stone microbiome species/strains. Each data point represents a single organism, with the diagonal line indicating equal abundance in the two cohorts. Each grey data point represents a single microbial species/strain that is present in both cohorts in each graph. Species/strains above the dotted line are enriched in the oral cavity (Healthy or FCGS) compared to the stone, while those below the line are enriched in the stone. The clustering pattern of data points with organisms around the center indicate a similar abundance/activity in each location. Microbes found exclusively in the stone are displayed along the top horizontal axis, parallel to the x-axis. Similarly, organisms exclusive to the oral cavity (Healthy or FCGS) are positioned along the far-right vertical axis, parallel to the y-axis. The boxes on each of the exclusive populations are expansions to provide names of top 10 organisms.

Given their well-established association with struvite urolithiasis, we specifically assessed the transcriptional activity of *S. pseudintermedius, K. pneumoniae*, and *P. mirabilis* across cohorts. *S. pseudintermedius* was significantly more active ($P < 0.01$ for both) in the stone microbiome compared to the healthy and FCGS groups, while *P. mirabilis* and *K. pneumoniae* were not significantly different between the stone and the oral cohorts.

Co-occurrence Patterns Differ by Niche

While specific taxa were unique to a given cohort, others were shared between the stone and oral groups but differed in relative transcriptional activity. We hypothesized that these microbes form sub-communities that comingle rather than act in isolation. To explore potential microbial interactions, we focused on a taxon found to differ significantly between the stone and oral cohorts. *Pasteurella*, a genus associated with the oral cavity, was significantly more abundant in both oral groups compared to the stone ($P < 0.01$ for both comparisons; Figure 2), but was also found in stones. The most transcriptionally active member of this genus across all three cohorts was *P. multocida* (Supplemental Figure 2). In all microbiomes, *P. multocida* exhibited extensive co-occurrence relationships, though the identity and direction of these associations varied markedly by location and disease status (Figure 5).

In the stone microbiome (Figure 5A), *P. multocida* was positively correlated with a large number of diverse organisms and displayed a signifcant correlation with stone-asociated organism, *K. pneumoniae* ($\rho = 0.94$, $P = 0.005$). In contrast, the healthy oral microbiome (Figure 5B) exhibited an opposing trend, with *P. multocida* showing mostly

negative correlations with other organisms. Notably, however, the trend of positive correlations with *Klebsiella* species persisted, as both *K. variicola* and *K. aerogenes* had very strong positive correlations with *P. multocida* in the healthy oral cavity (ρ = 0.94, P = 0.005 for both), indicating a consistent ecological association between these genera across niches. In the FCGS oral microbiome (Figure 5C), *P. multocida* displayed a smaller and more selective group of connections with other organisms.

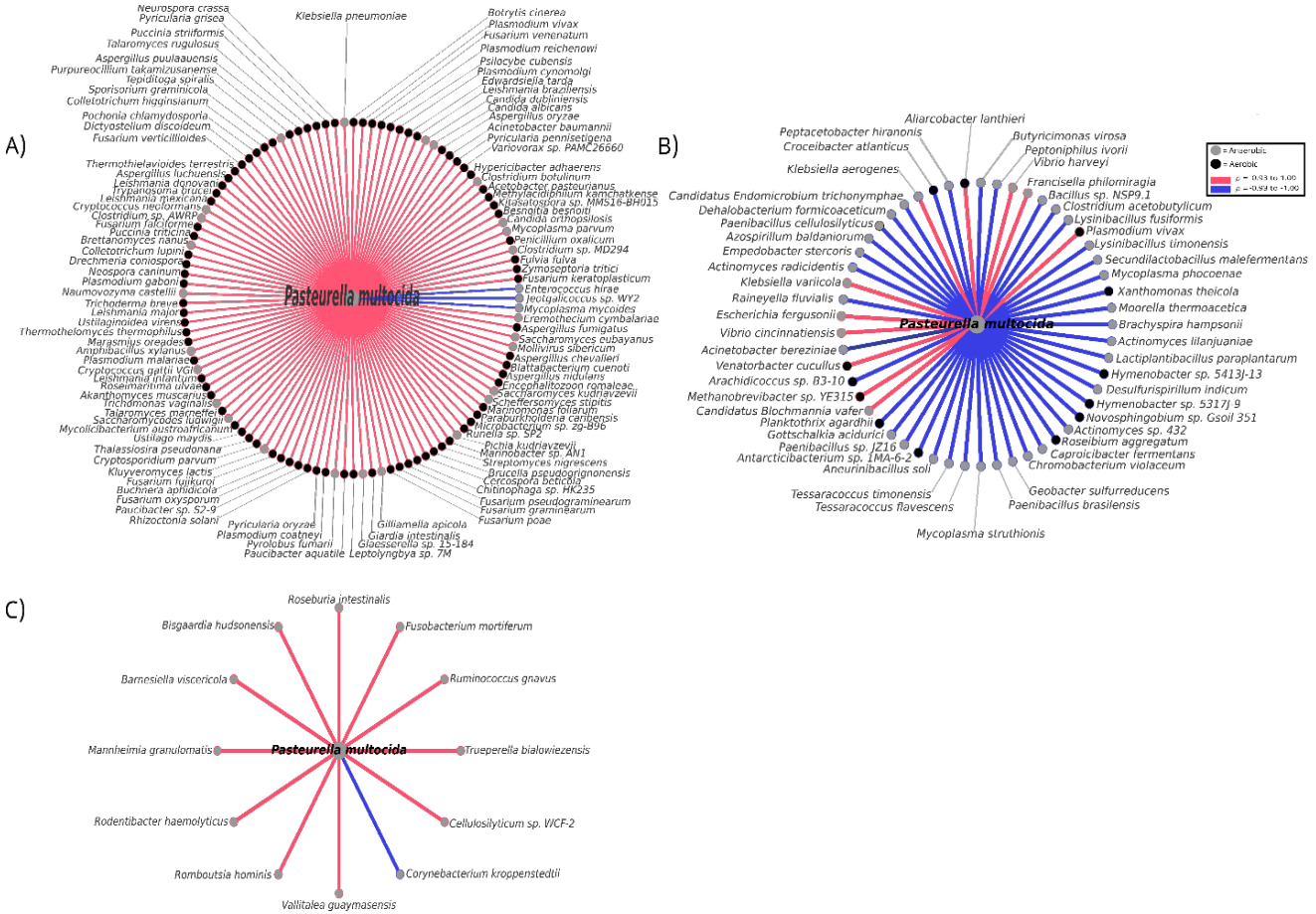

Figure 5. Co-occurrence plots at the strain- and species-level expression of *P. multoicida* in the A) stone, B) healthy, and C) FCGS cohorts. To explore potential microbial interactions, we focused on a taxon found to differ significantly between the stone and oral cohorts. Pasteurella, a genus traditionally associated with the oral cavity, was significantly more abundant in both oral groups compared to the stone ($p < 0.01$ for both comparisons; Figure 2). Pink edges represent positive correlations ($\rho = 0.93$ to 1.00), while blue edges represent negative correlations ($\rho = -0.93$ to -1.00). Node colors reflect the oxygen requirements of organisms, classified at the strain or species level when available, or otherwise inferred from genus-level taxonomy based on published literature. Co-occurrences shown were found to be statistically significant ($P < .05$). Spearman rank correlation coefficients showing as follows: A) ($|\rho| = 0.93$-1.00), B) ($|\rho| = 0.93$ to 099), C) ($|\rho| = 0.93$-1.00).

To refine our understanding of microbial interactions contributing to struvite stone formation, we next focused exclusively on the stone microbiome and examined correlations among the most transcriptionally active bacterial genera identified in this study (Figure 3). *Staphylococcus* was significantly more abundant in the stone microbiome than in both the healthy and FCGS oral cohorts ($P < .01$), and *Enterococcus* was significantly more abundant than in the healthy cohort ($P < 0.05$), with a trend toward increased abundance relative to FCGS. Based on these patterns, we constructed co-occurrence networks centered on the most transcriptionally active species of each genus in the stone microbiome (Supplemental Figure 2). Additional networks were constructed for notable organisms that co-occurred with *Staphylococcus* or *Enterococcus*, to assess their broader interaction patterns and evaluate whether similar correlation trends were observed across locations (Figure 6B, Supplemental Figure 3).

Staphylococcus pseudintermedius in the stone exhibited strong negative correlation (Figure 6A) with many organisms including *Limosilactobacillus fermentum* ($\rho = –0.83$, $P = 0.042$), a known probiotic organism. Given the observed inverse relationship between *S. pseudintermedius* and *L. fermentum*, a well-studied lactic acid bacterium (92), we next constructed a network centered on *L. fermentum* to further investigate this ecological interaction (Figure 6B). *S. pseudintermedius*, as well as other staphylococci were negatively correlated with *L. fermentum* (overall $|\rho| = 0.81–1.00$).

We next constructed targeted co-occurrence networks centered on *E. faecalis* (overall $|\rho| = 0.93–0.94$) (Figure 6C) and *K. pneumoniae* (overall $|\rho| = 0.94–1.00$)

(Figure 6D). *E. faecalis* was found to exhibit only negative correlations, with *Macrococcus canis* having a very strong negative correlation ($\rho = -0.94$, $P = 0.005$) (Figure 6C). *K. pneumoniae,* the most transcriptionally active *Klebsiella spp.* in the stone (Supplemental Figure 1) exhibited a very strong positive correlation with *P. multocida* ($\rho = 0.94$, $P < 0.001$) and very strong negative correlations with organisms including *Jeotgalicoccus sp. WY2* ($\rho = -0.99$, $P < 0.001$) (Figure 6D).

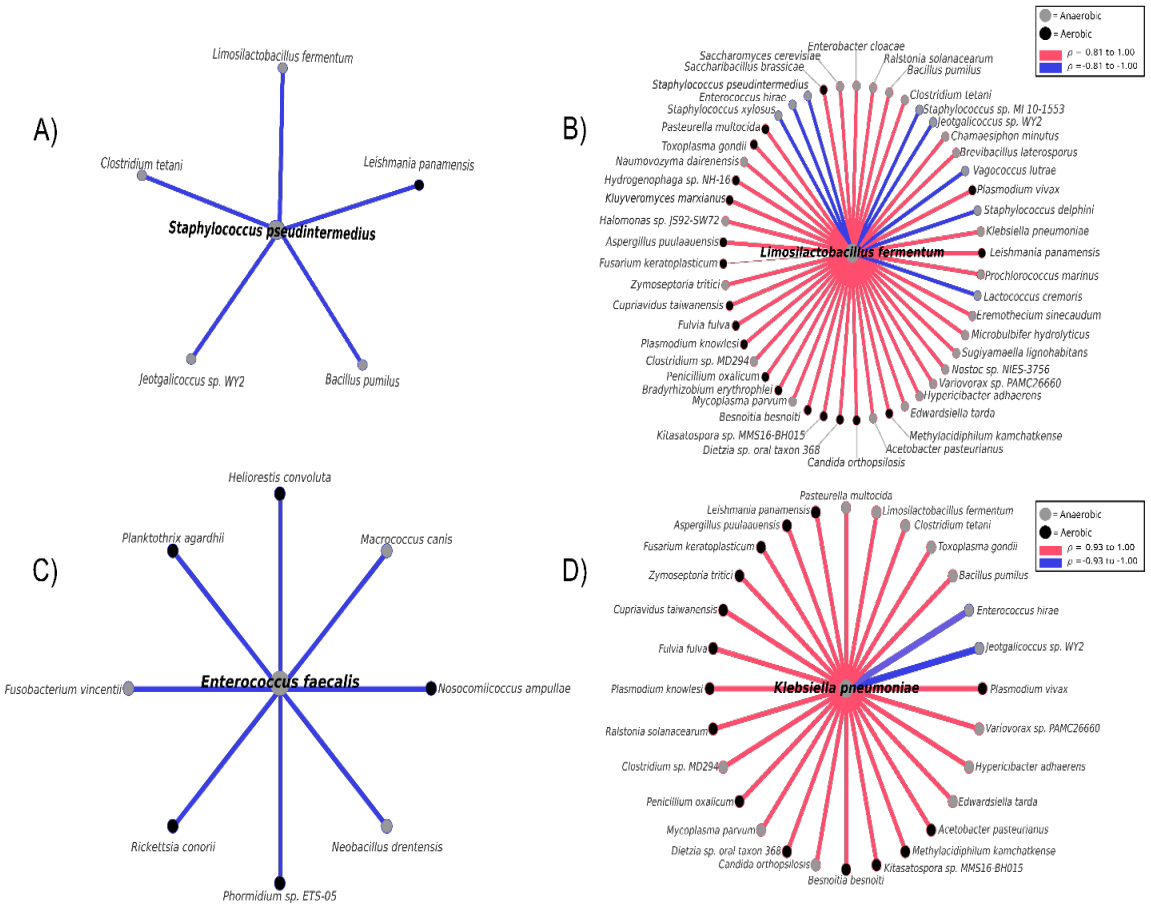

Figure 6. Co-occurrence plots at the strain- and species-level in organisms typically associated with the canine urinary tract identified in the stone. A threshold of $|\rho| \geq 0.81$-1.00 was applied for A) *S. pseudintermedius* and B) *L. fermentum. S. pseudintermedius* displayed a strong negative correlation with *L. fermentum* and given its previous use as a probiotic its co-occurrence plot was shown here. A threshold of $|\rho| \geq 0.93$-1.00 was applied for C) *E. faecalis* and D) *K. pneumoniae*. Pink edges represent positive correlations, while blue edges represent negative correlations. Node colors reflect the oxygen requirements of organisms, classified at the strain or species level when available, or otherwise inferred from genus-level taxonomy based on published literature. Co-occurrences shown were found to be statistically significant ($p<0.05$). Spearman rank correlation coefficients showing as follows: A) ($\rho = -0.81$ to -0.89), B) ($\rho = -0.81$ to -1.00), C) ($\rho = -0.94$ to -1.00), D) ($|\rho| = 0.93$ to 0.94).

Microbial Ammonia Production in the Stone

Using the same metatranscriptomic dataset we found abundant expression of pathway-associated genes in *Staphylococcus* and *Enterococcus*. We therefore prioritized these genera for deeper functional analysis, focusing on three processes central to struvite pathogenesis: ammonia production, biofilm formation, and phosphatase expression. Each of these processes is biologically and chemically relevant to struvite formation and may clarify the ecological roles of dominant taxa in the stone microbiome. Although cat struvite stones are traditionally considered sterile (93), our findings directly challenge this assumption. All stones, even those that were culture negative (Table 2), contained an active microbial community.

To further explore how these microbial consortia may be contributing to struvite stone formation in this species, we next analyzed gene expression across four major ammonia-producing pathways: urea hydrolysis via urease, the arginine deiminase (ADI) pathway, deamination of nitrogenous compounds, and dissimilatory nitrate reduction to ammonia (DNRA). Our results revealed abundant canonical gene expression linked to multiple ammonia-producing pathways in *Staphylococcus* and *Enterococcus*. In *Staphylococcus*, the urease, ADI, and deamination pathways were transcriptionally active, while *Enterococcus* expressed only the ADI and deamination pathways (Figure 7).

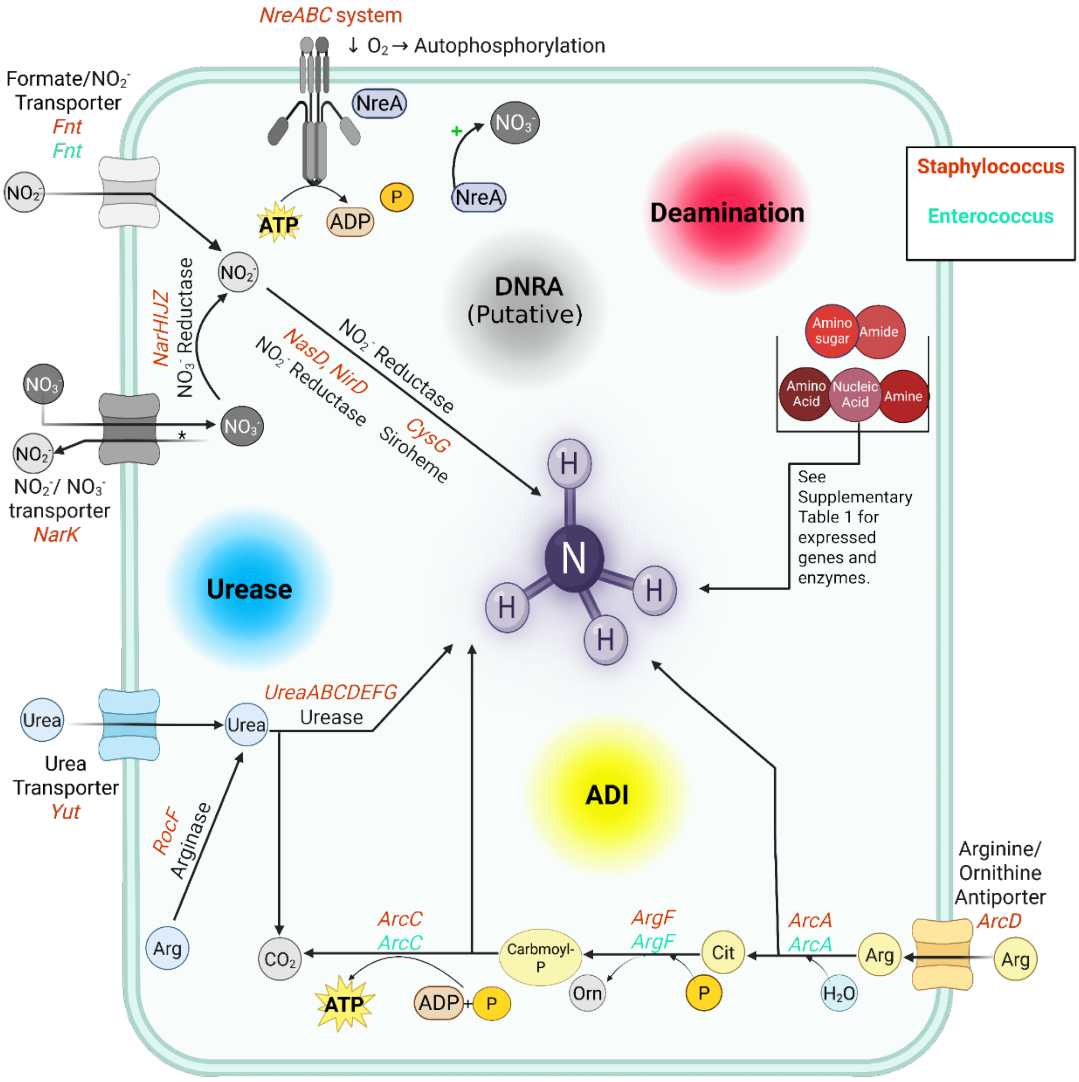

Figure 7. Summary Figure of Pathways Actively Expressed in *Staphylococcus* and *Enterococcus*, within the microbiome of the cat struvite urolith. CK= carbamate kinase, OTC= Ornithine carbmoyltransferase, ADI= Arginine Deiminase. *= During DNRA, nitrite (NO_2^-) may be exported if nitrite reductase capacity is exceeded to avoid excessive NO_2^- accumulation which can be toxic to the cell. During our analysis, it was discovered that Staphylococcus expressed sections of the DNRA (Dissimilatory Nitrate Reduction to Ammonia), nitrate reduction to nitrite. The NreABC nitrate-responsive two-component regulatory system was expressed by *Staphylococcus* which regulates nitrate and nitrite reductase expression during DNRA in response to oxygen and nitrate levels. However, for the purpose of quantifying ammonia production, this pathway was not considered for quantification of ammonia production. Created using Biorender.com.

Deamination accounted for the largest proportion of ammonia production by *Staphylococcus* (59.9%), followed by urease (34.1%), and ADI (6.1%) (Figure 8A). Both deamination and urease pathways were expressed at significantly higher levels in *Staphylococcus* than ADI ($p < 0.05$; Supplemental Figure 3A). *Staphylococcus* expressed nitrate reduction operon (*narHIJZK*) as well as the genes for the entire 2-component regulatory system *nreB/nreC*, which controls DNRA gene expression in response to local oxygen levels (Figure 7). However, canonical genes for the second step in the DNRA pathway, nitrite reduction to ammonia, which is catalyzed by a cytochrome c nitrite reductase (94), were not detected. Other functionally equivalent reductases were expressed but it remains to be proven that these genes can participate in DNRA. Therefore, this pathway was excluded from ammonia quantification in this analysis, even though genes associated with this general functional category were observed for the regulation and the entire first step of the pathway.

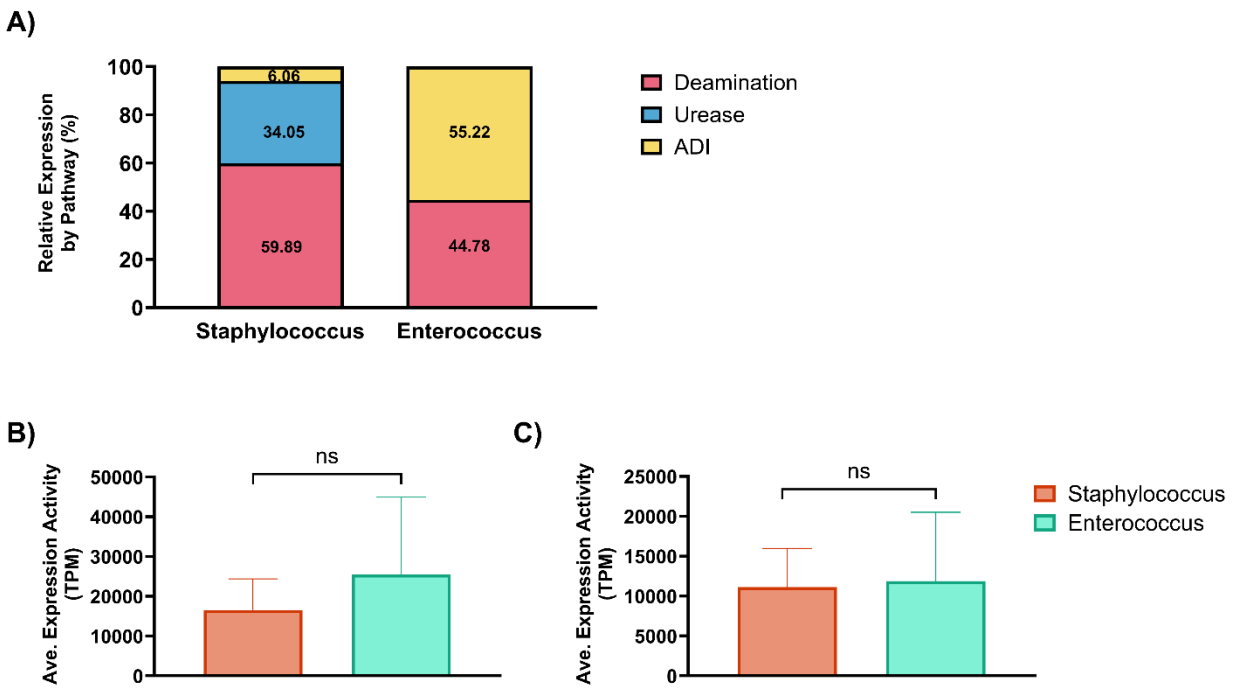

Figure 8. Comparison of pathway expression profiles across the two dominant genera; A) Expression values adjusted for the moles of ammonia produced per pathway. B) Average biofilm expression activity by genus. Pairwise comparisons between organisms were conducted using Wilcoxon signed-rank tests. ns = not significant. Bars represent the mean expression activity, with error bars indicating SEM. C) Average phosphatase expression activity by genus. Shapiro–Wilk tests were used to assess normality. As the data were not normally distributed, unpaired Wilcoxon signed rank sum tests were performed for both phosphatase and biofilm expression.

In contrast, *Enterococcus* expressed the ADI pathway primarily, which contributed more than half of its estimated total ammonia output (55.2%), compared to 44.8% from deamination (Figure 8A). Expression of the ADI and deamination pathways by *Enterococcus* was not statistically significant (Supplemental Figure 3B). Although *Staphylococcus* showed a trend toward higher expression of deamination reactions and *Enterococcus* trended toward higher expression of the ADI pathway, neither difference was statistically significant (Supplemental Figure 3C and 3D, respectively). When accounting for the estimated moles of ammonia produced per deamination reaction, both genera contributed comparable total ammonia-producing activity, indicating that

both organisms expressed similar amounts of ammonia-producing genes to produce ammonia (Supplemental Table 1).

Given that deamination was a predominant mechanism expressed by both genera to produce ammonia in the stone we defined the role of deamination in promoting struvite formation. To do this, the transcriptional activity of genes encoding enzymes that directly release free ammonia in deamination reactions, excluding those that use ammonia only as an intermediate (Supplemental Table 1). Both *Staphylococcus* and *Enterococcus* expressed genes needed to liberate ammonia from a wide range of nitrogen-containing substrates. These substrates include nucleotides such as adenosine and amino acids such as alanine, asparagine, ornithine, serine, and threonine, along with amino sugars such as glucosamine-6-phosphate (Supplemental Table 1). Beyond the shared deamination pathways, each genus also employed distinct mechanisms to generate ammonia. *Staphylococcus* uniquely expressed the histidine degradation pathway *(hutGHIU)*, which generates glutamate and formamide from histidine (95). In conjunction, the expression of formamidase *(fmdA)* allows hydrolysis of formamide to release a second mole of ammonia, resulting in a net yield of two moles of ammonia per histidine (95). In contrast, *Enterococcus* expressed the full pathway required to metabolize ethanolamine, a host-derived compound released during membrane turnover (96). Additionally, *Enterococcus* expressed transglutaminase, an enzyme that not only facilitates ammonia release through deamidation of glutamine residues but may also promote sugar/protein matrix cross-linking and stabilization of polymicrobial biofilms (97).

Biofilm Production in the Stone

Biofilm formation is a key microbial strategy for persistence in many environments, including the urinary tract and urinary stones (8,53). Both *Staphylococcus* and *Enterococcus* expressed biofilm genes associated with adhesion, matrix production, and extracellular remodeling (Supplemental Table 3). While *Enterococcus* exhibited approximately 1.5-fold higher expression of biofilm-associated genes compared to *Staphylococcus*, this difference did not reach statistical significance (Supplemental Figure 3), but indicated that both genera produced biofilms as part of their metabolism in stones.

Staphylococcus expressed a suite of genes associated with biofilm formation within the stone environment, including all four components of the *ica* operon *(icaA, icaB, icaC, icaD)*, which are critical for polysaccharide intercellular adhesin (PIA) synthesis, as well as the global regulator *sarA,* which enhances *ica* expression (98). Transcripts for *agrA, agrB, and agrD,* components of the *agr* quorum-sensing system were also expressed along with the complete *cidABC* operon. Multiple capsular biosynthesis genes were also expressed, including *capA, capB, capD, capI, capL, and capO*. Genes *femA, femB,* and *femX* were also expressed (99,100).

Enterococcus expressed several genes associated with biofilm formation in the stones, including some that overlapped with those found in *Staphylococcus,* as well as others that were distinct. Like Staphylococcus, Enterococcus expressed parts of the agr quorum-sensing system (*agrA* and *agrC*). Canonical biofilm genes including *srtA, srtC, and veg* were present. Additionally, *gelE* was expressed which encodes for a gelatinase that degrades host proteins and contributes to matrix remodeling (101).

Phosphate Production in the Stone

Expression of phosphate-releasing enzymes was similar between *Staphylococcus* and *Enterococcus* (Figure 9). *Staphylococcus* and *Enterococcus* expressed alkaline phosphatase (*phoB*) and alkaline phosphatase synthesis transcriptional regulator (*phoP*) (Supplemental Table 3). Additionally, both genera expressed acid phosphatases (*pgpB3* in *Staphylococcus, yodM* in *Enterococcus*). Both genera expressed *ppaC*, which encodes an inorganic pyrophosphatase that hydrolyzes pyrophosphate (PPi) to produce orthophosphate (PO_4^{3-}) (11). In *Staphylococcus*, additional expression of *ppx* and *rdgB* was observed. *Ppx* encodes an exopolyphosphatase that cleaves terminal phosphate groups from polyphosphate chains, while *rdgB* hydrolyzes purine nucleotides and generates PPi, which can then serve as a substrate for *PpaC*-mediated phosphate release (102,103). Further, *Enterococcus* expressed *acyP* that encodes an acylphosphatase to catalyze a direct route of PO_4^{3-} liberation through the cleavage of acyl-phosphate bonds (41).

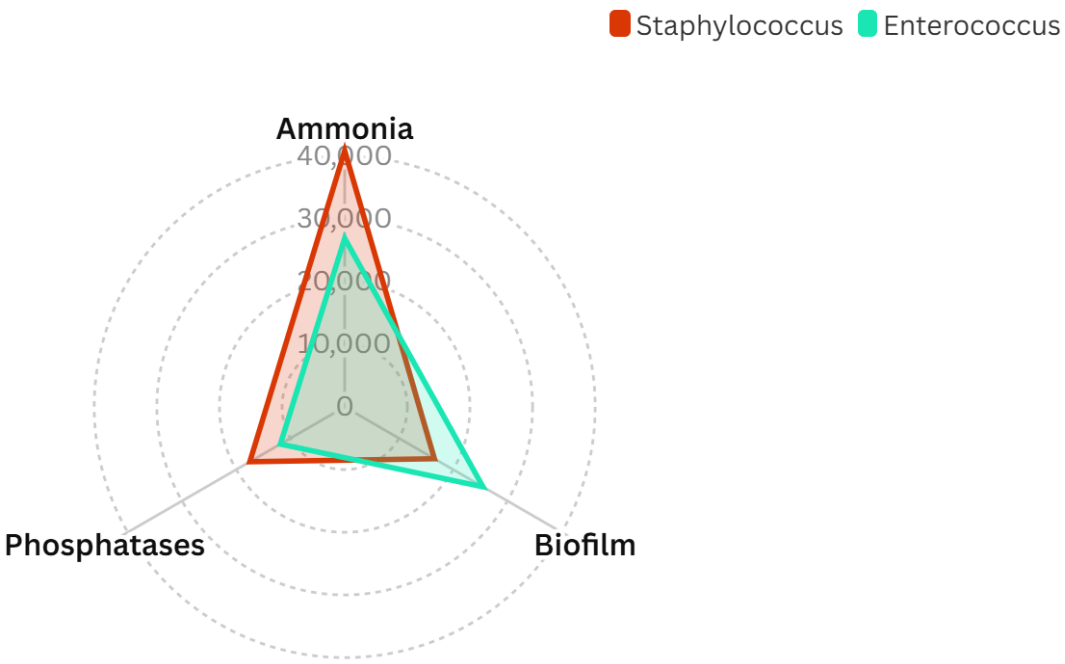

Figure 9. Radar plots of average pathway expression across keystone genera. Each plot compares expression levels of three functional pathway categories: 1) ammonia production that includes: ADI, deamination, urease-associated pathway, dissimilatory nitrite reduction, 2) biofilm expression, and 3) phosphatase expression. Average TPM-normalized expression adjusted for estimated ammonia yield per pathway is shown for *Staphylococcus and Enterococcus.*

DISCUSSION

Struvite urolithiasis in cats has long been considered sterile, with bacteria thought to play little role in stone formation (13). Our metatranscriptomic data challenge this view, revealing that feline struvite stones harbor diverse, transcriptionally active microbial communities. Dominant bacterial genera, including *Staphylococcus*, *Enterococcus*, expressed genes directly linked to struvite pathogenesis, including ammonia production, phosphate mobilization, and biofilm formation. Rather than being sterile, these stones appear to be ecological niches shaped by microbial metabolism.

Overlap in Community Membership Reveals an Oral/Stone Axis

Comparison of stone and oral microbiomes uncovered an oral–stone microbial axis. The healthy oral microbiome shared more taxa with stones than the FCGS cohort (Figure 1A and 1B), suggesting that barrier breakdown in FCGS is not the only route of microbial escape. Instead, selective enrichment within the stone environment may favor particular taxa regardless of disease status. Beta diversity analyses showed that stones were significantly different from healthy oral microbiomes but not from those of FCGS-affected cats (Figure 1D). This indicates that the overall microbial community of stones more closely resembles the oral microbiome in FCGS, which may predispose these taxa to persist in the urinary environment. In contrast, the healthy oral cavity harbors a broader array of low-abundance organisms, but these appear less suited to thrive under the selective pressures of the stone.

Comparison with Prior Literature and UCs

Half of the stones had yielded *Staphylococcus* on culture (Table 2) but metatranscriptomics revealed that even culture-negative stones contained rich microbial communities . All taxa historically associated with feline struvite were transcriptionally active in our dataset, confirming their relevance but also highlighting the vast under-detection by traditional culture (Figure 2). This underscores that culture-based approaches underestimate both diversity and function, and that molecular methods are needed to appreciate the full microbial contribution to struvite pathogenesis. Genera previously reported in the literature to be associated with struvite urolithiasis in cats were not only active in the stone microbiome, they were present in both the healthy and

FCGS microbiomes further suggesting that the oral cavity may serve as a reservoir for stone-associated organisms (Table 2 and Figure 2).

Abundant and Active Organisms in Each Microbiome

As we continued to investigate microbial membership between the three cohorts, we found that the stone microbiome was transcriptionally dominated by a diverse array of bacterial, fungal, and protozoal taxa, including *Staphylococcus*, *Klebsiella*, *Enterococcus*, *Clostridium*, *Bacillus*, *Aspergillus*, *Plasmodium*, and *Babesia* (Figure 3). Among the bacterial genera, *Staphylococcus*, *Klebsiella*, and *Enterococcus* have previously been implicated in struvite urolithiasis in cats (7,21,25). Although fungi and protozoa were not the focus of this study, their active presence within the stone microbiome suggests a potential role in pathogenesis that warrants further investigation. In contrast, oral microbiomes—both healthy and FCGS—were dominated by taxa such as *Moraxella*, *Porphyromonas*, and *Treponema*, established oral organisms in the cat (34,35). At the species/strain level, many taxa overlapped across niches but shifted in relative activity: *S. pseudintermedius*, *K. pneumoniae*, and *E. faecalis* were enriched in stones, whereas *P. gingivalis* and *T. denticola* were more active in oral sites (Figure 4A and 4B). This overlap, combined with the differential activity patterns, reinforces the concept of an oral–stone axis while highlighting the selective forces that shape microbial dominance in each niche. In the oral cavity, particularly in healthy cats the largely aerobic, nutrient-rich enviornment likely supports a, a broader community (104). In FCGS, chronic inflammation, tissue disruption, and altered nutrient availability shift this balance, enriching for taxa with pathogenic potential (34). The stone environment, by

contrast, functions as a narrow ecological bottleneck. Alkaline pH, limited nutrient and oxygen diffusion likely restrict the community to a smaller set of organisms capable of withstanding stress while actively contributing to struvite formation.

Co-occurrence Patterns Differ by Niche

P. multocida, detected in all three cohorts, allowed comparison of co-occurrence networks across stones, healthy oral, and FCGS oral microbiomes (Figure 5). Although most abundant orally, it was transcriptionally active in all niches and showed environment-specific interactions: positively correlating with diverse taxa including *K. pneumoniae* in stones, mostly negative correlations in healthy oral samples except with *Klebsiella spp*., and a more selective pattern in FCGS oral networks. These findings underscore the ecological flexibility of shared taxa across niches and disease states.

A strong negative correlation between *Limosilactobacillus fermentum* and *S. pseudintermedius* ($|\rho| = 0.83$) in stones suggests an antagonistic interaction with therapeutic potential (Figure 6). Multiple studies support the use of *L. fermentum* as a probiotic with broad-spectrum antimicrobial, immunomodulatory, and mucosal-protective properties across diverse host environments (92,105–111). Several strains exhibit direct antimicrobial activity against *Staphylococcus aureus*, a close relative of *S. pseudintermedius*, through the production of antibacterial proteins with potent lytic activity, induction of ATP leakage, disruption of cell membranes, and formation of co-aggregates that physically entrap and kill staphylococci (110). Additionally, *L. fermentum* produces organic acids and antibacterial proteins effective against a range of bacterial and fungal pathogens as it has been found to strengthen epithelial barrier

integrity, reduce pathogen adhesion, and modulates immune responses (92,105–111). These attributes support *L. fermentum* as a candidate probiotic to modulate urinary pathogens and potentially reduce struvite stone risk.

Microbial Ammonia Production in the Stone

In addition to urease-associated routes, multiple microbially mediated ammonia-producing routes including the ADI pathway and deamination of nitrogenous compounds were expressed by dominant taxa in the stone (Figure 7). In *Staphylococcus*, ammonia production was supported by urease (~34% of adjusted expression), with deamination pathways contributing ~60%, and the arginine deiminase (ADI) pathway the remainder (6%) (Figure 8). In addition to these pathways, *Staphylococcus* may engage in a non-canonical dissimilatory nitrate reduction to ammonia (DNRA) pathway was suggested by expression of nar operon genes (narKHIJZ), nitrate sensors (nreA, nreB/nreC) (113,114) (Supplemental Table 1). Although typical DNRA genes such as *nrfA* were absent, *Staphylococcus* expressed *nasD* and *nirD*, which encode siroheme-dependent nitrite reductases generally linked to assimilatory nitrate reduction. However, NasDE complexes in other organisms can function in both assimilatory and dissimilatory pathways depending on environmental context (115). The presence of *cysG*, essential for siroheme biosynthesis, and *fnt*, encoding a formate/nitrite transporter, further supports the operation of DNRA via non-canonical means (114). This mechanism could enable *Staphylococcus* to generate ammonia locally, especially within biofilm-dense, anaerobic niches of the stone.

Enterococcus expressed ADI and deamination pathways, including ethanolamine catabolism via the eut operon (Supplemental Table 1). Ethanolamine is a breakdown product of host membrane phospholipids and may be abundant in damaged or inflamed uroepithelial environments, an expected consequence of struvite stone formation (116). Facultative anaerobes that colonize the oral cavity have been found to express this same operon (96,117). The *eut* genes have also been found to be upregulated in clinical *E. coli* isolates from human UTIs (96,117), which are typically urease negative. This route may represent an underappreciated urease-independent source of ammonia contributing to urinary alkalinization and struvite crystallization, expanding the repertoire of bacteria that contribute to ammonia production in the cat struvite stone.

Biofilm Production in the Stone

Staphylococcus expressed a broad suite of genes supporting biofilm formation, including the full icaADBC operon and the global regulator *sarA*, which enhances ica expression (98). The icaADBC operon produces polysaccharide intercellular adhesin (PIA), a key component of multilayered biofilms, and PIA production has been functionally linked to the ADI ammonia-generating pathway (98,118). Expression of *femA, femB, and femX,* essential for peptidoglycan cross-linking and cell wall strength, further stabilizes the biofilm matrix and enhances resistance to host defenses (99). Collectively, these findings indicate that *Staphylococcus* biofilms in stones are highly adapted, coupling metabolic activity with structural reinforcement. Beyond structural components, *Staphylococcus* regulates biofilm formation and virulence via quorum sensing (121). *S. pseudintermedius* uses a system similar to *S. aureus*, but differences

in signaling peptides alter gene activation (121,122). Because many anti-virulence strategies target this interaction, the structural distinction suggests that therapies effective against *S. aureus* may not translate directly to *S. pseudintermedius,* highlighting the need for species-specific approaches (122).

Conversely, *Enterococcus* expressed a distinct biofilm gene set including *gelE* gelatinase, which degrades host matrix proteins facilitating tissue invasion and biofilm remodeling, sortases (*srtA, srtC*) anchoring surface adhesins, and *veg,* a gene linked to the transition from planktonic to sessile growth and upregulation of matrix genes (101,123). *Enterococcus* also expressed transglutaminase-like proteins capable of cross-linking matrix proteins and enhancing biofilm cohesion. In other Gram-positive bacteria, transglutaminases stabilize the biofilm matrix and anchor adhesins to the cell wall, contributing to mechanically resilient biofilms (101). This activity may help maintain a biofilm framework that traps mineral precursors such as phosphate, ammonium, and magnesium. Together with capsule biosynthesis genes, these factors suggest *Enterococcus* forms a flexible yet resilient biofilm structure capable of adapting to environmental changes.

Phosphate Production in the Stone

Both genera expressed alkaline and acid phosphatases enabling phosphate mobilization across fluctuating pH conditions, critical for struvite precipitation (Supplemental Table 3). The shared expression *of phoB* (encoding alkaline phosphatase or its homologs) alongside acid phosphatase genes such as *yodM* and *pgpB3* suggests a convergent microbial mechanism for phosphate acquisition that

operates efficiently under variable environmental conditions. This coordinated enzymatic activity is especially relevant to struvite stones, as alkaline phosphatase exhibits optimal function at the elevated pH levels conducive to struvite precipitation.

Although struvite stones are composed largely of phosphate, much of it is sequestered in the crystalline matrix. As the stone enlarges, particularly within biofilm-dense regions, phosphate becomes incorporated into struvite crystals and locally depleted, triggering bacterial phosphatase expression (124). Both *Staphylococcus* and *Enterococcus* displayed expression of the Pho regulon, a conserved system that regulates phosphate acquisition in response to limitation (125). Expression of *phoP*, a transcriptional regulator controlling alkaline phosphatase synthesis (125), suggests that the microbes are actively facilitating phosphate release under the alkaline conditions needed for struvite formation. Furthermore, expression of high-affinity phosphate transporters (pstSCAB–phoU operon) by both *Staphylococcus* and *Enterococcus* indicates active phosphate sensing, acquisition, and mobilization under local phosphate-limited conditions. The concurrent presence of phosphate-liberating enzymes and high-affinity transporters indicates these bacteria not only release phosphate from intracellular sources but also efficiently reclaim extracellular phosphate, sustaining the local PO_4^{3-} supply necessary for ongoing struvite formation.

CONCLUSION

This study challenges the long-standing assumption that struvite uroliths from cats are sterile by demonstrating that they harbor a diverse, transcriptionally active microbial community. Metatranscriptomic analysis revealed extensive taxonomic

overlap between the stone and oral microbiomes, particularly in cats affected by FCGS, suggesting a potential oral–stone axis. Hundreds of bacterial genera were identified in stones, including organisms previously associated with stones including *Staphylococcus, Enterococcus*, and *Klebsiella.* While many taxa were detected, functional analysis focused on *Staphylococcus* and *Enterococcus*, the most transcriptionally active genera within the stone microbiome. These organisms expressed multiple pathways relevant to struvite pathogenesis, including ammonia production via deamination and the arginine deiminase (ADI) pathway, urease activity (in *Staphylococcus*), phosphate liberation, and biofilm-associated genes. Importantly, ammonia production was not limited to urease, underscoring the contribution of alternative metabolic pathways. These findings support a model in which polymicrobial metabolic interactions within the stone microenvironment contribute to local biochemical conditions that favor struvite precipitation. By integrating microbial taxonomy and function across health states, this study provides new insights into the ecology of cat struvite uroliths and underscores the potential role of oral dysbiosis in stone pathogenesis.

Acknowledgments

The authors would like to thank B. Carol Huang from the UC Davis School of Veterinary Medicine for their technical expertise.

Funding

This work was supported by UCD School of Veterinary Medicine, The Center for Companion Animal Health at the UC Davis School of Veterinary Medicine and Soltero-Rivera startup funds. Financial support for AMF was supported by the MSTP T32 (NIH Grant T32GM136559), NIH TL1 Training Grant (5TL1DK139565-02) through the LAUNCH Program, UCSF. The funding sources were not involved in the study design, collection, analysis and interpretation of the data, in writing the report, or in the decision to submit this article for publication.

Data Availability Statement: Please contact the corresponding authors for data presented in this study.

Conflicts of Interest: The authors declare no conflicts of interest.

References

1. Hobday F. Urinary Calculi in Animals. J R Soc Med. 1922 Jun;15(Sect_Urol):69–72.

2. Kirk H. Urinary Calculi (Renal, Cystic, and Urethral). In: The Diseases of the Cat and Its General Management. Baillière, Tindall and Cox; 1925. p. 269–72.

3. Blout WP. Urinary Calculi. Vet J. 1931 Dec;87(12):561–76.

4. Defarges A, Evason M, Dunn M, Berent A. Urolithiasis in Small Animals. In: Clinical Small Animal Internal Medicine. Wiley; 2020. p. 1123–56.

5. Eyral V, Pichard D, Mariaud V, Manassero M, Maurey C. Struvite ureterolithiasis associated with ureolytic bacterial pyelonephritis in a cat. J Feline Med Surg Open Rep. 2025 Jan;11(1).

6. Albasan H, Osborne CA, Lulich JP, Lekcharoensuk C, Koehler LA, Ulrich LK, et al. Rate and frequency of recurrence of uroliths after an initial ammonium urate, calcium oxalate, or struvite urolith in cats. Sci Rep JAVMA. 2009 Dec;235(12).

7. Bohonowych RO, Parks JL, Greene RW. Cystic Calculi in Cats in a Hospital Population. J Am Vet Med Assoc. 1978;73(3):301–3.

8. Nickel JC, Costerton JW, Mclean' RJC, Olson M. Bacterial biofilms: influence on the pathogenesis, diagnosis and treatment of urinary tract infections [Internet]. Vol. 33, Journal of Antimicrobial Chemotherapy. 1994 p. 31–41. Available from: https://academic.oup.com/jac/article/33/suppl_A/31/723390

9. Flannigan R, Choy WH, Chew B, Lange D. Renal struvite stones - Pathogenesis, microbiology, and management strategies. Nat Rev Urol. 2014;11(6):333–41.

10. Çam S, Badıllı İ. The effect of NaCl, pH, and phosphate on biofilm formation and exopolysaccharide production by high biofilm producers of Bacillus strains. Folia Microbiol (Praha). 2024 Jun;69(3):613–24.

11. Sajid A, Arora G, Singhal A, Kalia VC, Singh Y. Protein Phosphatases of Pathogenic Bacteria: Role in Physiology and Virulence. Vol. 69, Annual Review of Microbiology. Annual Reviews Inc.; 2015. p. 527–47.

12. Danikowski KM, Cheng T. Alkaline Phosphatase Activity of Staphylococcus aureus Grown in Biofilm and Suspension Cultures. Curr Microbiol. 2018 Sep;75(9):1226–30.

13. Lulich JP, Berent AC, Adams LG, Westropp JL, Bartges JW, Osborne CA. ACVIM Small Animal Consensus Recommendations on the Treatment and Prevention of Uroliths in Dogs and Cats. J Vet Intern Med. 2016 Sep;30(5):1564–74.

14. Rivadeneyra MA, Gutierrez-Calderó A, Rivadeneyra AM, Ramos-Cormenzana A. A Study of Struvite Precipitation and Urease Activity in Bacteria Isolated from Patients with Urinary Infections and Their Possible Involvement in the Formation of Renal Calculi. Urol Int. 1999 Sep;63:188–92.

15. Wallace B, Chmiel JA, Al KF, Bjazevic J, Burton JP, Goldberg HA, et al. The Role of Urinary Modulators in the Development of Infectious Kidney Stones. J Endourol. 2023 Mar;37(3):358–66.

16. DiBartola SP, Chew DJ. Canine Urolithiasis. Compend Contin Educ Pract Vet. 1981 Mar;3(3):226–34.

17. Westropp JL, Sykes JE. Infections of the Genitourinary Tract. In: Sykes JE, editor. Greene's Infectious Diseases of the Dog and Cat. 5th ed. Elsevier; 2023. p. 1669–87.

18. Westropp JL, Stella JL, Buffington CAT. Interstitial cystitis—an imbalance of risk and protective factors? Vol. 5, Frontiers in Pain Research. Frontiers Media SA; 2024.

19. Dear JD, Larsen JA, Bannasch M, Hulsebosch SE, Gagne JW, Johnson EG, et al. Evaluation of a dry therapeutic urinary diet and concurrent administration of antimicrobials for struvite cystolith dissolution in dogs. BMC Vet Res. 2019 Aug;15(1):1–8.

20. Grauer GF. Feline Struvite & Calcium Oxalate Urolithiasis. Today's Veterinary Practice. 2015. p. 14–20.

21. Kopecny L, Palm CA, Segev G, Larsen JA, Westropp JL. Urolithiasis in cats: Evaluation of trends in urolith composition and risk factors (2005-2018). J Vet Intern Med. 2021 May;35(3):1397.

22. Houston DM, Vanstone NP, Moore AEP, Weese HE, Weese JS. Evaluation of 21426 feline bladder urolith submissions to the Canadian Veterinary Urolith Centre (1998–2014). Can Vet J. 2016 Feb;57(2):196–201.

23. Perry LA, Kass PH, Johnson DL, Ruby AL, Shiraki R, Westropp JL. Evaluation of culture techniques and bacterial cultures from uroliths. J Vet Diagn Invest. 2013 Mar;25(2):199–202.

24. Machado J da C, Renteria JM, Nascimento MM do, Cunha ACA, Vieira GM, Manso JEF. Association between urinary lithiasis, other than struvite by crystallography and non-ureolytic bacteria. Urolithiasis. 2024 Dec;52(1).

25. Detkalaya O, Kornkasem S, Vichukit K, Suksamranthaweerat M, Aponrat P. Association between uropathogens and the occurrence of magnesium ammonium phosphate and calcium oxalate in cats with urolithiasis: a retrospective study (2016-2021). J Feline Med Surg. 2025 Apr;27(4).

26. Palma D, Langston C, Gisselman K, McCue J. Feline Struvite Urolithiasis. Compendium: Continuing Education for Veterinarians®. Vetlearn.com; 2009. p. E1–8.

27. Kim Y, Carrai M, Leung MHY, Chin J, Li J, Lee PKH, et al. Dysbiosis of the Urinary Bladder Microbiome in Cats with Chronic Kidney Disease. 2021; Available from: https://doi.org/10.1128/mSystems

28. Aguiar-Pulido V, Huang W, Suarez-Ulloa V, Cickovski T, Mathee K, Narasimhan G. Metagenomics, metatranscriptomics, and metabolomics approaches for microbiome analysis. Vol. 12, Evolutionary Bioinformatics. Libertas Academica Ltd.; 2016. p. 5–16.

29. Matchado MS, Rühlemann M, Reitmeier S, Kacprowski T, Frost F, Haller D, et al. On the limits of 16S rRNA gene-based metagenome prediction and functional profiling. Microb Genomics. 2024 Feb;10(2).

30. Balboni A, Franzo G, Bano L, Arcangeli SD, Rizzardi A, Urbani L, et al. Culture-Dependent and Sequencing Methods Revealed the Absence of a Bacterial Community Residing in the Urine of Healthy Cats. Front Vet Sci. 2020 Aug;7.

31. Balboni A, Franzo G, Bano L, Urbani L, Segatore S, Rizzardi A, et al. No viable bacterial communities reside in the urinary bladder of cats with feline idiopathic cystitis. Res Vet Sci. 2024 Mar;168.

32. Lake BB, McAdams ZL, Ericsson AC, Reinero C, Gull T, Lyons BM. Feline urethral obstruction alters the urinary microbiota and comparison to oral, preputial, and rectal microbiotas. Am J Vet Res. 2025 Feb;86(2).

33. Joubran P, Roux FA, Serino M, Deschamps JY. Gut and Urinary Microbiota in Cats with Kidney Stones. Microorganisms. 2024 Jun;12(6).

34. Shaw CA, Soltero-Rivera M, Profeta R, Weimer BC. Case Report: Inflammation-Driven Species-Level Shifts in the Oral Microbiome of Refractory Feline Chronic Gingivostomatitis. Bacteria. 2025 Mar;4(1):1–0.

35. Shaw CA, Soltero-Rivera M, Profeta R, Weimer BC. Case Report: Shift from Aggressive Periodontitis to Feline Chronic Gingivostomatitis Is Linked to Increased Microbial Diversity. Pathogens. 2025 Mar;14(3).

36. Kleinstein SE, Nelson KE, Freire M. Inflammatory Networks Linking Oral Microbiome with Systemic Health and Disease. J Dent Res. 2020 Sep;99(10):1131–9.

37. Kislik G, Zhou L, Rubbi L, Pellegrini M. Age-correlated changes in the canine oral microbiome. Front Microbiol. 2024;15.

38. Lim MY, Kim JH, Nam YD. Oral microbiome correlates with selected clinical biomarkers in individuals with no significant systemic disease. Front Cell Infect Microbiol. 2023;13.

39. Lilenbaum W, Esteves AL, Souza GN. Prevalence and antimicrobial susceptibility of staphylococci isolated from saliva of clinically normal cats. Lett Appl Microbiol. 1999;28(6):448–52.

40. Abdolghanizadeh S, Salmeh E, Mirzakhani F, Soroush E, Siadat SD, Tarashi S. Microbiota insights into pet ownership and human health. Vol. 171, Research in Veterinary Science. Elsevier B.V.; 2024.

41. Lee DB, Verstraete FJM, Arzi B. An Update on Feline Chronic Gingivostomatitis. Vet Clin N Am - Small Anim Pract. 2020 Sep;50(5):973–82.

42. Vapniarsky N, Simpson DL, Arzi B, Taechangam N, Walker NJ, Garrity C, et al. Histological, Immunological, and Genetic Analysis of Feline Chronic Gingivostomatitis. Front Vet Sci. 2020 Jun;7.

43. Shariff A, Patil S, Bhandi S, Licari FW. Periodontitis linked with Urinary Tract Infections- Coincidence or Causality? In: Annual Research Symposium. Roseman University of Health Sciences, College of Dental Medicine; 2025. p. 37.

44. Huang IS, Huang SE, Kao WT, Chiang CY, Chang T, Lin CI, et al. Patients with chronic periodontitis are more likely to develop upper urinary tract stone: A nation-wide populationbased eight-year follow up study. PeerJ. 2018;2018(7).

45. Adamowicz K, Ribeiro ASL, Golda A, Wadowska M, Potempa J, Schmaderer C, et al. Bidirectional Interaction Between Chronic Kidney Disease and Porphyromonas gingivalis Infection Drives Inflammation and Immune Dysfunction. J Immunol Res. 2025;2025(1).

46. Soltero-Rivera M, Goldschmidt S, Arzi B. Feline chronic gingivostomatitis current concepts in clinical management. Vol. 25, Journal of Feline Medicine and Surgery. SAGE Publications Ltd; 2023.

47. Soltero-Rivera M, Shaw C, Arzi B, Lommer M, Weimer BC. Feline Chronic Gingivostomatitis Diagnosis and Treatment through Transcriptomic Insights. Pathogens. 2024 Mar;13(3).

48. Rodrigues MX, Bicalho RC, Fiani N, Lima SF, Peralta S. The subgingival microbial community of feline periodontitis and gingivostomatitis: characterization and comparison between diseased and healthy cats. Sci Rep. 2019 Dec;9(1).

49. Soltero-Rivera M, Vapniarsky N, Rivas IL, Arzi B. Clinical, radiographic and histopathologic features of early-onset gingivitis and periodontitis in cats (1997–2022). J Feline Med Surg. 2023 Jan;25(1).

50. Dolieslager SMJ, Riggio MP, Lennon A, Lappin DF, Johnston N, Taylor D, et al. Identification of bacteria associated with feline chronic gingivostomatitis using culture-dependent and culture-independent methods. Vet Microbiol. 2011 Feb;148(1):93–8.

51. Korkmaz SG, Ok M. Assessment of Selected Endothelial Damage Biomarkers in the Determination of Endothelial Damage in Cats With Gingivostomatitis. Vet Med Sci [Internet]. 2025 Sep;11(5). Available from: https://onlinelibrary.wiley.com/doi/10.1002/vms3.70525

52. Li Q, Ouyang X, Lin J. The impact of periodontitis on vascular endothelial dysfunction. Vol. 12, Frontiers in Cellular and Infection Microbiology. Frontiers Media S.A.; 2022.

53. Espinosa-Ortiz EJ, Gerlach R. Struvite Stone Formation by Ureolytic Biofilms. In: The Role of Bacteria in Urology. Springer International Publishing; 2019. p. 61–70.

54. Schultz LN, Connolly J, Lauchnor E, Hobbs TA, Gerlach R. Struvite stone formation by ureolytic biofilm infections. In: The Role of Bacteria in Urology. Springer International Publishing; 2015. p. 41–9.

55. Schaffer JN, Norsworthy AN, Sun TT, Pearson MM. Proteus mirabilis fimbriae- and urease-dependent clusters assemble in an extracellular niche to initiate bladder stone formation. Proc Natl Acad Sci U S A. 2016 Apr;113(16):4494–9.

56. Li X, Zhao H, Lockatell CV, Drachenberg CB, Johnson DE, Mobley HLT. Visualization of Proteus mirabilis within the matrix of urease-induced bladder stones during experimental urinary tract infection. Infect Immun. 2002;70(1):389–94.

57. Low WW, Kass PH, Ruby AL, Westropp JL. Evaluation of trends in urolith composition and characteristics of dogs with urolithiasis: 25,499 cases (1985–2006). J Am Vet Med Assoc. 2010 Jan;236(2):193–200.

58. Kopecny L, Palm CA, Segev G, Westropp JL. Urolithiasis in dogs: Evaluation of trends in urolith composition and risk factors (2006-2018). J Vet Intern Med. 2021 May;35(3):1406–15.

59. Burggraaf ND, Westgeest DB, Corbee RJ. Analysis of 7866 feline and canine uroliths submitted between 2014 and 2020 in the Netherlands. Res Vet Sci. 2021 Jul;137:86–93.

60. Kong N, Ng W, Vivan L, Weimer BC. Production and Analysis of High Molecular Weight Genomic DNA for NGS Pipelines Using Agilent DNA Extraction Kit (p/n 200600) [Internet]. Agilent Technologies; 2014. Available from: http://100kgenome.

61. Kong N, Ng W, Foutouhi A, Huang BC, Weimer BC, Kelly L. Quality Control of High-Throughput Library Construction Pipeline for KAPA HTP Library Using an

Agilent 2200 TapeStation [Internet]. 2014 Jan p. 1–8. Available from: http://100kgenome.vetmed.ucdavis.edu/

62. Beck KL, Haiminen N, Chambliss D, Edlund S, Kunitomi M, Huang BC, et al. Monitoring the microbiome for food safety and quality using deep shotgun sequencing. Npj Sci Food. 2021 Dec;5(1).

63. Haiminen N, Edlund S, Chambliss D, Kunitomi M, Weimer BC, Ganesan B, et al. Food authentication from shotgun sequencing reads with an application on high protein powders. Npj Sci Food 2019 31. 2019 Nov;3(1):1–11.

64. Bolger AM, Lohse M, Usadel B. Trimmomatic: A flexible trimmer for Illumina sequence data. Bioinformatics. 2014 Aug;30(15):2114–20.

65. Ewels P, Magnusson M, Lundin S, Käller M. MultiQC: Summarize analysis results for multiple tools and samples in a single report. Bioinformatics. 2016 Oct;32(19):3047–8.

66. Andrews S. FastQC: A quality control tool for high throughput sequence data. Babraham Bioinformatics; 2010.

67. Wood DE, Lu J, Langmead B. Improved metagenomic analysis with Kraken 2. Genome Biol. 2019 Nov;20(1).

68. Lu J, Breitwieser FP, Thielen P, Salzberg SL. Bracken: Estimating species abundance in metagenomics data. PeerJ Comput Sci. 2017;2017(1).

69. Grabherr MG, Haas BJ, Yassour M, Levin JZ, Thompson DA, Amit I, et al. Full-length transcriptome assembly from RNA-Seq data without a reference genome. Nat Biotechnol. 2011 Jul;29(7):644–52.

70. Patro R, Duggal G, Love MI, Irizarry RA, Kingsford C. Salmon provides fast and bias-aware quantification of transcript expression. Nat Methods. 2017;14(4):417–9.

71. Seemann T. Prokka: Rapid prokaryotic genome annotation. Bioinformatics. 2014 Jul;30(14):2068–9.

72. Cantalapiedra CP, Herṇandez-Plaza A, Letunic I, Bork P, Huerta-Cepas J. eggNOG-mapper v2: Functional Annotation, Orthology Assignments, and Domain Prediction at the Metagenomic Scale. Mol Biol Evol. 2021;38(12):5825–9.

73. Huerta-Cepas J, Szklarczyk D, Heller D, Hernández-Plaza A, Forslund SK, Cook H, et al. EggNOG 5.0: A hierarchical, functionally and phylogenetically annotated orthology resource based on 5090 organisms and 2502 viruses. Nucleic Acids Res. 2019 Jan;47(D1):D309–14.

74. Wen T, Niu G, Chen T, Shen Q, Yuan J, Liu YX. The best practice for microbiome analysis using R. Protein Cell. 2023 Oct;14(10):713–25.

75. Basbas C, Garzon A, Schlesener C, Heule M van, Profeta R, Weimer BC, et al. Unveiling the microbiome during post-partum uterine infection: a deep shotgun sequencing approach to characterize the dairy cow uterine microbiome. Anim Microbiome. 2023 Dec;5(1).

76. Batagelj V. Python Packages for Networks. In: Encyclopedia of Social Network Analysis and Mining. Springer New York; 2018. p. 1–10.

77. Xu JZ, Sun JX, Miao LT, Zhang SH, Wang WJ, Liu CQ, et al. Interconnections between urolithiasis and oral health: a cross-sectional and bidirectional Mendelian randomization study. Front Med. 2023;10.

78. Xu ZJ, Chen L, Tang QL, Li D, He CJ, Xu CL, et al. Differential oral and gut microbial structure related to systemic metabolism in kidney stone patients. World J Urol. 2024 Dec;42(1).

79. Guo S, Wu G, Liu W, Fan Y, Song W, Wu J, et al. Characteristics of human oral microbiome and its non-invasive diagnostic value in chronic kidney disease. Biosci Rep. 2022 May;42(5).

80. Parkhomenko E, Fazio AD, Tran T, Thai J, Blum K, Gupta M. A Multi-Institutional Study of Struvite Stones: Patterns of Infection and Colonization. J Endourol. 2017 May;31(5):533–7.

81. Pressler BM, Vaden SL, Lane IF, Cowgill LD, Dye JA. Candida spp. Urinary Tract Infections in 13 Dogs and Seven Cats: Predisposing Factors, Treatment, and Outcome. J Am Anim Hosp Assoc. 2003 May;39(3):263–70.

82. Litster A, Thompson M, Moss S, Trott D. Feline bacterial urinary tract infections: An update on an evolving clinical problem. Vol. 187, Veterinary Journal. 2011. p. 18–22.

83. Bailiff NL, Westropp JL, Jang SS, Ling GV. Corynebacterium urealyticum urinary tract infection in dogs and cats: 7 cases (1996-2003). Sci Rep Retrosp Study JAVMA. 2005 May;226(10):1676–80.

84. Olender A, Bogut A, Bańska A. The role of opportunistic Corynebacterium spp. in human infections. Vol. 17, European Journal of Clinical and Experimental Medicine. Publishing Office of the University of Rzeszow; 2019. p. 157–61.

85. Ling GV. Urinary Stone Disease. In: Lower Urinary Tract Diseases of Dogs and Cats: Diagnosis, Medical Management, Prevention [Internet]. Mosby-Year Book, Inc.; 1995. p. 144–77. Available from: https://uc-nrlf.caiasoft.com/reports/caiasoftBRW.php

86. Thompson RB, Stamey TA. Bacteriology of Infected Stones*. Urology. 1973 Dec;2(6):627–33.

87. Osborne CA, Lulich JP, Kruger JM, Polzin DJ, Johnston GR, Kroll RA. Medical dissolution of feline urocystoliths. J Am Vet Med Assoc. 1990;29(7):1053–63.

88. Ling GV, Ruby AL, Johnson DL, Thurmond M, Franti CE. Renal calculi in dogs and cats: prevalence, mineral type, breed, age, and gender interrelationships (1981-1993). J Vet Intern Med Am Coll Vet Intern Med. 1998;12(1):11–21.

89. Griffith DP. Struvite stones. Kidney Int. 1978 May;13(5):372–82.

90. Freshwater A. Why your housecat's trite little bite could cause you quite a fright: A study of domestic felines on the occurrence and antibiotic susceptibility of Pasteurella multocida. Zoonoses Public Health. 2008 Oct;55(8–10):507–13.

91. Krumbeck JA, Reiter AM, Pohl JC, Tang S, Kim YJ, Linde A, et al. Characterization of oral microbiota in cats: Novel insights on the potential role of fungi in feline chronic gingivostomatitis. Pathogens. 2021 Jul;10(7).

92. Rodríguez-Sojo MJ, Ruiz-Malagón AJ, Rodríguez-Cabezas ME, Gálvez J, Rodríguez-Nogales A. Limosilactobacillus fermentum CECT5716: Mechanisms and therapeutic insights. Vol. 13, Nutrients. MDPI AG; 2021. p. 1–22.

93. Cannon AB, Westropp JL, Ruby AL, Kass PH. Evaluation of trends in urolith composition in cats: 5,230 cases (1985-2004). J Am Vet Med Assoc. 2007 Aug;231(4):570–6.

94. Wang C, He T, Zhang M, Zheng C, Yang L, Yang L. Review of the mechanisms involved in dissimilatory nitrate reduction to ammonium and the efficacies of these mechanisms in the environment. Vol. 345, Environmental Pollution. Elsevier Ltd; 2024.

95. Bender RA. Regulation of the Histidine Utilization (Hut) System in Bacteria. Microbiol Mol Biol Rev. 2012 Sep;76(3):565–84.

96. Sintsova A, Smith S, Subashchandrabose S, Mobley HL. Role of Ethanolamine Utilization Genes in Host Colonization during Urinary Tract Infection. Infect Immun. 2018 Mar;86(3):1–10.

97. Boisvert H, Lorand L, Duncan MJ. Transglutaminase 2 is essential for adherence of Porphyromonas gingivalis to host cells. Proc Natl Acad Sci U S A. 2014;111(14):5355–60.

98. Zhu Y, Weiss EC, Otto M, Fey PD, Smeltzer MS, Somerville GA. Staphylococcus aureus biofilm metabolism and the influence of arginine on polysaccharide intercellular adhesin synthesis, biofilm formation, and pathogenesis. Infect Immun. 2007 Sep;75(9):4219–26.

99. Rahman S, Nath S, Mohan U, Das AK. Targeting Staphylococcal Cell-Wall Biosynthesis Protein FemX Through Steered Molecular Dynamics and Drug-Repurposing Approach. ACS Omega. 2023 Aug;8(32):29292–301.

100. Moormeier DE, Endres JL, Mann EE, Sadykov MR, Horswill AR, Rice KC, et al. Use of microfluidic technology to analyze gene expression during Staphylococcus aureus biofilm formation reveals distinct physiological niches. Appl Environ Microbiol. 2013 Jun;79(11):3413–24.

101. Mohamed JA, Huang DB. Biofilm formation by enterococci. J Med Microbiol. 2007 Dec;56(12):1581–8.

102. Gajadeera CS, Zhang X, Wei Y, Tsodikov OV. Structure of inorganic pyrophosphatase from Staphylococcus aureus reveals conformational flexibility of the active site. J Struct Biol. 2015 Feb;189(2):81–6.

103. Davies O, Mendes P, Smallbone K, Malys N. Characterisation of multiple substrate-specific (d)ITP/(d)XTPase and modelling of deaminated purine nucleotide metabolism. BMB Rep. 2012 Apr;45(4):259–64.

104. Anderson JG, Rojas CA, Scarsella E, Entrolezo Z, Jospin G, Hoffman SL, et al. The Oral Microbiome across Oral Sites in Cats with Chronic Gingivostomatitis, Periodontal Disease, and Tooth Resorption Compared with Healthy Cats. Animals. 2023 Nov;13(22).

105. D'ambrosio S, Ventrone M, Fusco A, Casillo A, Dabous A, Cammarota M, et al. Limosilactobacillus fermentum from buffalo milk is suitable for potential biotechnological process development and inhibits Helicobacter pylori in a gastric epithelial cell model. Biotechnol Rep. 2022 Jun;34.

106. Sarmah M, Deka M. Probiotic properties of Limosilactobacillus fermentum strain TPGMS1 isolated from gut microflora of Tai-Phake community of Assam. J Appl Nat Sci. 2024;16(4):1771–9.

107. Gan BS, Kim J, Reid G, Cadieux P, Howard JC. Lactobacillus fermentum RC-14 Inhibits Staphylococcus aureus Infection of Surgical Implants in Rats [Internet]. Vol. 185, The Journal of Infectious Diseases. American Society for Cell Biology; 2002 p. 9–13. Available from: https://academic.oup.com/jid/article/185/9/1369/938551

108. Pato U, Riftyan E, Yusmarini, Rossi E, Putri AA, Karvina S, et al. Sustainable Encapsulation of Limosilactobacillus fermentum Using Cellulose Microfiber Hydrogel:Antimicrobial and Immunomodulatory Effects Against Staphylococcus aureus. Adv Anim Vet Sci. 2025;13(3):533–43.

109. Yaikhan T, Wonglapsuwan M, Pahumunto N, Nokchan N, Teanpaisan R, Surachat K. Probiogenomic analysis of Limosilactobacillus fermentum SD7, a probiotic candidate with remarkable aggregation abilities. Heliyon. 2025 Feb;11(3).

110. Abramov VM, Kosarev IV, Machulin AV, Priputnevich TV, Deryusheva EI, Nemashkalova EL, et al. Limosilactobacillus fermentum 3872 That Produces Class III Bacteriocin Forms Co-Aggregates with the Antibiotic-Resistant Staphylococcus aureus Strains and Induces Their Lethal Damage. Antibiotics. 2023 Mar;12(3).

111. Park DY, Hwang J, Kim Y, Lee D, Kim YY, Kim HS, et al. Antimicrobial activity of Limosilactobacillus fermentum strains isolated from the human oral cavity against Streptococcus mutans. Sci Rep. 2023 Dec;13(1).

112. Speziale P, Geoghegan JA. Biofilm formation by staphylococci and streptococci: Structural, functional, and regulatory aspects and implications for pathogenesis. Vol. 5, Frontiers in Cellular and Infection Microbiology. Frontiers Research Foundation; 2015.

113. Yang S, Meng X, Zhen Y, Baima Q, Wang Y, Jiang X, et al. Strategies and mechanisms targeting Enterococcus faecalis biofilms associated with endodontic infections: a comprehensive review. Vol. 14, Frontiers in Cellular and Infection Microbiology. Frontiers Media SA; 2024.

114. Durand S, Guillier M. Transcriptional and Post-transcriptional Control of the Nitrate Respiration in Bacteria. Vol. 8, Frontiers in Molecular Biosciences. Frontiers Media S.A.; 2021.

115. Nakano MM, Hoffmann T, Zhu YI, †, Jahn and D. Nitrogen and Oxygen Regulation of Bacillus subtilis nasDEF Encoding NADH-Dependent Nitrite Reductase by TnrA and ResDE. J Bacteriol. 1998;180(20):5344–50.

116. Garsin DA. Ethanolamine utilization in bacterial pathogens: Roles and regulation. Vol. 8, Nature Reviews Microbiology. 2010. p. 290–5.

117. Dadswell K, Creagh S, McCullagh E, Liang M, Brown IR, Warren MJ, et al. Bacterial microcompartment-mediated ethanolamine metabolism in Escherichia coli urinary tract infection. Infect Immun. 2019;87(8).

118. Peng Q, Tang X, Dong W, Sun N, Yuan W. A Review of Biofilm Formation of Staphylococcus aureus and Its Regulation Mechanism. Vol. 12, Antibiotics. MDPI; 2023.

119. Vlaeminck J, Lin Q, Xavier BB, Backer SD, Berkell M, Greve HD, et al. The dynamic transcriptome during maturation of biofilms formed by methicillin-resistant Staphylococcus aureus. Front Microbiol. 2022 Jul;13.

120. Doeve J, Roquero DM, Holton GH, Mach K, Liao J. Bacteria Promotes Calcium Oxalate Crystal Aggregation Through Biofilm Formation. Vol. 211, The Journal of Urology. 2024.

121. Gray B, Hall P, Gresham H. Targeting agr- and agr-like quorum sensing systems for development of common therapeutics to treat multiple gram-positive bacterial infections. Sens Switz. 2013;13(4):5130–66.

122. Little SV, Bryan LK, Hillhouse AE, Cohen ND, Lawhon SD. Characterization of agr Groups of Staphylococcus pseudintermedius Isolates from Dogs in Texas. mSphere. 2019 Apr;4(2).

123. Lei Y, Oshima T, Ogasawara N, Ishikawa S. Functional analysis of the protein veg, which stimulates biofilm formation in bacillus subtilis. J Bacteriol. 2013 Apr;195(8):1697–705.

124. Kelliher JL, Radin JN, Kehl-Fie TE. PhoPR contributes to staphylococcus aureus Growth during phosphate starvation and pathogenesis in an environment- specific manner. Infect Immun. 2018 Oct;86(10).

125. Santos-Beneit F. The Pho regulon: A huge regulatory network in bacteria. Vol. 6, Frontiers in Microbiology. Frontiers Media S.A.; 2015.

SUPPLEMENTAL FIGURES

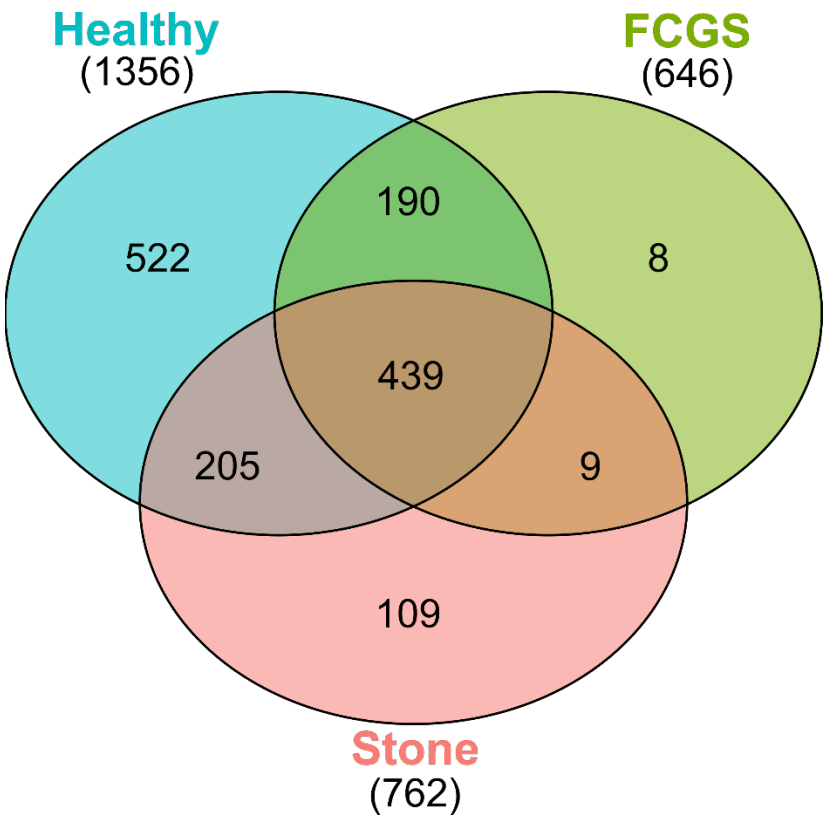

Supplemental Figure 1. Venn diagram of the unique and overlapping genera between the stone, healthy, and FCGS cohorts

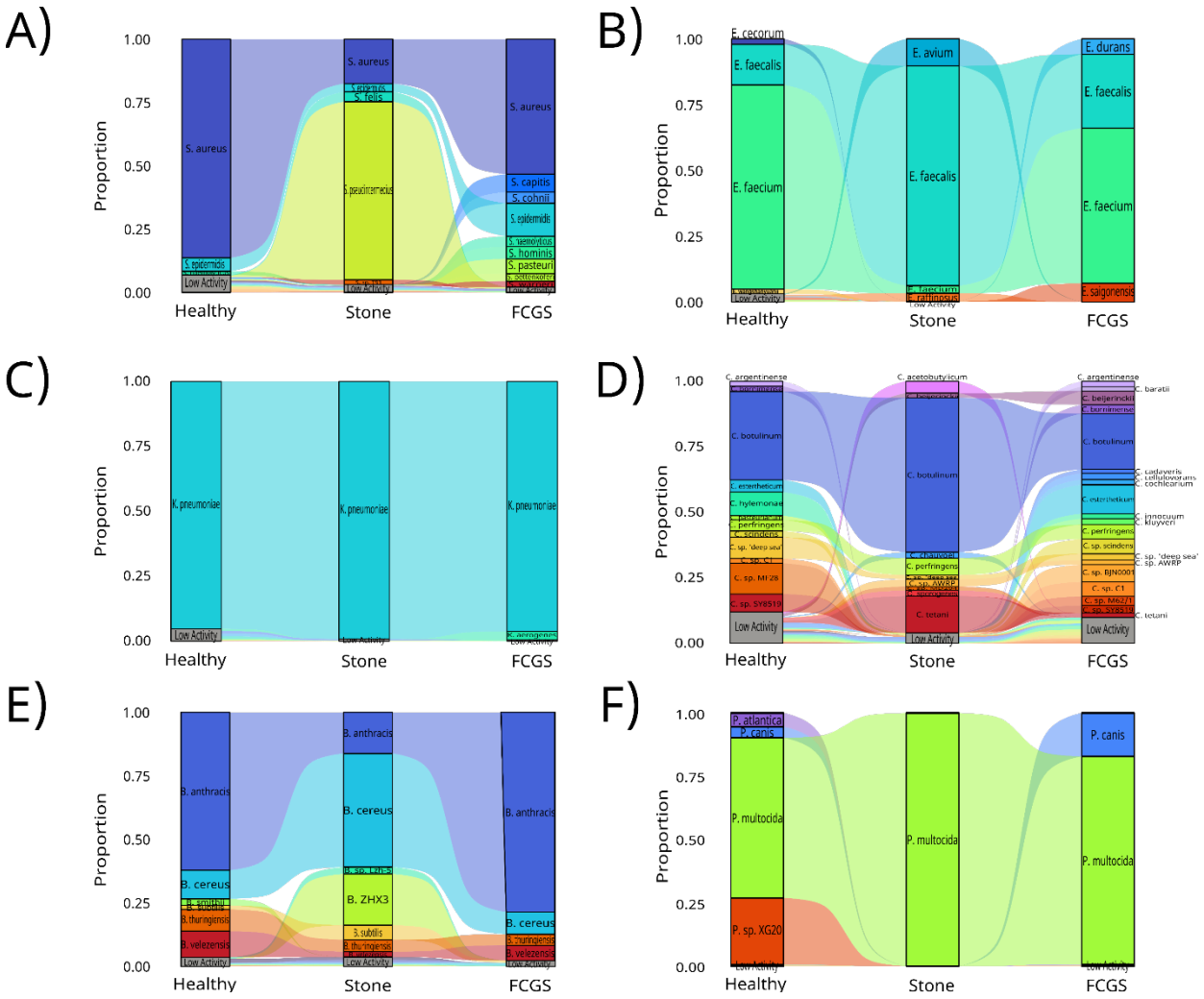

Supplemental Figure 2. Species- and strain-level shifts between keystone genera (proportion > 01; Fig 4). in the Healthy, Stone, and FCGS microbiomes. Alluvial plot displaying species/strain composition on the strata and species/strain shifts on the alluvia Organisms with less than 0.15 of the total proportion of reads in the microbiome were collapsed into the 'Mixed' category.

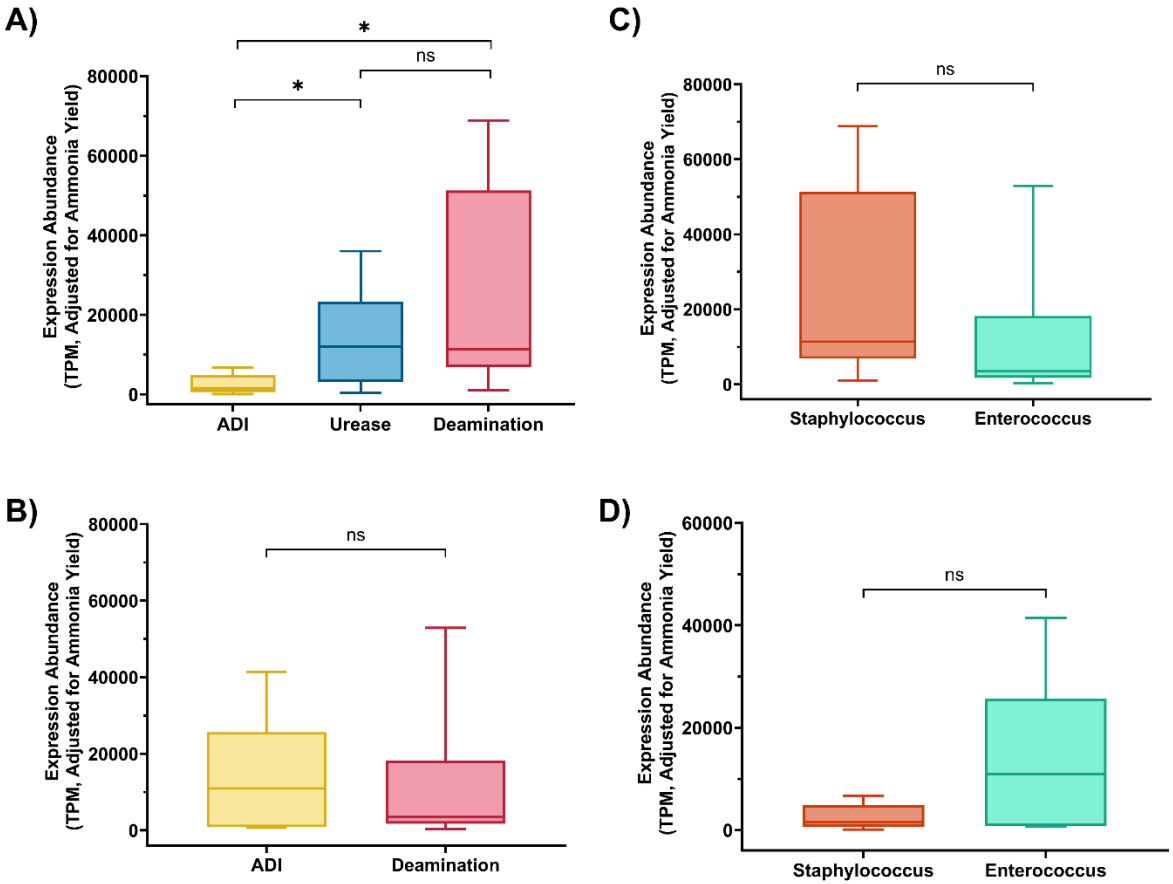

Supplemental Figure 3. Expression Abundance of Ammonia Producing Pathways. Panels A–C display expression abundance of ADI, urease, and deamination pathways in panel A is Staphylococcus, B is Enterococcus after adjusting for the ammonia yield per pathway. The urease pathway includes expression values for *rocF, yut, and ureABCDEFG.* Deamination includes genes detailed in Supp Table 1. Panels C and D show differences in expression abundance of (C) Deamination and (D) ADI by genus.

Supplemental Table 1. Deamination Gene Expression in *Staphylococcus* and *Enterococcus* in the Cat Stone.

The TPM-normalized expression values were adjusted values were computed based on estimated ammonia yield per pathway as described follows: deamination:1-2 depending on substrate, urease: 2, ADI: 2, which represents that total amount of ammonia produced by the reaction or pathway.

Enzyme	EC Number	*Staphylococcus*	*Enterococcus*	Gene(s)
Adenine deaminase	3.5.4.2	0	1	*ade*
Adenosine deaminase	3.5.4.4	1	1	*add*
4-amino-4-deoxychorismate lyase	4.1.3.38	1	0	-
Alanine dehydrogenase	1.4.1.1	1	1	*ald*
Arginine decarboxylase	4.1.1.19			-
L-asparaginase	3.5.1.1	1	1	*ansB (Enterococcus and Staphylococcus), asnA2 (Staphylococcus)*
Cytosine deaminase	3.5.4.1	0	1	-
dCMP deaminase	3.5.4.12	1	1	*comEB*
dctp deaminase	3.5.4.13	1	0	*dcd*
Ethanolamine ammonia lyase	4.3.1.7	0	1	*eutA, eutB, eutC, eutH, eutN, eutP, eutQ*
glucosamine-6-phosphate deaminase	3.5.99.6	1	1	*nagB*
Glu Leu Phe Val dehydrogenases	1.4.1.2	0	1	*gdhA*
GMP reductase	1.7.1.7	1	0	*guaC*
Guanine deaminase	3.5.4.3	0	1	*guaD*

Histidine degradation (with formamide degradation): Histidine Ammonia lyase, Urocanate hydratase, Imidazolonepropionase, Formiminoglutamase, Formamidase	3.5.3.8 4.3.1.3 4.2.1.49 3.5.2.7 3.5.3.8 3.5.1.49	2	0	*hutG, hutH, hutU, hutI, fmdA*
Nicotinamidase	3.5.1.19	1	0	*pncA*
Belongs to the Glu Leu Phe Val dehydrogenases family	1.4.1.2	1	0	-
Metal-dependent amidase aminoacylase carboxypeptidase	3.5.1.4	1	0	*amd*
Ornithine cyclodeaminase	4.3.1.12	1	1	*snbA* *snbB* *rapL* *(Staphylococcus)* *- (Enterococcus)*
Porphyromonas-type peptidyl-arginine deiminase	3.5.3.15	0	1	*aguA*
L-serine dehydratase	4.3.1.17	1	1	*sdaA* *sdaAA* *sdaAB*
Threonine deaminase	4.3.1.19	1	1	*ilvA*
Threonine dehydratase	4.3.1.17	1	1	*tdcB*
Transglutaminase	2.3.2.13	0	1	-
Total		**17**	**16**	

Supplemental Table 2. Biofilm-Associated Gene Expression in *Staphylococcus* and *Enterococcus* in the Stone

Genus Expressing	Description	Gene
Enterococcus	5-bromo-4-chloroindolyl phosphate hydrolysis protein	-
Enterococcus	cell adhesion	-
Enterococcus	Collagen binding domain	-
Staphylococcus	C-terminus of bacterial fibrinogen-binding adhesin	-
Staphylococcus	enzyme involved in biosynthesis of extracellular polysaccharides	-
Enterococcus	Glucan-binding protein C	-
Enterococcus	glycerophosphoryl diester phosphodiesterase	-
Staphylococcus	involved in biosynthesis of extracellular polysaccharides	-
Staphylococcus	peptidoglycan catabolic process	-
Staphylococcus	Peptidoglycan polymerase that catalyzes glycan chain elongation from lipid-linked precursors	-
Staphylococcus and Enterococcus	Putative adhesin	-
Staphylococcus	Regulator	*agrA*
Staphylococcus	Essential for the production of a quorum sensing system signal molecule, the autoinducing peptide (AIP). This quorum sensing system is responsible for the regulation of the expression of virulence factor genes. Involved in the proteolytic processing of AgrD, the precursor of AIP.	*agrB*
Staphylococcus	Staphylococcal AgrD protein	*agrD*
Staphylococcus	Bacterial capsule synthesis protein PGA_cap	*capA*
Staphylococcus	Mur ligase middle domain	*capB*
Staphylococcus	Capsule biosynthesis CapC	*capC*
Staphylococcus	Belongs to the UDP-glucose GDP-mannose dehydrogenase family	*capO*
Staphylococcus	Increases the activity of extracellular murein hydrolases possibly by mediating their export via hole formation. Inhibited by the antiholin-like proteins LrgAB. In an unstressed cell, the LrgAB products probably inhibit the function of the CidAB proteins. When a cell is stressed by the addition of antibiotics or by other factors in the environment, the CidAB proteins possibly oligomerize within the bacterial cell membrane, creating lesions that disrupt the proton motive force, which in turn results in loss of cell viability.	*cidB*
Staphylococcus	Belongs to the TPP enzyme family	*cidC*

Enterococcus	Polysaccharide biosynthesis protein	*cps2J*
Enterococcus	Catalyzes the stereoinversion of LL-2,6- diaminoheptanedioate (L,L-DAP) to meso-diaminoheptanedioate (meso- DAP), a precursor of L-lysine and an essential component of the bacterial peptidoglycan	*dapF*
Enterococcus	Belongs to the D-alanine--D-alanine ligase family	*ddl*
Enterococcus	Catalyzes the first step in the D-alanylation of lipoteichoic acid (LTA), the activation of D-alanine and its transfer onto the D-alanyl carrier protein (Dcp) DltC. In an ATP-dependent two-step reaction, forms a high energy D-alanyl-AMP intermediate, followed by transfer of the D-alanyl residue as a thiol ester to the phosphopantheinyl prosthetic group of the Dcp. D-alanylation of LTA plays an important role in modulating the properties of the cell wall in Gram-positive bacteria, influencing the net charge of the cell wall	*dltA*
Staphylococcus	Lysin motif	*ebpS*
Staphylococcus	Catalyzes the reversible conversion of 2- phosphoglycerate into phosphoenolpyruvate. It is essential for the degradation of carbohydrates via glycolysis	*eno*
Enterococcus	Fibronectin-binding protein A N-terminus (FbpA)	*FbpA*
Staphylococcus	Catalyzes the incorporation of amino acid(s) into the interchain peptide bridge of peptidoglycan, using aminoacyl-tRNA as amino acid donor	*femX*
Enterococcus	Zinc metalloprotease (elastase)	*gelE*
Enterococcus	Glycerophosphoryl diester phosphodiesterase family	*glpQ*
Enterococcus	Glycerophosphoryl diester phosphodiesterase family	*glpQ4*
Enterococcus	belongs to the glutamate--cysteine ligase type 1 family. Type 2 subfamily	*gshF*
Staphylococcus	N-acetylglucosaminyltransferase that catalyzes the polymerization of single monomer units of UDP-N-acetylglucosamine to produce the linear homopolymer poly-beta-1,6-N-acetyl-D- glucosamine (PNAG, also referred to as PIA), a biofilm adhesin polysaccharide. Requires IcaD for full activity	*icaA*
Staphylococcus	Catalyzes the N-deacetylation of poly-beta-1,6-N-acetyl- D-glucosamine (PNAG, also referred to as PIA), a biofilm adhesin polysaccharide	*icaB*
Staphylococcus	transferase activity, transferring acyl groups other than amino-acyl groups	*icaC*
Staphylococcus	-	*icaD*
Staphylococcus	transcriptional regulator IcaR	*icaR*
Enterococcus	Ami_2	*lytA*

Enterococcus	Functions as a peptidoglycan terminase that cleaves nascent peptidoglycan strands endolytically to terminate their elongation	*mltG*
Enterococcus	Binding-protein-dependent transport system inner membrane component	*modB*
Enterococcus	First step of the lipid cycle reactions in the biosynthesis of the cell wall peptidoglycan	*mraY*
Enterococcus	Catalyzes the addition of L-lysine to the nucleotide precursor UDP-N-acetylmuramoyl-L-alanyl-D-glutamate (UMAG) in the biosynthesis of bacterial cell-wall peptidoglycan	*murE*
Enterococcus	Belongs to the metallo-dependent hydrolases superfamily. NagA family	*nagA*
Enterococcus	Bacterial extracellular solute-binding proteins, family 5 Middle	*oppA1*
Enterococcus	Bacterial extracellular solute-binding proteins, family 5 Middle	*oppA2*
Enterococcus	Binding-protein-dependent transport system inner membrane component	*oppB*
Enterococcus	Binding-protein-dependent transport system inner membrane component	*opuCB*
Enterococcus	Binding-protein-dependent transport system inner membrane component	*opuCD*
Enterococcus	ABC-type spermidine putrescine transport system, permease component I	*potB*
Enterococcus	Binding-protein-dependent transport system inner membrane component	*potC*
Staphylococcus and Enterococcus	Sortase family	*srtA*
Enterococcus	ABC transporter substrate-binding protein PnrA-like	*tcsA*
Staphylococcus and Enterococcus	Biofilm formation stimulator VEG	*veg*
Enterococcus	Polysaccharide biosynthesis protein	*yabM*
Enterococcus	Polysaccharide biosynthesis protein	*ytgP*
Enterococcus	Putative adhesin	*yvlB*
Enterococcus	5-bromo-4-chloroindolyl phosphate hydrolysis protein	-
Enterococcus	cell adhesion	-
Enterococcus	Collagen binding domain	-

Supplemental Table 3. Phosphatase Gene Expression in *Staphylococcus* and *Enterococcus*

Genus Expressing	Description	Gene
Enterococcus	Bifunctional serine threonine kinase and phosphorylase involved in the regulation of the pyruvate, phosphate dikinase (PPDK) by catalyzing its phosphorylation dephosphorylation	-
Enterococcus	endonuclease exonuclease phosphatase family protein	-
Staphylococcus and Enterococcus	Histidine phosphatase superfamily (branch 1)	-
Staphylococcus	PA-phosphatase related membrane protein	-
Enterococcus	Pfam:Y_phosphatase3C	-
Enterococcus	Type I phosphodiesterase / nucleotide pyrophosphatase	-
Staphylococcus and Enterococcus	Belongs to the acylphosphatase family	*acyP*
Enterococcus	HAMP (Histidine kinases, Adenylyl cyclases, Methyl binding proteins, Phosphatases) domain	*arlS*
Enterococcus	Catalyzes the stereoinversion of LL-2,6- diaminoheptanedioate (L,L-DAP) to meso-diaminoheptanedioate (meso- DAP), a precursor of L-lysine and an essential component of the bacterial peptidoglycan	*dapF*
Enterococcus	Endonuclease/Exonuclease/phosphatase family	*exoA*
Enterococcus	Firmicute fructose-1,6-bisphosphatase	*fbp*
Enterococcus	Histidine phosphatase superfamily (branch 1)	*gpmB*
Staphylococcus	Endonuclease/Exonuclease/phosphatase family	*hlb*
Enterococcus	Phosphatidylglycerophosphatase A	*ltrC*
Enterococcus	Catalyzes the addition of L-lysine to the nucleotide precursor UDP-N-acetylmuramoyl-L-alanyl-D-glutamate (UMAG) in the biosynthesis of bacterial cell-wall peptidoglycan	*murE*
Staphylococcus	acid phosphatase family protein	*pgpB3*
Staphylococcus and Enterococcus	Alkaline phosphatase	*phoB*
Staphylococcus and Enterococcus	Phosphate starvation-inducible protein PhoH	*phoH*
Staphylococcus and	Alkaline phosphatase synthesis transcriptional regulatory protein	*phoP*

Enterococcus		
Staphylococcus and Enterococcus	Plays a role in the regulation of phosphate uptake	*phoU*
Staphylococcus and Enterococcus	Inorganic pyrophosphatase	*ppaC*
Staphylococcus	Purple acid Phosphatase, N-terminal domain	*ppe1*
Staphylococcus	Exopolyphosphatase	*ppx*
Enterococcus	Belongs to the low molecular weight phosphotyrosine protein phosphatase family	*ptpA*
Staphylococcus	Pyrophosphatase that catalyzes the hydrolysis of nucleoside triphosphates to their monophosphate derivatives, with a high preference for the non-canonical purine nucleotides XTP (xanthosine triphosphate), dITP (deoxyinosine triphosphate) and ITP. Seems to function as a house-cleaning enzyme that removes non-canonical purine nucleotides from the nucleotide pool, thus preventing their incorporation into DNA RNA and avoiding chromosomal lesions	*rdgB*
Enterococcus	Modulates RecA activity	*recX*
Staphylococcus	Serine phosphatase RsbU regulator of sigma subunit	*rsbU*
Staphylococcus	HAMP (Histidine kinases, Adenylyl cyclases, Methyl binding proteins, Phosphatases) domain	*saeS*
Staphylococcus and Enterococcus	Sigma factor PP2C-like phosphatases	*stp*
Staphylococcus and Enterococcus	Inositol monophosphatase	*suhB*
Staphylococcus	endonuclease exonuclease phosphatase	*XK27_02140*
Enterococcus	HAMP (Histidine kinases, Adenylyl cyclases, Methyl binding proteins, Phosphatases) domain	*yclK*
Enterococcus	Acid phosphatase homologues	*yodM*
Staphylococcus and Enterococcus	Mitochondrial PGP phosphatase	*yqeG*
Enterococcus	Bifunctional serine threonine kinase and phosphorylase involved in the regulation of the pyruvate, phosphate dikinase (PPDK) by catalyzing its phosphorylation dephosphorylation	*yqfL*

Staphylococcus	Belongs to the low molecular weight phosphotyrosine protein phosphatase family	*ywlE*
Enterococcus	Bifunctional serine threonine kinase and phosphorylase involved in the regulation of the pyruvate, phosphate dikinase (PPDK) by catalyzing its phosphorylation dephosphorylation	-
Enterococcus	endonuclease exonuclease phosphatase family protein	-
Staphylococcus and Enterococcus	Histidine phosphatase superfamily (branch 1)	-
Staphylococcus	PA-phosphatase related membrane protein	-
Enterococcus	Pfam:Y_phosphatase3C	-
Enterococcus	Type I phosphodiesterase / nucleotide pyrophosphatase	-
Staphylococcus and Enterococcus	Belongs to the acylphosphatase family	*acyP*
Enterococcus	HAMP (Histidine kinases, Adenylyl cyclases, Methyl binding proteins, Phosphatases) domain	*arlS*
Enterococcus	Catalyzes the stereoinversion of LL-2,6- diaminoheptanedioate (L,L-DAP) to meso-diaminoheptanedioate (meso- DAP), a precursor of L-lysine and an essential component of the bacterial peptidoglycan	*dapF*
Enterococcus	Endonuclease/Exonuclease/phosphatase family	*exoA*
Enterococcus	Firmicute fructose-1,6-bisphosphatase	*fbp*
Enterococcus	Histidine phosphatase superfamily (branch 1)	*gpmB*
Staphylococcus	Endonuclease/Exonuclease/phosphatase family	*hlb*
Enterococcus	Phosphatidylglycerophosphatase A	*ltrC*
Enterococcus	Catalyzes the addition of L-lysine to the nucleotide precursor UDP-N-acetylmuramoyl-L-alanyl-D-glutamate (UMAG) in the biosynthesis of bacterial cell-wall peptidoglycan	*murE*

Chapter 5:

Conclusion

CONCLUSION

The overarching hypothesis of this dissertation was that struvite uroliths in dogs and cats contain transcriptionally active, polymicrobial communities that promote stone formation through pathways beyond urease activity, with the oral microbiota serving as a potential reservoir for urinary stone-associated organisms. To test this hypothesis, a review of the current state of knowledge regarding microbial contributions to struvite urolithiasis was conducted as we aimed to characterize the taxonomic and functional profiles of struvite stone microbiomes and evaluate overlap with the oral microbiome in dogs and cats.

Chapter 1 reviewed the current understanding of struvite urolithiasis across species, with focus on dogs and cats, highlighting the limitations of traditional diagnostic approaches and the underappreciated role of the urinary microbiome in disease pathogenesis. While urease-producing bacteria have been long associated with struvite formation in both humans and dogs, the underlying mechanisms in cats remain poorly characterized, with many cases occurring in the absence of identifiable pathogens. However, evidence from both human and veterinary studies increasingly supports a more complex, polymicrobial model in which additional metabolic pathways—beyond urease—contribute to ammonia production, pH elevation, and struvite precipitation in the urinary tract. Aerobic urine cultures (AUCs) have remained the gold standard diagnostic for this condition for many decades. Yet the limitations of AUCs, along with other factors such as biofilm formation, complicate both diagnosis and treatment, as AUCs often fail to capture the full extent of microbial diversity present in the urinary tract. These challenges underscore the clinical value of advanced molecular tools such

as metatranscriptomics, which are used in the following chapters to improve our understanding of the microbial activity within struvite stones. Although this dissertation centers on struvite stone formation, a comparison to the oral microbiome was included to explore potential microbial overlap across niches and evaluate whether extra-urinary sources might contribute to stone-associated communities.

In *Chapter 2*, we hypothesized that struvite uroliths from dogs harbor transcriptionally active, polymicrobial communities that contribute to stone formation, and that the healthy dog oral microbiome may serve as a potential reservoir for these organisms and we used metatranscriptomic sequencing address this. Despite the distinct environmental conditions of the oral cavity and urinary tract, we observed substantial taxonomic overlap between the two niches. Approximately 74% of genera identified in stone samples were also present in the oral microbiome, and nearly half (47%) of species- or strain-level taxa were shared, suggesting a possible oral–stone microbial axis in dogs. The presence of *Porphyromonas*, a well-established oral pathogen, within the stone microbiome further supports this connection. The most transcriptionally active members of the stone microbiome included facultative and strict anaerobes: *Staphylococcus*, *Enterococcus*, *Bacillus*, and *Porphyromonas*. Struvite formation appears to be shaped not by a single urease-producing organism, but by the cooperative interactions of a broader microbial community with diverse ammonia producing methods. Urease-associated ammonia production was found to only occur in *Staphylococcus* of all the most transcriptionally active taxa, accounting for only 28.3% of all ammonia-producing expression by that genus. Notably, although several taxa were shared between oral and stone microbiomes, the co-occurrence partners of these

organisms differed across niches, suggesting that microbial interactions are highly niche-specific and shaped by local environmental pressures. Functional profiling revealed expression of multiple ammonia-generating pathways—including urease, the ADI pathway, and deamination of nitrogenous substrates—as well as transcripts associated with dissimilatory nitrite reduction, suggesting alternative routes of ammonia production under oxygen-limited conditions. Concurrent expression of biofilm and phosphatase associated genes also suggests that these organisms contribute to a shared extracellular matrix that promotes microbial persistence and supports continued mineral deposition within the urinary tract.

Finally, in *Chapter 3* we hypothesized that struvite stones from cats are not sterile and instead,they also harbor transcriptionally active microbial communities and exhibit evidence of polymicrobial involvement. To further explore the oral/stone axis, we examined health and FCGS samples to determine if the microbiome overlaps between these locations. Investigation into the oral microbiome of both healthy and FCGS-affected individuals allowed for evaluation of whether oral disease alters microbial composition in a way that contributes to colonization of the urinary tract and stone formation. The stone microbiome displayed marked overlap in community membership with both healthy and FCGS-associated oral microbiomes. At the species/strain level, 64.7% of stone-associated taxa were also present in the healthy oral microbiome, while 61.7% overlapped with the FCGS oral microbiome. Further analysis revealed that the stone and FCGS communities were more compositionally similar, reflecting shared dominance by a smaller number of highly active taxa. This supported the hypothesis that FCGS increases the likelihood of the same organisms being present in both the

oral cavity and the stone, reinforcing the existence of a potential oral–stone axis in cats. The stone microbiomes of cats were more taxonomically diverse and compositionally heterogeneous than those observed in dogs, with a broader range of transcriptionally active facultative anaerobes, including organisms previously associated with struvite stones including *Staphylococcus*, *Enterococcus,* and *Klebsiella.* Co-occurrence network analysis identified structured microbial sub-communities within the stone, with one of the most striking patterns being the strong inverse association between *Staphylococcus pseudintermedius* and *Limosilactobacillus fermentum*. This antagonistic relationship may reflect microbial competition or niche partitioning. This finding is important because it suggests that *L. fermentum* may antagonize *S. pseudintermedius* within the stone environment. As an extensively studied probiotic, the presence of *L. fermentum* raises the potential for therapeutic strategies that promote beneficial taxa to limit pathogenic colonization and reduce stone risk.

Biochemically functional profiling of stone samples revealed consistent expression of genes involved in ammonia production via multiple routes in a small number of organisms. As in the dog struvite urolith, urease gene expression occurred exclusively in *Staphylococcus* and only comprised 34.1% of all ammonia-producing expression by that genus. Phosphate mobilization and biofilm formation was found to be highly active which further supports a microbial role in struvite stone formation in cats. Overall, our findings demonstrate that cat struvite stones contain a robust, transcriptionally active microbiome, refuting the long-held assumption in the field that these stones are sterile. The observed overlap with oral microbes, particularly in FCGS-

affected patients, points to a potential connection between oral health and susceptibility to stone formation.

These findings support the presence of polymicrobial communities in both dog and cat struvite stones that drive the biochemical conditions necessary for struvite crystallization, expanding the current understanding of urolithiasis beyond traditional culture-based paradigms focused solely on urease activity. The detection of an oral–stone microbial axis, especially in states of oral disease, suggests that oral health may influence stone microbiota composition and disease risk. While the study is limited by sample size and the inherent challenges of host–microbe metatranscriptomic analysis, it establishes a foundation for integrating microbial functional data into future diagnostic and therapeutic strategies. By jointly examining taxonomic composition and transcriptional activity, this work offers new insights into the active roles of stone-associated microbes and highlights potential targets for intervention. Modulating key taxa or targeting specific microbial pathways may offer new opportunities to improve patient care through more precise and informed diagnostic and therapeutic strategies in the future. Overall, this work advances the field by demonstrating the utility of transcriptomic profiling in identifying active microbial contributors to stone formation and underscores the importance of adopting an integrated, community-level approach to understanding and managing urolithiasis in veterinary medicine. Importantly, this works provides the basis for an oral-stone axis in multiple animal species leading to new insights into risk factors for stone formation as well as new approaches for diagnostic and therapeutic options.

Future Directions

This dissertation lays the foundation for a deeper understanding of the microbiome's role in struvite urolithiasis and highlights several key directions for future research. The consistent presence of transcriptionally active microbes in both dog and cat stones warrants larger-scale studies to further support and build upon the findings. Broader sampling may also clarify whether specific community structures or keystone taxa predict stone recurrence or severity. While this work identified ammonia-producing pathways and taxa involved in biofilm and phosphate metabolism within the stone, further research is needed to clarify the functional roles of individual microbes and the microbial interactions or crosstalk that collectively promote stone formation. Additionally, the discovery of an oral–stone microbial axis raises new questions about microbial translocation and systemic reservoirs. Longitudinal studies could determine whether oral dysbiosis precedes urinary colonization and stone formation. Experimental models might test whether oral microbiome modulation, via probiotics or oral hygiene interventions, alter risk for stone development. Finally, these findings have strong translational potential for both veterinary and human health. Incorporating microbial functional profiling into diagnostics could help identify high-risk patients who may be missed by traditional culture methods. As molecular tools become more accessible, precision-based approaches, such as targeted microbial therapies or functional diagnostics, may improve outcomes and reduce recurrence in both clinical and veterinary settings.